



National Library
of Canada

Bibliothèque nationale
du Canada

Canadian Theses Service

Service des thèses canadiennes

Ottawa, Canada
K1A 0N4

NOTICE

The quality of this microform is heavily dependent upon the quality of the original thesis submitted for microfilming. Every effort has been made to ensure the highest quality of reproduction possible.

If pages are missing, contact the university which granted the degree.

Some pages may have indistinct print especially if the original pages were typed with a poor typewriter ribbon or if the university sent us an inferior photocopy.

Reproduction in full or in part of this microform is governed by the Canadian Copyright Act, R.S.C. 1970, c. C-30, and subsequent amendments.

AVIS

La qualité de cette microforme dépend grandement de la qualité de la thèse soumise au microfilmage. Nous avons tout fait pour assurer une qualité supérieure de reproduction.

S'il manque des pages, veuillez communiquer avec l'université qui a conféré le grade.

La qualité d'impression de certaines pages peut laisser à désirer, surtout si les pages originales ont été dactylographiées à l'aide d'un ruban usé ou si l'université nous a fait parvenir une photocopie de qualité inférieure.

La reproduction, même partielle, de cette microforme est soumise à la Loi canadienne sur le droit d'auteur, SRC 1970, c. C-30, et ses amendements subséquents.



National Library
of Canada

Bibliothèque nationale
du Canada

Canadian Theses Service Service des thèses canadiennes

Ottawa, Canada
K1A 0N4

The author has granted an irrevocable non-exclusive licence allowing the National Library of Canada to reproduce, loan, distribute or sell copies of his/her thesis by any means and in any form or format, making this thesis available to interested persons.

The author retains ownership of the copyright in his/her thesis. Neither the thesis nor substantial extracts from it may be printed or otherwise reproduced without his/her permission.

L'auteur a accordé une licence irrévocable et non exclusive permettant à la Bibliothèque nationale du Canada de reproduire, prêter, distribuer ou vendre des copies de sa thèse de quelque manière et sous quelque forme que ce soit pour mettre des exemplaires de cette thèse à la disposition des personnes intéressées.

L'auteur conserve la propriété du droit d'auteur qui protège sa thèse. Ni la thèse ni des extraits substantiels de celle-ci ne doivent être imprimés ou autrement reproduits sans son autorisation.

ISBN 0-315-55506-8

Canada

THE UNIVERSITY OF ALBERTA

**THE DISTRIBUTION AND THERMAL STABILITY OF OXYGEN IN SOME
REPRESENTATIVE CANADIAN COALS**

by

CHANDRAWATEE (SEEPERSADSINGH) ANGLE

A THESIS

**SUBMITTED TO THE FACULTY OF GRADUATE STUDIES AND RESEARCH IN
PARTIAL FULFILLMENT OF THE REQUIREMENTS FOR THE DEGREE OF
MASTER OF SCIENCE**

IN

MINERAL ENGINEERING

DEPARTMENT OF MINING, METALLURGICAL AND PETROLEUM ENGINEERING

EDMONTON, ALBERTA

FALL 1989

THE UNIVERSITY OF ALBERTA
RELEASE FORM

NAME OF AUTHOR CHANDRAWATEE (SEEPERSADSINGH) ANGLE

TITLE OF THESIS THE DISTRIBUTION AND THERMAL STABILITY OF
OXYGEN IN SOME REPRESENTATIVE CANADIAN COALS

DEGREE MASTER OF SCIENCE

YEAR THIS DEGREE GRANTED FALL 1989

Permission is hereby granted to THE UNIVERSITY OF ALBERTA LIBRARY to reproduce single copies of this thesis and to lend or sell such copies for private, scholarly or scientific purposes only.

The author reserves other publication rights, and neither the thesis nor extensive extracts from it may be printed or otherwise reproduced without the author's written permission.

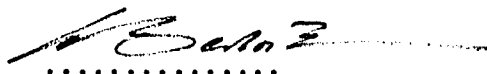
(SIGNED)*Changle*.....
PERMANENT ADDRESS:

.....6332-14 Ave.....
.....Edmonton, Alberta.....
.....T6L 1S4, CANADA.....

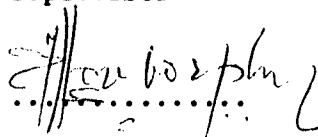
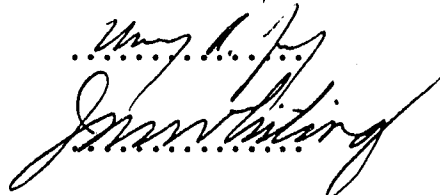
DATED ...*12-10-89*.....

THE UNIVERSITY OF ALBERTA
FACULTY OF GRADUATE STUDIES AND RESEARCH

The undersigned certify that they have read, and recommend to the Faculty of Graduate Studies and Research for acceptance, a thesis entitled **THE DISTRIBUTION AND THERMAL STABILITY OF OXYGEN IN SOME REPRESENTATIVE CANADIAN COALS** submitted by **CHANDRAWATEE (SEEPERSADSINGH) ANGLE** in partial fulfillment of the requirements for the degree of **MASTER OF SCIENCE in MINERAL ENGINEERING**


.....

Supervisor


.....

.....

Date ...12-10-89...

Dedication

For my children, Daryan, Trisha and Kiri

The powers of the mind are endless, the seemingly impossible becomes possible when you decide that it is so and act on it. A dream becomes reality when you pursue it with desire, nurture it with the positive energy from yourself and those who can dream with you.

ABSTRACT

The seemingly atypical behaviour of Western Canadian coals in many utilization technologies may be related to differences in the distribution of oxygen in reactive functional groups rather than differences in elemental composition. There is a paucity of such data for Canadian coals. European Carboniferous coals, for which data are available, cannot be used because of differences in formative history.

The distribution of oxygen in reactive functional groups -COOH , -OH , and =CO were determined for 10 Canadian coals of three geological ages. Focus was on the plentiful low rank coals, and others were selected to compare Cretaceous age coals with equivalent Carboniferous coals. The consequences of mild pyrolysis on the distribution of O-bearing functional groups were investigated by slow heating at 200°C and 300°C : fast heating was used to study decarboxylation of low rank coals.

Automated titrimetry allowed some refinement of the classical wet analytical procedures used. Fourier Transform Photoacoustics Infrared Spectroscopy (FTIR-PAS) was used for qualitative confirmation of chemical modifications and completion of reactions.

Oxygen concentrations in O-bearing functional groups follow the sequence $[\text{O}_{\text{OH}}] > [\text{O}_{\text{CO}}] > [\text{O}_{\text{COOH}}]$ and versus total oxygen, are described by regression lines. Wide variations in concentrations of oxygen in O-bearing functional groups among coals of similar elemental composition indicate that coal

reactivities vary as well. The distribution of oxygen in O-bearing functional groups partially conform with data reported in the literature.

Molecular rearrangements occur at slow heating and fast heating, but at slow heating most coals show increased =CO and -OH . The extent of decarboxylation depends on temperature and rate of heating. Chemical changes entail small losses in total oxygen. The results may be explained by any of three pathways involving loss of -COOH : reversible anhydride formation, quinone formation, and/or CO release with free radical stabilization by -OH .

Acknowledgement

For the help and contribution of many who generously gave of themselves towards the success of this thesis, I am grateful.

Dr. N. Berkowitz, my advisor, with whom I have had the privilege of very stimulating discussions about coal. Since my 12 years of research experience on coal centered around surface and colloid properties, his wisdom and knowledge in coal chemistry introduced me into new dimensions of thinking about coal. His time and criticisms were valuable keys to improvement.

Dr. T.D. Brown, director of CANMET/CRL, for approving and supporting my study goals, and for helpful suggestions. Dr. H.A. Hamza, CANMET manager, for his belief in my potential, worth, and abilities. He values growth in people as assets, took the necessary risks to support my endeavors. My colleague and friend A. Mo, whose helping hand and encouragement made coping easier.

Randolph P. Angle, my husband, for his encouragement and support throughout. My three children, Daryan, Trisha, and Kiri who, despite their young age, were understanding and supportive.

N. Aikman for providing library assistance. The Department of Mining, Metallurgical and Petroleum Engineering committee for accepting me from another discipline. Last, but not least, I thank all those whose positive attitude towards my endeavors made the heavy load lighter.

This work was financially supported by CANMET for which I am grateful.

Table of Contents

Chapter	Page
1. Introduction	1
1.1 The Impact of Oxygen on Surface Properties of Coals.	2
1.2 The Significance of Oxygen in Conversion Processes .	5
1.3 The Significance of Diagenetic and Metamorphic History on Oxygen in Coal.....	7
1.4 Historical perspective.....	9
1.5 Other Considerations	12
1.6 Approach to Study.....	13
2. Literature Review.....	16
2.1 Oxygen in Coal.....	16
2.2 Analytical Procedures.....	18
2.2.1 Total Oxygen	19
2.2.2 Functional Group Analysis.....	20
2.2.2.1 Instrumental Techniques.....	20
2.2.2.2 Wet Chemical Methods.....	25
2.3 Methods Selected.....	35
3. Experimental.....	37
3.1 Choice of Coal Samples.....	37
3.2 Sampling	40
3.3 Apparatus and Instrumentation	41
3.4 Materials.....	41
3.5 Protonation	43

Table of Contents

Chapter	Page
3.6 Mild Pyrolysis.....	44
3.6.1 Slow Heating	44
3.6.2 Fast Heating	45
3.7 Wet Chemical Methods.....	45
3.7.1 Automatic Potentiometric Titrimetry.....	46
3.7.2 Analysis of [O] in Hydroxyl Groups.....	48
3.7.3 Analysis of [O] in Carboxylic Groups.....	50
3.7.4 Analysis of [O] in Carbonyl Groups.....	52
3.8 Carbon, Hydrogen, and Nitrogen (CHN) Analyses....	53
3.9 Proximate Analyses.....	54
3.10 Fourier Transform Infrared Photoacoustic Spectroscopy (FTIR-PAS).....	54
 4. Results and Discussion I. Distribution of Oxygen Functional Groups in Coals.....	56
4.1 Introduction	56
4.2 Trends of Oxygen-Bearing Functional Group Concentrations.....	59
4.3 Variations in Oxygen Distribution in Canadian coals	67
4.3.1 Low Rank U.Cretaceous/Tertiary Coals	67
4.3.2 High Rank U.Cretaceous/Tertiary and Carboniferous Coals	69
4.4 Regional Metamorphic Effects	70

Table of Contents

Chapter	Page
4.5 Observations respecting Experimental Methods	72
4.6 Qualitative Variations among Coals as detected by FTIR-PAS.....	76
5. Results and Discussion II- Thermal Stability.....	78
5.1 Introduction	78
5.2 Slow Heating	85
5.2.1 Thermal stability of Hydroxyl Oxygen.....	85
5.2.2 Thermal stability of Carbonyl Oxygen	89
5.2.3 Thermal stability Carboxyl Oxygen.....	92
5.3 Effects of Rapid heating on Carboxyl Oxygen	94
5.3.1 Comparison of Slow and Fast Heating Effects..	94
5.4 Inferences and Explanations of Observed Trends ...	96
5.5 Qualitative Observations of Coal Chemistry after Pyrolysis	99
5.6 Ramifications of Heating Rate Effects.....	99
6. Conclusions.....	113
6.1 Distribution of Oxygen in Functional Groups.....	113
6.2 Thermal Stability of Canadian Coals.....	116
6.3 Recommendations.....	117
References.....	119

Table of Contents

Chapter	Page
Appendix 1 - Detailed Experimental Data on O-Bearing Functional Groups in Protonated and Heat- Treated Coals	137
Appendix 2 - Elemental Analyses of Protonated and Heat- Treated Coals.....	150
Appendix 3 - Proximate Analyses of Protonated and Heat- Treated Coals.....	161
Appendix 4 - FTIR-PAS Spectra of Protonated, Chemically Modified and Heat Treated Coals	172
Appendix 5 - List of Chemicals and Time Table of Experimental Plan.....	185

List of Tables

Table		Page
1	Identification, Source and Rank of Coals	38
2	Description of Original Coal Characteristics.....	39
3	Weight percentage of Oxygen in O-bearing Functional Groups in Coal dried in vacuo, 70°C to 100°C for 20h. 57	
4	Weight Percentage of Oxygen in O-bearing Functional Groups as a Fraction of Total Oxygen in coal dried in vacuo at 70°C - 100°C for 20h.....	58
5	Oxygen Distribution after Slow Heating (200°C, N ₂ 8cc/min, 20h), all concentrations in weight percentage daf coal.....	82
6	Oxygen Distribution after Slow Heating (300°C, N ₂ 8cc/min, 0.5h), all concentrations in weight percentage daf coal	83
7	Comparison of Oxygen in Carboxyl Groups for low rank coals rapidly heated in N ₂ (12cc/min).....	84

Appendix 1

1-10	Detailed Data on Oxygen Distribution in Protonated and Heat-treated Coals.....	137
------	---	-----

Appendix 2

1-10	Elemental Analyses of Protonated and Heat- treated Coals.....	150
------	--	-----

Appendix 3

1-10	Proximate Analyses of Protonated and Heat-treated Coals.....	161
------	---	-----

List of Figures

Figure	Description	Page
	Chapter 3	
1	Photograph of apparatus for refluxed reactions.....	42
2	Sampling apparatus for automatic titration.....	47
	Chapter 4	
3	Weight percentage of oxygen in O-bearing functional groups ($x = -OH, =CO, -COOH$) $[Ox]$ versus total oxygen $[O]$	60
4	Oxygen in O-bearing functional groups ($x = -OH, =CO, -COOH$), as a fraction of the total oxygen $[O]$ versus $[O]$. Solid lines indicate the empirical $f([O])$ plotted against $[O]$..	62
5	Weight percentage of oxygen in O-bearing functional groups ($x = -OH, =CO, -COOH$) $[Ox]$ versus %C	63
6	Weight percentage of oxygen in O-bearing functional groups versus %C (a) after Blom. et al., 1957) (b) Canadian coals (cumulative plots).....	65

Figure	Description	Page
7	Typical titration and derivative curves of unbuffered filtrate of ion exchanged hydrolysate of acetylated coal. Titrant is .05M NaOH.....	73
8	Titration and derivative curves for filtrate from a coal exchanged against barium acetate and buffering capacity is undiluted. Titrant is .05M NaOH.....	74
9	Titration and derivative curves of filtrate from a coal exchanged against barium acetate. Buffering capacity is reduced and $\text{Ba}(\text{OH})_2$ precipitates. Titrant is .05M NaOH.	75
10	Typical FTIR-PAS spectra for low rank coals (subbit.C. #2 & #4, lignite #1 and subbit.B #7) (Appendix 4).....	173
11	FTIR-PAS spectra of different rank Western Canadian Coals #11 (subbit. C), #10 (hvb) and #20 (mhb) (Appendix 4).....	174
12	FTIR-PAS spectra of U.Cretaceous coals #11 (subbit. C) and #10 (hvb) (Appendix 4).....	175

Figure	Description	Page
13	FTIR-PAS spectra of similar rank (hvb) coals which differ in geological age (#10 is U.Cret./Tert., #14 is Carb.) (Appendix 4)...	176
14a	Typical FTIR-PAS spectra of a protonated coal (subbit.C #4) (Appendix 4).....	177
14b	Typical FTIR-PAS spectra of a Ba-exchanged coal (subbit.C #4) (Appendix 4)	178
14c	Typical FTIR-PAS spectra of an acetylated coal (subbit.C #4) (Appendix 4).....	179
14d	Typical FTIR-PAS spectra of a coal (subbit.C #4) hydrolysed after acetylation (Appendix 4).....	180
14e	Typical FTIR-PAS spectra of an oximated coal (subbit.C #11) (Appendix 4).....	181

Chapter 5

5.1	Linear regression plots of $[O_{OH}]$ versus $[O]$ for low and high rank coals after slow heating at (i) 100°C (20h) in vacuo, (ii) 200°C (20h) and (iii) 300°C (0.5h) in N_2 (8cc/min).....	86
-----	---	----

Figure	Description	Page
5.2	Linear regression plots of $[O_{CO}]$ versus $[O]$ for low and high rank coals after slow heating at (i) 100°C (20h) in vacuo, (ii) 200°C (20h) and (iii) 300°C (0.5h) in N_2 (8cc/min).....	90
5.3	Linear regression plots of $[O_{COOH}]$ versus $[O]$ for low and high rank coals after slow heating at (i) 100°C (20h) in vacuo, (ii) 200°C (20h) and (iii) 300°C (0.5h) in N_2 (8cc/min).....	93
5.4	Comparison of $[O_{COOH}]$ versus $[O]$ for low rank coals after slow and fast heating at 200°C (0.5h) and 300°C (0.5h). Solid lines are regression plots for fast heated coals.....	95
5.5	FTIR-PAS spectra of coal #11 (subbituminous C) after slowly heated to 200°C (20h) and 300°C (0.5h) in N_2 (8cc/min) (Appendix 4).....	182
5.6	FTIR-PAS spectra of coal #14 after slow heating at 200°C (20h) and 300°C (0.5h) in N_2 (8cc/min), compared with original coal dried at 100°C (20h) in vacuo (Appendix 4).....	183

Figure	Description	Page
5.7	FTIR-PAS spectra of coal #9 (subbit. C) after slow heating at 200°C in N ₂ (8cc/min) compared with the original coal dried in vacuo (Appendix 4).....	184
5.8	Fraction of total oxygen in C-bearing functional groups of protonated lignite #1 dried at (i) 100°C (20h) and after slow heating in N ₂ (8cc/min) at (ii) 200°C (20h), (iii) 300°C (0.5h).....	101
5.8a	Fraction of total oxygen in carboxyl group of lignite #1 after fast heating in N ₂ (12cc/min) 0.5h at (i) 200°C and (ii) 300°C.....	102
5.9	Fraction of total oxygen in O-bearing functional groups of protonated subbit. C #2 dried at (i) 100°C (20h) and after slow heating in N ₂ (8cc/min), at (ii) 200°C (20h), (iii) 300°C (0.5h).	103
5.9a	Fraction of total oxygen in carboxyl group of protonated subbit. C #2 dried at (i) 100°C (20h) and after fast heating in N ₂ (12cc/min) for 0.5h at (i) 200°C (ii) 300°C.....	104

Figure	Description	Page
5.10	Fraction of total oxygen in O-bearing functional groups of protonated subbit. B #7 dried at (i) 100°C (20h) and after slow heating in N ₂ (8cc/min) at (ii) 300°C (0.5h).....	105
5.10a	Fraction of total oxygen in carboxyl group of protonated Subbit. B #7 dried at (i) 100°C (20h) in vacuo and after fast heating in N ₂ (12cc/min) for 0.5h, at (ii) 200°C and (iii) 300°C.....	106
5.11	Fraction of total oxygen in O-bearing functional groups of protonated subbit. C #9 dried at (i) 100°C (20h) in vacuo and slowly heated in N ₂ (8cc/min) at (ii) 200°C (20h) (iii) 300°C (0.5h)..	107
5.11a	Fraction of total oxygen in carboxyl group of protonated subbit.B #9 dried at (i) 100°C (20h) in vacuo and after fast heating in N ₂ , (12cc/min) for 0.5h, at (i) 200°C (ii) 300°C.....	108
5.12	Fraction of total oxygen in O-bearing functional groups of protonated subbit. C #11 dried at (i) 100°C (20h) in vacuo and after slow heating in N ₂ (8cc/min) at (ii) 200°C (20h), (iii) 300°C (0.5h)	109

Figure	Description	Page
5.13	Fraction of total oxygen in O-bearing functional groups of protonated hvb U. Cret /Tert #10 dried at (i) 100°C (20h) in vacuo and after slow heating in N ₂ (8cc/min) at (ii) 200°C (20h) (iii) 300°C (0.5h)	110
5.14	Fraction of total oxygen in O-bearing functional groups of protonated hvb Carb. #14 dried at (i) 100°C (20h) in vacuo and after slow heating in N ₂ (8cc/min) at (ii) 200°C (20h) (iii) 300°C (0.5h)111	111
5.15	Fraction of total oxygen in O-bearing functional groups of protonated hvb Carb. #16 dried at (i) 100°C (20h) in vacuo, and after slow heating in N ₂ (8cc/min) at (i) 200°C (20h) (ii) 300°C (0.5h) 112	112

LIST OF PHOTOGRAPHIC PLATES

Plate	Page
1	Photograph of apparatus for refluxed reactions.....42

CHAPTER 1

INTRODUCTION

When exposed to air, freshly mined coals lose moisture rapidly and oxidize. Coal quality deteriorates on weathering: bituminous metallurgical coals (see note 1) lose commercial value by oxidative destruction of their caking properties and thermal coals lose calorific value (see note 2). Lower rank coals react more rapidly with oxygen than the higher ranks (Berkowitz, 1979).

Alberta's coals (see note 3) have been reported to exhibit atypical behaviour in many aspects. For example, subbituminous coals yield substantially less tar in low temperature carbonization assays than rank correlations would lead one to expect (Selvig & Ode, 1957), and metallurgical coals do not conform with well established relationships between petrographic compositions and coke strength (Shapiro & Gray, see note 4; Neavel, 1981a). It was reported that the oxygen content was higher for a given reflectance than in Appalachian coals (Ignasiak & Berkowitz, 1974). Whether these anomalies are the result of faster maturation, or of the depositional history of Alberta coals, cannot be answered until the coals are compared with the Eastern Canadian Carboniferous counterparts. Data on the distribution of oxygen functional groups may provide a basis for understanding these anomalies.

The paucity of information on the distribution of oxygen in coals of Alberta and other parts of Canada prompted this

study. In addition, reliable data for freshly mined coals will provide a better understanding of the role of oxygen functional groups in coal processing, conversion and utilization. Much of what is inferred about the role of O-functional groups in coal reflects observations on the impact of weathering on coal properties. The same groups that already exist in the fresh coals are more abundant in the weathered coals. For example, in processing coals, surface properties are important and these are affected by O-bearing functional groups. Knowledge of the distribution of oxygen groups in Canadian coals is important to coal utilization engineers and geologists as well as to coal chemists.

1.1 The Impact of Oxygen on the Surface Properties of Coals

Cleaning or selective removal of impurities from coals is commonly necessary to meet market specifications. The cleaning process exploits differences in the properties of coal and associated impurities, and is most often based on differences in specific gravity. However, as the particles become finer, specific gravity differences are progressively overshadowed by surface properties which, in turn, are largely influenced by the distribution of oxygen functional groups.

These groups govern many behavioural facets of coal fines by conferring polar characteristics on the coal. The polar groups, especially -OH, are centers for facilitating H-bonding of sorbates such as alcohols and H_2O (Kini et al., 1956). The efficiency of such processes as oil agglomeration and flotation,

which involve interaction of coal surfaces with nonpolar oils, is primarily dependent on the relative hydrophobicities of the coal surfaces. The deterioration of oil-agglomerating properties has thus been attributed to carboxyl groups and, to a lesser extent, to hydroxyl groups (Du Plessis et al., 1985).

Flotation depends on interaction of coal particle surfaces with air bubbles. Collectors, conditioners and other surface active agents are normally used to enhance differences in hydrophobicity between coal and gangue particles. The presence of oxidized coal particles, even in small quantities, has been shown to significantly influence coal flotability (Somasundaran, 1988). Large differences in surface properties of floated and sedimented coals were shown by infrared spectroscopy (Angle et al., 1988) to be associated with oxygen functional groups.

In both flotation and agglomeration, the wettability of the coal is important. The oxygen functional groups have been tied to wettability characteristics (Murata, 1982). A shift of wetting tension, measured by a film flotation technique which uses alcohol to change the surface tension of the continuous phase, is found along with differences between oxidized and nonoxidized coals. This provides a quantifiable measure of changes in surface energy induced by increased oxygen functional groups (Fuerstenau et al., 1987). Interaction of organically bound oxygen with solvents is strong and causes the coals to swell and heat up as well (Attar & Hendrikson, 1982).

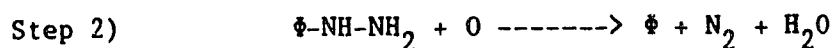
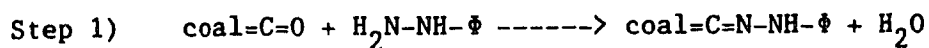
There is no doubt that moisture in coals would cause difficulties in all surface-dependent processes, including

preparing high-calorific coals for market. Drying coals with high oxygen contents is more difficult than drying coals with low oxygen contents (Attar & Hendrikson, 1982). Adsorption of moisture as influenced by oxygen functional groups was observed in the early 40's and was later reiterated by Schafer (1972) for low rank Australian coals, then by Tartarelli & Belli (1985) for European coals. Schafer (1979) correlated moisture adsorption with carboxyl content and showed that the cationic forms of the carboxyl groups retained higher moisture. The higher valence cations retained more moisture. Charge characteristics of coals have also been attributed to polar groups (Angle & Hamza, 1983).

Variability in the distribution of different oxygen functionalities has contributed to the relative heterogeneity of the populations of finely charged particles. These charges confer stability on suspended fine coal particles in a washery (Angle & Hamza, 1983). Selective adsorption of polymeric flocculants was shown to depend on the charges of these coal fines (Angle & Hamza, 1987). In the search for evidence of selectivity in the cleaning of coals, the clean and raw feed coals were removed from a pilot washery operation and compared using electrokinetics and Fourier Transform Infrared Spectroscopy. Definitive differences in the clean and raw coals were shown by the different band intensities of oxygen functional groups and also by charges conferred by these functional groups on the coal particles (Angle et al., 1985). The clean coals showed lower intensities in the 1700cm^{-1} bands assigned to -COOH , than the raw coals, and at the same time were less negatively charged and more hydrophobic.

addition of excess sodium hydroxide which converts the ammonium ion to ammonia that can be neutralized by distilling it into a saturated boric acid solution; and the borate is titrated against standard HCl. With coal, converting the N in oxime to NH_4^+ may produce erroneous results if the former forms N_2 . Refinements of this procedure via new designs of instrumentation overcome some of the difficulties (Harris & Kratochvil, 1981). As in any multistep reaction in quantitative analysis, accumulated experimental errors can be expected.

Satisfactory results were obtained (Ihnatowicz, 1952; Blom et al. 1957) by determining coal-carbonyl via a reaction with phenylhydrazine in sodium acetate at 90°C.



Step 2 is accomplished by an oxidizing agent such as Fehling's solution. Nitrogen in the reaction product was determined by volumetric analysis.

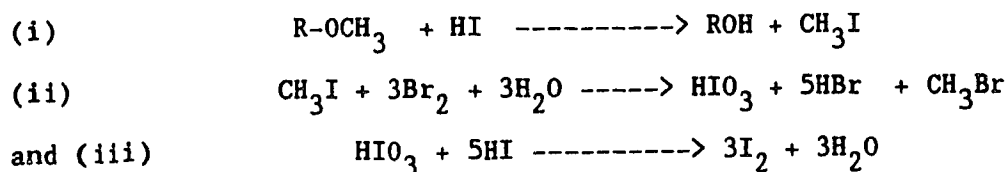
Other reactions involve reduction of carbonyl by titanous chloride (Blom et al. 1957). Specific reactions of ketonic carbonyl with dinitrophenyl hydrazine have been also used (Kroger et al., 1965). Detailed accounts of several other, not commonly used, wet methods of analysis have been described by van Krevelen (1961).

Carbonyl-oxygen has also been studied by FTIR spectroscopy, and some success has been achieved in comparative studies. Painter et al. (1981) as well as Bouman & Freriks (1980) observed the changes in intensity of the 1600cm^{-1} peak during coal oxidation. The former found no change during oxidation at 100°C but the latter noted quite pronounced intensity increases. On the other hand, Tooke & Grint (1983), using British coals, found that deoxygenation (via pyrolysis in nitrogen) caused the intensity of 3300cm^{-1} -OH band to increase while diminishing the 1600cm^{-1} (=CO) band. There is still much controversy over assignments to the 1600cm^{-1} peak (Painter et al., 1981a). Earlier, Ignasiak et al. (1972) had strongly disagreed with the carbonyl assignment because their results showed increased intensity of the 1600cm^{-1} peak with phenolic -OH increases, not with carbonyl. Data obtained quantitatively or qualitatively by FTIR should be treated with caution for this region. Good analytical data via wet chemistry should be obtained for comparison with such data.

Other Functional Groups

Estimation of all oxygen groups which are not considered reactive are normally lumped together and are calculated by difference from total oxygen determined by indirect or direct methods. Reactive peroxides, which are relatively unstable, only occur in weathering coals. They are described as "interim forms" (in which two adjacent carbons bond), prior to dissociation, to water and carbon oxides. They are often described in mechanistic pathways of coal oxidation (Berkowitz, 1989).

Other groups are methoxyl $\text{O}-\text{CH}_3$, ethers, furans and pyrans which are considered unreactive in nature, and so there are limited analytical methods available. Methoxyl may be an exception and can be measured by the Zeisl method (Blom et al., 1957) which entails



Iodometric titration against sodium thiosulphate is then used to determine the iodine concentration.

There are many ether forms, and analysis of ether-oxygen in coal has not been convincingly proven. The methods used most often are cleavage of ether by HI at 135°C in KOH and acetylating the $-\text{OH}$ formed (Bhaumik et al., 1962); or reduction by sodium in liquid ammonia (Takegami et al., 1964; Kroger et al., 1964; Lazarova & Angelova, 1968)

Most of these methods have inherent deficiencies. For example HI does not react with diaryl ethers; Na in liquid ammonia will cleave diaryl but not dialkyl ethers. There are also several complex side reactions (Berkowitz, 1989).

2.3 Methods Selected

The present work undertaken, involves measurement of the three reactive O -bearing functional groups. Based on this review, wet analytical methods are used. In addition, the

concentrations are presented as a fraction of the total oxygen determined by difference from the elemental analyses. FTIR-PAS is used only as a qualitative check on completion of the reaction.

CHAPTER 3

EXPERIMENTAL

3.1 Choice of Coal Samples

It has been recognized by many workers that differences in coal reactivity pertaining to combustion, solvent extraction, liquefaction and beneficiation processes cannot be attributed to rank dependency alone (Given, 1960; Berkowitz, 1979; Attar, 1982). This fact and the importance of depositional and metamorphic histories on coal properties (Raj, 1976; Abdel-Baset et al., 1978; Chafee et al., 1981; Given, 1984) determined the choice of coals.

The ten coals selected were of different ranks and geological history, and represented Tertiary, Cretaceous and Carboniferous coals. The samples were drawn from the sample bank of the coal conversion laboratory, Department of Mining, Metallurgical and Petroleum Engineering, University of Alberta. The exception is coal #20 which was obtained from Cardinal River Mines Ltd. The coals are identified in Table 1 which summarizes the geographic location, geological age, and rank. Their elemental and petrographic analyses are shown in Table 2.

The five subbituminous Upper Cretaceous/Tertiary coals (#2, #4, #7, #9, #11) were sampled from locations a few hundred kilometers apart and chosen to represent coals with broadly similar diagenetic and geochemical histories. One L. Paleocene (Tertiary) lignite (#1) was obtained from Saskatchewan and represented the lowest rank coal of this suite. The U.

Table 1. Identification, Source and Rank of Coals

Coal	Geological Era Formation	Location	(ASTM) Rank
1	L. Paleocene Ravens Craig Fm.	Estevan, Sask.	lignite A
2	U. Cretaceous, L. Horseshoe Canyon Fm.	Castor- Battle River, Alta.	subbit. C
4	U. Cretaceous, Horseshoe Canyon Fm.	Drumheller, Alta.	subbit. C
7	U. Cretaceous, Scollard member Paskapoo Fm.	Highvale Mine, Wabamun, Alta.	subbit. B
9	U. Cretaceous, L. Horseshoe Canyon Fm.	South Tofield, Alta.	subbit. C
10	U. Cretaceous / Tertiary , Paskapoo Fm.	Obed Marsh, Obed, Alta.	hvb
11	U. Cretaceous, L. Horseshoe Canyon Fm.	Vesta Mine, Sheerness, Alta.	subbit. C
14	L. Carboniferous (Pennsylvanian)	Lingan Mine, Cape Breton, N.S.	hvb
16	L. Carboniferous (Pennsylvanian)	Phalen Mine, Cape Breton, N.S.	hvb
20	U. Cretaceous / Tertiary	Cardinal River Mine, Cardinal River, Alta.	mvb

Table 2 Description of original coal characteristics

Coal	Petrographic Analysis ^{a,c}				Ultimate Analysis (daf) ^b				
	Vitrinite %	Exinite Liptinite %	Inertinite %	Vitrinite Reflectance	%C	%H	%N	%S	%O
1					73.4	5.0	2.1	0.6	18.9
2	93.2	0.4	6.4	0.47±0.04	74.9	5.1	1.4	0.6	18.0
4	93.0	2.2	3.2						
7	74.6	2.1	23.3	0.48±0.04	75.9	4.6	1.0	1.1	17.4
9	92.0	4.0	3.0	0.42±0.04	75.2	5.0	1.5	0.6	17.7
10	92.0	4.5	3.0		74.8	4.2	1.8	0.3	18.9
11	73.3	0.3	26.3	0.43±0.04	75.4	5.1	1.4	0.6	17.5
14	85.1	5.7	5.9		85.5	5.4	1.6	2.6	4.9
16	90.4	3.8	4.0		84.8	5.2	1.5	0.9	7.6

^{a, b} Taken from Berkowitz et al. (1988).

^b Coals 14, 16 taken from G. Koropchuk MSc Thesis, U of A, 1989.

^c Petrographic Analyses of coals 4, 10, 14, and 16 were generously performed by Ken Pratt, ISPG, Calgary, Alberta.

Cretaceous/Tertiary hvb and mvb coals (#10 and #20) from the Foothills and Mountain Regions of Alberta were selected as examples of Western Canadian bituminous coals for comparison with Carboniferous Eastern Canadian coals of similar rank. The latter (#14 and #16) were obtained from Cape Breton (Nova Scotia) and may be similar to those studied by Blom et al. (1957).

3.2 Sampling

The crushed coals were stored with excess moisture in sealed polythene bags at -10°C . Aliquots of these samples, each about 300 grams, were removed as required and partly dried in a desiccator in vacuo at room temperature. Before opening, the desiccator was purged with nitrogen gas. The crushed coals were then ground to -200 mesh (Tyler) using a Retzch pulverizer. Previous studies (Ruberto & Cronauer, 1978) showed that this size was optimum for the chosen methods of analysis. Since the coal was fairly moist and the samples were small, grinding required only about 10 seconds, and air oxidation of the samples was therefore minimal. The prepared samples were then quickly removed and stored under CO_2 in amber-colored bottles.

Before further use, the coals were riffled in a nitrogen filled glove bag, split into 50g portions, and transferred to polyethylene bottles, covered with de-ionized water, sealed in heat-sealed Kapak pouches (originally designed for food storage) which had been purged with ultrahigh pure (UHP) nitrogen, and subsequently frozen until needed further. This procedure

preserved the chemistry of the fresh coals until further analysis.

3.3 Apparatus and Instrumentation

The following equipment and instrumentation were used in this work:

Fisher Model AE 160 Analytical balance; Leco CHN-600 Elemental Analyser; Fisher Model 490 Coal Analyzer; Fisher Isotemp vacuum oven Model 281A; Perkin Elmer TGS-2/TADS System; CANMET/CRL Automatic Titration System for solids and liquids; Bruker 113V-PAR Fourier Transform Infrared Spectrometer with Photoacoustic Cell (EG&G Princeton); Fisher Thermolyne Combustion Tube Furnace; Retzch Pulverizer by Brinkman; Fisher Magnetic Stirrer; Millipore RO-20 and Milli-Q Water System. The Condenser assembly is shown in Fig. 1.

3.4 Materials

All chemicals were ACS grade and were obtained from Fisher Scientific. The Amberlite Rexyn IR-120 H ion exchange resin was obtained from Aldrich Chemicals. Details pertaining to the chemicals and supplies are set out in Appendix 5. Water used in this work was purified by a MillRO-20 and Milli-Q water purification system made by Millipore Corp. All solutions were prepared with degassed water which was either boiled or sonicated to eliminate dissolved carbon dioxide. Sodium hydroxide solutions (0.05M) were made from pellets and standardized against

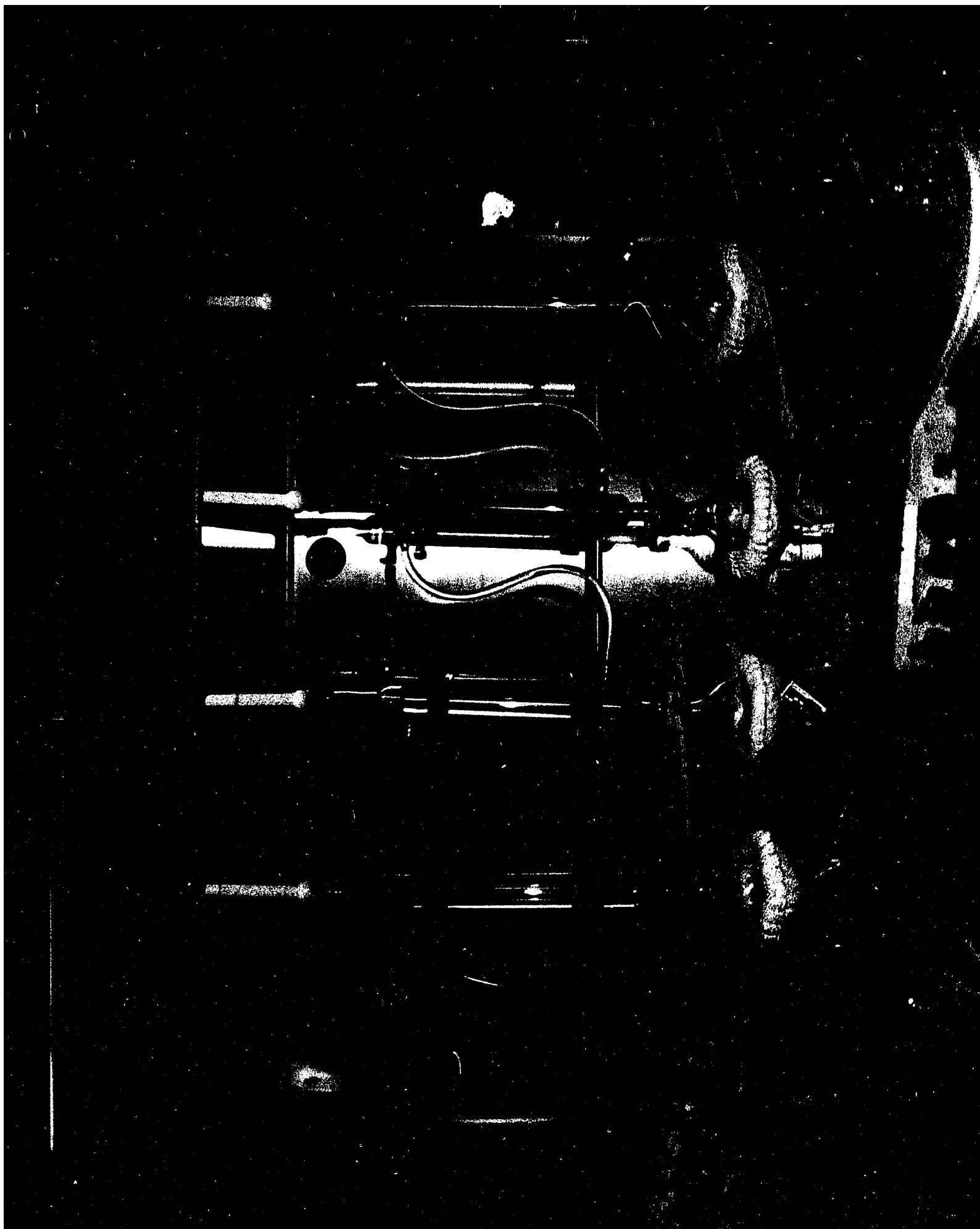


Fig.1. Photograph of apparatus for refluxed reactions.

potassium hydrogen phthalate as primary standard. Buffer solutions of pH 7.0, 8.0, and 4.0 were phosphate-based (See section 3.7.1 to follow).

3.5 Protonation

Pretreatment with concentrated hydrochloric acid as a required step in the determination of oxygen containing functional groups in coal has been emphasized by earlier workers (Ruberto & Cronauer 1978). Such pretreatment ensures that salts are absent and that oxygen functional groups are in the free protonated form. Ruberto and Cronauer's work on lignites demonstrated that higher carboxylic acid concentrations are recorded with HCl-pretreated samples.

Protonation was carried out by mixing 30 grams of coal with 300ml 2M HCl in a 500ml beaker covered with parafilm, and then magnetically stirring the slurry gently for approximately 12 hours (i.e overnight). After acidification, the coal was filtered on 7cm #42 Whatman hardened ashless filter papers in 7cm disposable Buchner funnels. The solids were washed with (18M Ω resistivity) purified water until chloride-free washings were recorded by silver nitrate.

The clean coal was placed in an oven which was then evacuated and repeatedly purged with ultra high purity nitrogen, and finally dried in vacuo at 70°C or 100°C for 20hrs. If there was too much moisture in the coal, spluttering would occur at 100°C, and in such cases 70°C was chosen. In some cases, drying at 70°C was followed by drying at 100°C in order to observe

possible differences in functional group composition after different drying histories.

The dried samples were placed in vials which were purged with UHP nitrogen, and sealed in nitrogen-filled Kapak thermo-seal pouches. The sealed pouches were then stored at -10°C . During the subsequent analyses, the coal powders were kept in UHP nitrogen-purged desiccators. After all analyses were completed, the samples were resealed in N_2 -filled Kapak pouches and refrozen for storage.

3.6 Mild Pyrolysis

3.6.1 Slow Heating

For thermal stability studies, the protonated samples were heated in a stream of UHP nitrogen (8cc/min) in a Fisher Scientific 281A Isotemp Vacuum Oven. The oven was first repeatedly (3-4 volume changes) purged with UHP nitrogen and then set to specific temperatures (100°C , 200°C , or 300°C) as desired. Heating to the selected temperature took about 1.5h. The heating rates were approximated as $3.5^{\circ}\text{C}/\text{min}$ to 100°C , $3.8^{\circ}\text{C}/\text{min}$ to 200°C , and $3.4^{\circ}\text{C}/\text{min}$ to 300°C . Samples were held at 100°C for 20h, at 200°C for 20h and at 300°C for 0.5h. These periods were deemed sufficient for attainment of equilibria. Several coals were usually run simultaneously, with nitrogen flowing at 8 cc/min.

At the end of the heating period, the samples were allowed to cool to room temperature in flowing nitrogen over some

6h-8h. The cooled samples were then placed in Kapak heat-seal pouches that were purged, filled with nitrogen and heat-sealed.

3.6.2 Fast Heating

In order to observe the effects of fast heating on the thermal stability of $-COOH$, a tube furnace preheated to $200^{\circ}C$ or $300^{\circ}C$, was used. A constant stream of UHP nitrogen was maintained at 12 cc/min. Up to 3 gm of protonated coal in a ceramic crucible was pushed into the mid-third of the furnace from the downstream end of the tube, and the temperature in this zone was recorded by a thermocouple and a digital thermometer. Temperature rises due to exothermicity were prevented by increasing the flow rate of the nitrogen gas.

Final temperatures were maintained for exactly 0.5 hr, after which the boat was pulled out and the coal transferred to nitrogen-filled glass bottles that were quickly placed in a desiccator and rapidly cooled to room temperature by a fast stream of N_2 . (Cooling took approximately 0.5h). The samples were then analysed for $[-COOH]$ by the methods described in the following sections.

3.7 Wet Chemical Methods

The distribution of oxygen in three oxygen-containing functional groups was determined by measuring the concentrations of carboxyl ($-COOH$), carbonyl ($=CO$), and hydroxyl ($-OH$), the last of which is mainly present in coal in phenolic form. In order to present the data on a dry ash free basis (daf), all samples were

subjected to proximate analyses. All measurements of O-bearing functional groups were replicated two or more times. When different batches of the same coal were replicated, the measurements were averaged after a standard Q-test and the standard deviations were pooled. The timetable for the different analyses is presented in the form of a flow chart in Appendix 6.

3.7.1 Automatic Potentiometric Titrimetry

All titrations were performed with an automatic potentiometric titration system developed at CANMET and described by Angle et al. (1988). The sampling system is shown schematically in Fig. 2. Liquids to be titrated were degassed with UHP nitrogen for 10 minutes, then titrated with .05M NaOH. The pH versus volume of titrant was continuously measured and stored by the computer. The equivalence point was calculated from the volume of titrant at the maximum of the first derivative plot and this volume was used in the calculations. NaOH was standardized against potassium hydrogen phthalate (Harris & Kratochvil, 1981). The sensing pH electrode was glass with a silver/silver chloride reference electrode.

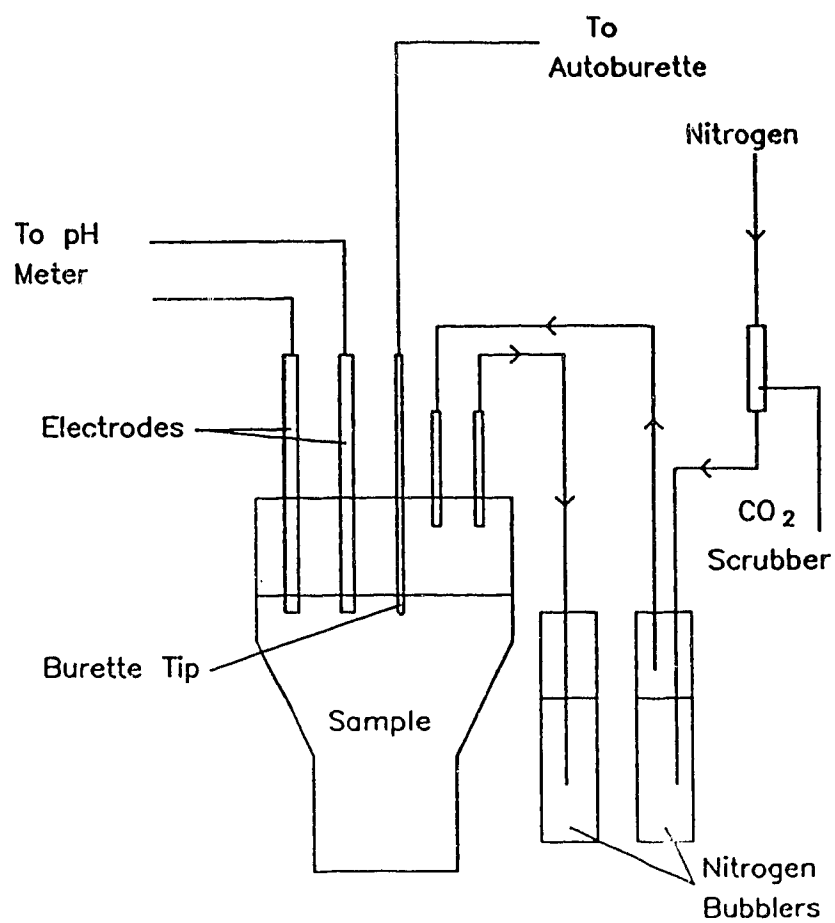
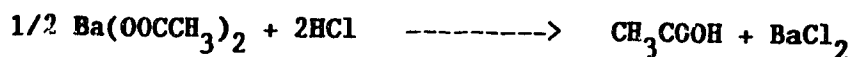
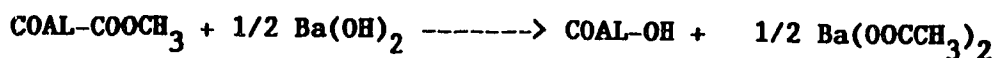
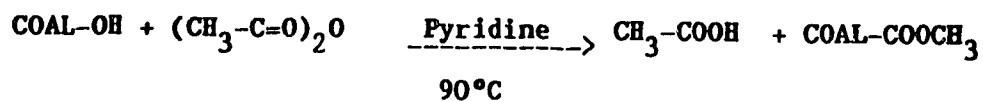


Fig. 2. Sampling apparatus of Automatic Titration

3.7.2 Analysis of [O] in Hydroxyl Groups

Analysis of oxygen in -OH can be represented by



These analyses are described in three steps: coal acetylation, hydrolysis of acetylated coal, and analysis of the hydrolysate.

Quantitative determination of [-OH] was carried out by a modification of the procedure developed by Blom et al. (1957). Ion exchange was used instead of distillation to obtain the equivalent acetic acid (Hatami et al., 1967; Takeya et al., 1965), and [CH₃COOH] was automatically titrated potentiometrically. The time frame of the reactions is detailed in a flow chart in Appendix 5.

The protonated coals were first acetylated by refluxing 1.0 gram of coal in 30ml of 1:2 acetic anhydride and pyridine for 20 hours. After refluxing, 200ml of de-ionized water was slowly added to the cooled reaction mixture. After cooling to room temperature, the acetylated coal was filtered on Whatman #42 hardened ashless filter paper, washed with de-ionized water until free of acid (by pH measurement) and pyridine (by odor). All filtrates were discarded, and the clean acetylated coal was dried

in an oxygen-free evacuated oven at 100°C for 20 hours. This treatment was earlier proved to be adequate for removal of tenaciously held pyridine from coal (Liotta, 1979; Collins et al., 1976).

Precisely 0.3 g of the acetylated coal was wetted with a few drops of methanol, and 2 g of barium hydroxide added to the coal in a 250ml round bottom flask. Thereafter, 40ml of de-ionized water was added with some teflon boiling stones. The acetylated coals were hydrolysed by refluxing for 20 hours at low heat. The condenser assembly is shown in Fig. 1.

After hydrolysis, the mixture was filtered on #50 5cm Whatman hardened ashless filter paper. The solids were washed with de-ionized water and the filtrate was quantitatively transferred to a 200ml volumetric flask which was made up to volume with the washings. The solids were again dried in vacuo at 100°C. Both the acetylated and hydrolysed coals were qualitatively analysed by FTIR-PAS to check completion of the reactions (see Sec. 3.10).

The barium acetate contained in the filtrate was converted to acetic acid by exchanging 50ml aliquots of the filtrate on an ion exchange column made up of Amberlite IR 120 (type H) Rexyn resin. The eluent (250 ml) was titrated as previously outlined, and oxygen in [-OH] was calculated (Blom et al., 1957; Hatami et al., 1967; Takeya et al., 1965) from

$$[O_{OH}] = \frac{4x(X_t - X_b) \times F}{S - 4x42(X_t - X_b)}$$

where

Xt = millimoles of titrant at equivalence point

Xb = millimoles of blank

4 = 200ml/50ml i.e. four runs per sample of exchangeable barium acetate.

42 = Mol.wt of acetylated coal- Mol. wt of original coal.

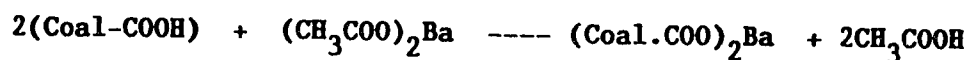
= Coal-(00CCH₃) - Coal-OH = 12x2 + 16x2 + 1x3 - 16 - 1

F = 16x100x1/(100 - %H₂O - %Ash)

S = Weight of acetylated coal in grams.

3.7.3 Analysis of [O] in Carboxylic Acid Groups

Carboxyl protons are exchanged with barium in barium acetate, thus liberating free acetic acid which is then titrated.



Carboxyl (-COOH) groups were determined by a modification of Schaffner's method, which is itself an adaptation of classical methods that employed calcium acetate instead of barium acetate. A similar procedure was also used by Takeya et al. (1965) and Hatami et al. (1967) in studies of Japanese coals. The optimum reaction time of 67h, as determined by Takeuchi & Berkowitz (1988) for Canadian coals, was adopted, and further refinements included automated titrimetry for determination of the acid content (Angle et al., 1988).

0.3 gm aliquots of the protonated coals were weighed out on a Fisher model AE160 analytical balance, and transferred to a

150 ml polyethylene Erlenmeyer flask in order to avoid dissolution of -OH groups in glass flasks. To aid wetting of the coal, a few drops of methanol were introduced and then 100ml of barium acetate (15.333g/l; pH=8.25) were added to the coal. Air in the flask was replaced by UHP nitrogen, and the flask sealed, gently swirled, and allowed to stand for 67 hours. During this time, the flask was intermittently swirled by hand.

Following completion of the reaction, the solids were filtered on Whatman #50 ashless filter paper, washed with barium acetate and then with de-ionized water. Care was taken to avoid dilution of the buffered filtrate in order to avoid barium hydroxide precipitation. The washed filtrate was quantitatively transferred to a 150ml flask, and acetic acid titrated as outlined in Section 3.7.1. All protonated coal samples were barium acetate exchanged in duplicates or more as required. A control barium acetate solution was treated like the coal samples and its titrant volume was used to calculate the millimole value of the blank which was subsequently subtracted from the sample data.

Oxygen in [-COOH] was calculated by

$$[O_{COOH}] = \frac{(X_t - X_b) \times 32 \times 0.1}{M}$$

where

X_t = millimoles of titrant at equivalence point

X_b = millimoles of titrant of blank

M = grams of daf coal

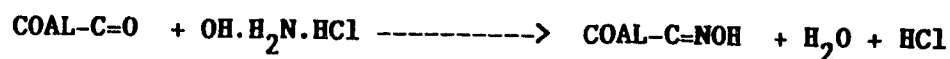
32 = 2 x the atomic weight of oxygen

0.1 = 100 / 1000, for conversion to %

and is reported on a dry ash free basis (daf).

3.7.4 Analysis of [O] in Carbonyl Groups

Carbonyl was determined by the classical method developed by Blom et al (1957) and summarized by Van Krevelen (1961). This method takes advantage of the reaction between =CO and hydroxylamine to form the corresponding oxime. The success of this reaction was confirmed by FTIR-PAS (see Sec. 3.10 and Appendix 4).



0.7g aliquots of the protonated coals were weighed into 250ml round bottom flasks, 1.0 g of hydroxylamine hydrochloride added, and 15ml pyridine was introduced. Teflon boiling chips (10 pieces) were added, and the mixture was swirled gently to dissolve the hydroxylamine hydrochloride before refluxing at low heat. Refluxing proceeded for 20 hours at a gentle boil.

After refluxing, the mixture was cooled to room temperature and 40ml water added under swirling. Concentrated HCl (18ml) was then added slowly to avoid heating by this exothermic reaction. The reaction mixture was allowed to cool and coal was filtered off on Whatman #42 ashless filter paper. The coal was repeatedly washed with de-ionized water until free of pyridine and the pH was the same as that of de-ionized water. The sample was dried at 100°C for 20hr in vacuo.

The dried coals were analysed, for nitrogen, using a Leco CHN analyser. Controls (without hydroxylamine hydrochloride) were run simultaneously. The increase in nitrogen content of the coal is directly related to the original carbonyl concentration in the coal and was calculated by subtracting the nitrogen content of the control from that of the sample. [O] in =CO was calculated from

$$[\text{O}_{\text{CO}}] = \frac{16 (\text{N}' - \text{N}) \times F}{14 \times 100}$$

N' = nitrogen in oximated coal

N = nitrogen in the control

F = $1/(100 - \% \text{H}_2\text{O} - \% \text{ash})$

16 = atomic weight of oxygen

14 = atomic weight of nitrogen

In all cases the controls gave the same result as the original protonated coals.

3.8 Carbon, Hydrogen and Nitrogen (CHN) Analyses

C, H, and N analyses were determined with a LECO CHN-600 Analyser. The equipment was calibrated for C and N by ξ - dosing, and for H by burning standard sugars. All coal samples were analysed in triplicate or more (as necessary for rechecking the data). [O] was determined "by difference" and %S was assumed

to be negligible. All data was reported on a dry ash free basis (daf).

3.9 Proximate Analyses

Proximate analyses followed ASTM Standards D3172 and D3173. Where ample sample was available, a Fisher Model 490 Coal Analyser was used; otherwise a Perkin Elmer TGS-2 thermogravimetric system linked to a TADS data station was used. The latter method was more suitable for the mildly pyrolyzed coal samples. Comparative tests of the two methods showed them to furnish substantially identical results.

3.10 Fourier Transform Infrared using Photoacoustic

Spectroscopy (FTIR-PAS)

As indicated in Chapter 2, this method is now fairly widely used for surface characterization of coals and in this study provided qualitative checks on quantitative determination of oxygen in reactive functional groups. All protonated coals and their analytical derivatives were analysed by Fourier Transform Infrared Spectroscopy to corroborate that reactions had, in fact, gone to completion. The technique was also applied to samples which had been subjected to heat treatment.

A Bruker 113V-PAR model spectrometer and an EG&G Princeton model PAS cell which accommodated about 25mg of coal were used. In this technique, the spectra were recorded under nitrogen (see Sec. 2.2.2.1, Chapter 2). Spectra were collected over the range 4000cm^{-1} to 400cm^{-1} at a resolution of 4 cm^{-1} and

averaged from ten files of 250 scans per file. All samples were ratioed against a Fisher carbon lampblack reference powder.

CHAPTER 4

RESULTS AND DISCUSSION-I: DISTRIBUTION OF OXYGEN FUNCTIONAL GROUPS

4.1 Introduction

Data on the distribution of oxygen in functional groups are presented in two formats. The first shows the concentration of oxygen in each functional group ($[O_{OH}]$, $[O_{CO}]$, and $[O_{COOH}]$) expressed as a weight percentage of the coal mass (Table 3). The second shows the concentration of oxygen in each functional group as a percentage of the total oxygen in the coal ($[O_{OH}]/[O]$, $[O_{CO}]/[O]$ and $[O_{COOH}]/[O]$), (Table 4). Detailed data are presented in Tables 1-10, Appendix 1. Total oxygen $[O]$ was determined "by difference" from elemental analyses and is shown in Tables 1-10, Appendix 2. All values are presented on a dry ash free (daf) basis. The required proximate analyses are summarized in Appendix 3.

Data encompass Alberta Upper Cretaceous/Tertiary subbituminous coals of the Plains (#'s 2,7,9,11) and higher ranked (hvb and mvb) U. Cretaceous coals of the Foothills (#10) and Mountain Regions (#20) respectively. The lignite (#1) was from Estevan, Saskatchewan. Tables 3 & 4 present summaries of average concentrations of oxygen in O-bearing functional groups, measured after drying at 70°C and /or 100°C (see Appendix 1 for details), along with %C and $[O]$. Tables 3 & 4 show pooled standard deviations from the mean of replicates. The larger

**Table 3 Weight Percentage Oxygen in O-bearing functional groups
in coal dried in vacuo, 70°C - 100°C** for 20 hrs .**

Coal	[O] ^b	[OOH]	[OCO]	[OCOOH]	[Ores] ^a	[C]
1	22.4±0.5	8.5±0.1	4.3±0.0	4.0±0.1	5.6±0.5	70.6±0.4
2	22.0±0.9	10.4±0.6	4.7±0.3	3.2±0.3	3.7±0.4	70.7±1.5
4	21.4±0.7	9.2±0.6	4.1±0.1	2.4±0.0	5.7±0.2	71.4±0.2
9	20.8±1.0	8.5±0.1	4.4±0.2	3.1±0.1	4.8±1.0	71.9±0.1
11	21.0±0.3	10.0±0.0	3.5±0.1	2.7±0.4	4.8±0.0	72.5±2.1
7	19.8±0.8	8.8±0.2	3.6±0.4	3.5±0.1	3.9±0.1	73.7±1.1
10	17.1±0.4	8.5±0.5	3.5±0.4	1.2±0.3	3.9±0.0	75.6±0.4
16	9.3±0.7	5.2±0.5	1.1±0.2	0.1±0.0	2.9±0.4	82.5±0.2
14	9.8±0.5	3.2±0.3	1.4±0.2	0.3±0.0	4.9±0.4	82.7±0.5
20	6.9±0.5	1.1±0.0	0.01±0.0	0.3±0.0	5.5±0.4	87.2±1.3

** Original data (coals dried at 70 - 100°C) for each group were averaged and standard deviations pooled.

a. $\%[\text{Ores}] = \%[\text{O}] - (\%[\text{OOH}] + \%[\text{OCO}] + \%[\text{OCOOH}])$.

b. $\%[\text{O}] \cong 100 - \%[\text{C} + \text{H} + \text{N}]$.

Standard deviations less than ± 0.05 are rounded to ± 0.0 .

Table 4 Weight Percentage of Oxygen in O-bearing functional groups as a fraction of total oxygen in daf coal (dried in vacuo, 70°C - 100°C for 20 hrs) .**

Coal	[O] ^a	$\frac{[\text{O}^{\text{H}}]}{[\text{O}]}$	$\frac{[\text{O}^{\text{CO}}]}{[\text{O}]}$	$\frac{[\text{O}^{\text{COOH}}]}{[\text{O}]}$	$\frac{[\text{O}^{\text{res}}]}{[\text{O}]}$	% C	% S ^b
1	22.4 ± 0.4	38.0 ± 0.8	19.2 ± 0.4	17.9 ± 0.5	25.0 ± 2.5	70.6 ± 0.4	0.6
2	22.0 ± 0.9	47.4 ± 3.3	21.4 ± 1.5	14.5 ± 1.4	16.8 ± 1.8	70.7 ± 1.5	0.6
4	21.4 ± 0.7	43.0 ± 3.2	19.1 ± 0.8	11.2 ± 0.3	26.7 ± 2.1	71.4 ± 0.2	0.6
9	20.8 ± 1.0	40.9 ± 2.0	21.2 ± 1.5	14.9 ± 0.9	23.1 ± 4.8	71.9 ± 0.1	0.6
11	21.0 ± 0.3	47.7 ± 1.0	16.7 ± 0.5	12.9 ± 1.9	22.7 ± 0.4	72.5 ± 2.1	0.6
7	19.8 ± 0.8	44.4 ± 2.0	18.2 ± 2.2	17.7 ± 0.8	19.7 ± 1.0	73.7 ± 1.1	1.0
10	17.1 ± 0.4	49.7 ± 3.0	20.5 ± 2.0	7.0 ± 1.8	22.8 ± 0.5	75.6 ± 0.4	0.3
16*	9.3 ± 0.7 (8.4)	55.9 ± 6.7 (61.9)	11.8 ± 2.4 (15.1)	1.1 ± 0.1 (1.2)	31.2 ± 5.3 (23.8)	82.5 ± 0.2	0.9
14*	9.8 ± 0.5 (7.3)	32.7 ± 3.6 (43.8)	14.3 ± 2.1 (19.2)	3.1 ± 0.2 (4.1)	49.9 ± 4.5 (32)	82.7 ± 0.5	2.5
20	6.9 ± 0.5	16.1 ± 1.1	0.2 ± 0.0	4.4 ± 0.3	79.4 ± 10.0	87.2 ± 1.3	

a. $\%[\text{O}] \approx 100 - \%[\text{C} + \text{H} + \text{N}]$.

b. Approximate sulfur content based on Table 2, Chapt 3 (literature values).

c. $[\text{O}^{\text{res}}] = \%[\text{O}] - (\%[\text{OOH}] + \%[\text{OCO}] + \%[\text{O}^{\text{COOH}}])$

* Eastern Canadian coals bracketed values are for $\%[\text{O}] \approx 100 - \%[\text{C} + \text{H} + \text{N} + \text{S}]$.

** Average values of 70°C and 100°C data, standard error pooled.

standard deviations, especially in %C are indicative of sampling errors of different batches of coal mass taken from the same location. Fig.3 shows $[O_x]$ versus $[O]$ (where x is the O-bearing functional group) and Fig.4 shows plots of $[O_x]/[O]$ versus $[O]$ for all coals. Fig.5 shows regression lines of $[O_x]$ versus %C. For direct comparison with Fig. 6a which shows $[O_x]$ versus %C as reported for European Carboniferous coals (Blom et al., 1957), Fig.6b presents the data of Fig.5 plotted cumulatively.

4.2. Trends of Oxygen-Bearing Functional Group Concentrations

Clear trends emerge from either data set, with concentrations of O-bearing functional groups falling into the sequence

$$[O_{OH}] > [O_{CO}] > [O_{COOH}].$$

The one exception was #20 (mvp) for which

$$[O_{OH}] > [O_{COOH}] > [O_{CO}].$$

Possible reasons for this deviation are discussed in section 4.3.

Fig.3 illustrates these trends. As $[O]$ increases, $[O_{OH}]$, $[O_{CO}]$ and $[O_{COOH}]$ increase linearly, and least square regression lines can be fitted to the data. The slopes of these lines correspond with the above trend. The greatest slope corresponds to $[O_{OH}]$ versus $[O]$, and the smallest slope relates to $[O_{COOH}]$. The linear equations for the O-bearing groups are

It is from such observations that inferences have been drawn about the role of O-bearing functional groups in fresh coals. Such inferences tend to be validated by the fact that concentrations of acidic functional groups (-OH, -COOH) decrease with increasing rank and coal surfaces change slowly from hydrophilic to hydrophobic. Of course, in weathered coals this hydrophilicity is increased along with O-bearing functional group concentrations.

1.2 The Significance of Oxygen in Conversion Processes

Whereas surface related processes leave the coals relatively intact and easy linkages can be made to oxidation of the coal, conversion processes such as liquefaction and pyrolysis degrade the coal material depending on the conditions and severity (Whitehurst, 1978). The material left after conversion consists of a mixture of the coal extract and a solid char which does not resemble the original coal (Neavel, 1981).

Observations on oxygen contents and inferences respecting its influence on conversion processes have been derived from analysis of coal extracts and "model" materials (Trehella & Grint, 1988). It was shown that, generally, there is a loss of the less stable oxygen forms in conversion processes, and mostly phenolic functional forms are left in the extracts (Attar & Hendrikson, 1982). Carboxylic acids were absent from the extracts (Ruberto & Cronauer, 1978). The decreased oxygen content of coal explained by scission of ether bridges (Fisher & Eisner, 1937), has been linked to changes in solubilities in H donor solvents

(Takegami et al., 1963). Szladow & Given (1978) suggested that hydrogenolysis of hydroxyl groups occurs after ethers are depleted.

The difference in structure before and after conversion processes can be described by statistical correlations (Whitehurst, 1978; Abdel-Baset et al., 1978). In many of these processes reaction rates and temperature play a major interdependent role. The extent of conversion depends on process severity such as, rate, extent and temperature of heating.

Oxygen in the coal consumes the much needed hydrogen required for forming oils. On the other hand, oxygen in the form of OH stabilizes free radicals and so prevents recombination of small fragments into higher molecular weight species (McKeogh, 1983; Attar & Hendrikson, 1982). This occurs to a large extent with low rank coals (Zhou, Dermes & Crynes, 1984).

Low rank coals were found to differ from higher ranks in rates and the degree of conversion. With low rank coals, conversion rates are slower. Conversion occurs to a lesser extent than with higher rank coals under similar conditions (Whitehurst, 1978). Whether this is the case because of the contribution of the oxygen functionalities or to open pore structures which facilitate accessibility of reagents has not been clearly defined (Lucht, 1983). If the ability to access specific bonds in the coal matrix is a prerequisite for successful processing of coals to higher energy fuels, the exact distribution of oxygen in coal must be known (Attar & Hendrikson, 1982). The application of Attar's kinetic model of coal

liquefaction demands data on oxygen functional groups (Attar, 1978).

1.3 The Significance of Diagenetic and Metamorphic History on Oxygen in Coal

The premise that the depositional environment and geochemical prehistory influences the composition and reactivities of coals has been broadly invoked by several workers (Chafee et al., 1981 for Australian brown coals, (called lignites in North America); Given, 1984 and Raj, 1976 for USA coals; Berkowitz 1979, for Canadian coals). This influence would be more important with the lower rank, less mature coals which have not been homogenized over time, or by geothermal gradients and /or tectonism.

"Normal metamorphic development" produces a coal that depends on the geothermal gradients. It refers to the alteration of the coal through compaction, dehydration, and removal of functional groups via condensation reactions. These are caused by sustained heat flow from the earth's interior which are associated with the geothermal gradients. Gradients may vary between 10°C to 30°C per kilometer of depth. Reactions that are believed to occur are the elimination of peripheral substituent groups such as -OH, -COOH, -OCH₃ and a simultaneous increase in the molecular weight of the condensed coal product (Berkowitz, 1979). Hence the properties associated with increased rank are also as a function of depth of burial in undisturbed strata.

These properties are indicated in Hilt's rule and stem from normal metamorphism (Teichmuller & Teichmuller, 1968).

"Regional metamorphic development" of coals occurs by further changes induced by increased differential pressures and temperatures of orogeny, or indirect exposure to increased localized temperatures superimposed on geothermal gradients. Alberta's Cretaceous coals were quickly matured because of orogeny and so rank may not follow correlations with conventional "coal systematics" (see Sec. 1.4). This phenomenon per se does not tell much about the actual chemistry of the maturing processes or the coal's structure.

It has been suggested that variability in structure is directly related to the history of the coal material, based on the diagenetic pathways and metamorphic processes rather than entirely rank related (Given, 1960, 1978; Raj, 1976). Diagenesis and variability in original plant material would seem to influence the composition of low rank coals. This depends on whether the plants were highly lignified conifers and deciduous types as in the Cretaceous, or alternatively, the lower plant forms such as ferns, hedges and mosses as in the Carboniferous. The Carboniferous coals developed in tropical climates which influenced homogenization of the premordial mass (van Krevelen, 1963; Banks, 1970) prior to maturation into higher rank coals.

We can therefore tie the final coal material to the degradative path only within limits. The higher rank coals, such as anthracites, are homogenized and undifferentiated. On the other hand, the differences in sapropelic and humic coals are

clearly definitive. The former developed by putrefaction of vegetable debris in an anaerobic setting and therefore have less oxygen in their structure than the latter, which were exposed to oxygen before inundation.

In Alberta coals, earlier evidence suggested that rapid maturation of coals may also have affected the nature of the chemical reactions which occurred in metamorphic development of coals (Berkowitz et al., 1974). Therefore, shallow burial of the plains coals, contrasted with large overburden deposited on coal during regional metamorphism (that occurred in the foothills during orogeny), and the age difference between Western and Eastern Canadian coals, suggested that the distribution of O-functionalities may be dissimilar varying between regions as well as in comparison to the European coals.

1.4 Historical Perspective

Many inferences about coal behaviour are based on statistical correlations of coal properties with elemental compositions. This accumulated body of information, termed "coal systematics", in the past was based primarily on Carboniferous coals. Correlations involving oxygen were mainly derived from total oxygen contents.

Total oxygen was determined indirectly, by difference, from the elemental analysis, i.e.

$$[O] = 100\% - [C + H + N + S]\%$$

where [] means concentration in weight-percent. Total oxygen was linked to rank and used to predict related coal properties. Later, there was recognition that some of coal's reactivity can be related to the distribution of oxygen in different functional groups (Georgiadis, 1947; Ihnatowicz, 1952; Blom et al. 1957). Others seized on the notion that some properties and behaviour of coal could be explained in terms of the distribution of oxygen in the functional groups.

Extensive literature on oxygen distributions in different coals appeared. Studies on analytical determination of O-bearing functional groups on coals were developed quickly. These studies were generally performed on coals which were most conveniently located and/or were easily available to the investigator. Most of the research was based on adaptations of the methods developed previously. For example, Blom et al. modified the methods of Syskow & Kucharenko (1947) on Moscow brown coals, of Ihnatowicz (1952) on Polish coals, and Georgiadis (1952) on other European coals. These classical methods were modified in order to eliminate observed shortcomings such as reaction times, and for comparative studies of methods and coals.

Nonaqueous titration techniques for determining total acidic [-OH] were developed by Brooks & Maher (1957) working with Australian brown coals. These techniques were adapted and compared with newer methods by Maher & Schafer (1976). The distribution of oxygen-bearing groups in one form or another for coals of many parts of the world were reported in the literature. Some dealt with British "bright" coals (Brown & Wyss, 1955;

Wyss, 1956; Horton, 1958), with Indian lignites (Mazumdar et al 1957; Iyengar & Ghosh 1957), with Australian brown coals (Brooks et al., 1958; Bhaumik et al., 1962; Schafer, 1970a,1970b; Maher & Schafer, 1976), with Japanese Cretaceous coals (Hatami et al., 1967; Takeya et al. 1965), and with US coals (Given, 1962; Abdel-Basset et al., 1978). There is still a paucity of such data for Canadian coals.

From these studies, generalizations about oxygen distributions were developed. They made disproportionate use of the results of Blom et al.(1957) for vitrains of Carboniferous coals which were extrapolated further to low rank coals. These quantitative data on the concentrations of O-bearing functional groups were widely applied irrespective of the geological and geographic origins of the coals of concern.

According to these generalizations, the fraction of oxygen in -OH increases with increasing rank of the coal and reaches a maximum of 70% in coals with 85%C-86%C. Coals with more than 90%C display rapidly diminishing [-OH], and only about 30% of total oxygen exist as -OH (Horton, 1958). On the other hand, Wyss (1956) reported that [-OH] accounts for 40% of total oxygen in most coals with less than 90%C. Others claimed [-OH] ranges between 0-11% of coal mass or equivalent to about 60% of total oxygen in bituminous coals (Dryden, 1963). Phenolic -OH diminishes with increasing rank and is absent in coals with greater than 89%C (Yohe & Blodgett, 1947; Brown, 1955).

It was reported that there were no appreciable amounts of carboxyl or methoxyl groups in bituminous coals. Some of these

groups may persist in small amounts in the lower rank brown, lignitic and subbituminous coals (Dryden, 1963). In brown coals as much as 30% of the total oxygen is contained in $-COOH$, but this falls off rapidly with increasing rank. At 75%C, $[-COOH]$ amounts to 4% of total oxygen, and at higher ranks it disappears completely. It was also claimed that carbonyl oxygen accounted for about 5%-10% of total oxygen throughout a wide range as rank increases from 65%C to 90%C (Horton, 1958).

Although these concentrations were not found to be universal when data for coals from other geological eras were collected, they persisted as estimates. They were used to illustrate changing properties of coal maturing under normal metamorphism. Often the results were presented without geological history and were used as fact irrespective of the type of coals being illustrated.

1.5 Other Considerations

In hypothesizing about the role of oxygen, some of the behavioural differences between coals may also reflect the distribution in oxygen as it affects steric factors and molecular configurations which are important for reactivity. While some functional groups are integrated within ring structures others are found only peripheral to the rings or along chains. In such cases, the ease of dissociation of a proton from one peripheral group is affected by the proximity of another group. Thus, where the structural configuration affects coal chemistry, quantitative data on the oxygen distributions of

functional groups may add little to the understanding of mechanisms. Many models of coal structure have been proposed to better understand the apparent behaviour of the coals, and some of these account for spatial arrangements of O-bearing functional groups. These models represented an assemblage which portrayed some essential chemical characteristics in coal as they were then understood. Among the numerous proposed models, none was successful in accounting for the complexity in coal's behaviour. Given (1961) based his model on vitrinite rich coal at 84%C. Wender et al. (1981) and Wiser (1973) referred only to bituminous coals. At that time little information was available for low rank coals.

1.6 Approach to Study

In this study ten coals were examined. Five very similar coals were of subbituminous rank; one was a lignite; three were high volatile bituminous (hvb) coals - two of Carboniferous age (collected in Nova Scotia) and the other of Cretaceous age (collected in Alberta); and one was a medium volatile bituminous (mvb) coal collected in the Foothills region of Alberta, 50 kilometers south west from the hvb coal. These were selected because of the high reserve of low rank coals in Western Canada. The experimental data were intended to clarify relationships between this hvb coal of the Canadian Plains and their Eastern Canadian Carboniferous counterparts.

Data on the distribution of oxygen-bearing functional groups in coals of the Alberta Plains would establish the extent

to which the work of Blom et al. on Carboniferous coals is generally applicable. With this in mind, the distribution of the three dominant oxygen-bearing functional groups, -COOH , -OH , and =CO , in lignite, subbituminous and bituminous coals compare with Blom's data.

Since preheating of caking coals at low temperatures appears to alter their caking properties, extractability and solubilities (Berkowitz, 1978), it was decided to investigate the relationship between mild pyrolysis and the distribution of functional groups for some of the coals. This was studied by determining $[\text{-OH}]$, $[\text{-COOH}]$, and $[\text{=CO}]$ after heating at 200°C (20hr) and 300°C (0.5hr). Decarboxylation was also explored by rapidly heating low rank coals to 200°C (0.5hr) and 300°C (0.5hr). All these data were expected to provide some basis for explaining behavioural differences between Western (Cretaceous) and Eastern (Carboniferous) coals.

This chapter has shown the usefulness of data on distribution of oxygen in functional groups. Chapter 2 reviews the published literature on analysis of oxygen in coal, and chapter 3 describes the experimental procedures used in this study. The distributions of O-bearing functional groups are presented and discussed in chapter 4. Chapter 5 addresses the changes that occur in these functional groups as a result of thermal treatments. Results are summarized in chapter 6.

footnotes

1. Metallurgical coals are coals which are suitable and most commonly used for coke production. These maybe high

volatile bituminous for bulk or low to medium volatile bituminous for strength. Coals are graded according to their value for specific use, employing whatever empirically applicable test parameters are appropriate to that use. This includes ash content, moisture, calorific value, rank and petrographic composition (Chemistry of Coal Utilization, 2nd supplementary Vol., Elliot, M.E. ed. Chapter 3).

2. Rank only express the progressive metamorphism of coals from lignite to anthracite. However coals are categorized into ranks depending coal properties. Among these are elemental analysis, calorific value, moisture (van Krevelen, 1961; Berkowitz, 1979).

3. Alberta has about 75% of Canada's thermal coal resources (Smith, 1989). Thermal coals (for heat and electricity) are high volatile bituminous (hvb) and subbituminous (subbit.) generally found in the Plains of Alberta. Metallurgical coals, which are low and medium volatile bituminous coals (mvb), are found in the Rocky Mountain and Foothills regions (1988 coal directory of the Coal Association of Canada).

4. For Shapiro and Gray Correlation, see "Introduction to Coal Technology" by N. Berkowitz or "Chemistry of Coal Utilization" 2nd Supplementary volume, ed. M.E. Elliot p.148

CHAPTER 2

LITERATURE REVIEW

This chapter briefly discusses oxygen as it occurs in coal, and describes the most common analytical methods reported in the literature. It emphasizes analytical methodologies and presents key experimental data as well as the inferences derived from them. Experimental findings from some of the classic research in the field have been summarized in in-depth reviews by Attar & Hendrikson (1982) and by Zhou, Dermes & Crynes (1984). A related review by Berkowitz (1988) discusses mechanisms of atmospheric coal oxidation. Material from the newer literature as it pertains to methods is included here.

2.1 Oxygen in Coal

Oxygen is an integral part of coal. It constitutes a major part of the building blocks of the plant material from which coal is derived, and occurs in coal in diverse forms. Organically bound oxygen is part of the structural network of the coal material and inorganic oxygen is associated with moisture as well as with mineral matter in the coal. Organic oxygen occurs in functionalities such as carboxyl (-COOH), carbonyl (=CO) and hydroxyl (-OH). These groups are all polar and reactive in comparison to oxygen in ether structures (R-O-R) or heterocycles such as furan (Blom et al., 1957; Ihnatowicz, 1952; Van Krevelen, 1961). Reactive peroxides (O-O), and hydroperoxides (H-O-O-H) do not occur in fresh coals, but are found in weathered coals. -OH

is present in predominantly phenolic form; current knowledge indicates that there is no alcoholic -OH (Berkowitz, 1988). =CO occurs in ketonic or quinoid form or in lactones. Linear as well as cyclic ethers occur as Ar-O-Ar, Ar-O-Al, Al-O-Al which (Ar = aromatic ring, al = Aliphatic chain). Because of such diverse forms, analytical methods are not available to distinguish between these ethers and quantitative data for ethers are often suspect (Blom et al., 1957).

The current thinking on functional group-rank relationship (which is based primarily on Carboniferous coals and normal metamorphism) is that -COOH, -OH and =CO all decrease during metamorphism, and hence as coal rank increases. The highest rank coals therefore are left exclusively with heterocyclics, ether structures and possibly low concentrations of quinoid =CO groups. For US coal populations studied by Abdel-Baset et al. (1978) a linear correlation between carbon content and [-OH] suggested that [-OH] can be a parameter defining rank in the same manner as carbon content.

Transformation of oxygen functionalities during coalification is explained by two possible pathways (Attar & Hendrikson, 1982). One involves reactions that eliminate oxygen in the form of water and carbon dioxide, and the other reactions that condense oxygen into more stable functions. These reactions may occur simultaneously or sequentially. Examples are, alcohols --> ethers, aliphatics--> alicyclics and/or hetero-aromatic structures. Oxygen serves as one type of linkage in aromatic structures (Ouchi & Imuta, 1973). In ether form it is a

crosslinking agent (Liotta et al., 1983). In its hydroxyl form it is responsible for structures which participate as weak hydrogen bonding agents in coal (Liotta, 1979; Kini et al., 1958; Horton, 1958).

In whatever form these functionalities occur, oxygen is the most abundant heteroatom in coal, generally much more so than sulfur and nitrogen. The determination of oxygen is therefore of primary concern, with methods of analysis determined by interest, need and, often convenience.

Most of the published data on oxygen in coal can be categorized into: (i) "original" in as-mined coals, (ii) coal extracts, (iii) coals depolymerized via pyrolysis or hydrolysis and (iv) oxidized coals (Attar & Hendrikson 1982). In this work direct investigation of the as-mined and slightly pyrolyzed coals were the primary concerns.

2.2 Analytical Procedures

Analysis of oxygen in coals may entail determination of total oxygen or determination of individual forms of oxygen. The former employs three specific methods to date: i) oxygen-by-difference, ii) neutron activation, and iii) combustion. The latter employs wet chemical methods using specific reactions for individual oxygen groups, or modern surface-sensitive instrumental techniques such as spectroscopy, or a combination of wet chemical and spectroscopic methods.

2.2.1 Total Oxygen

2.2.1.1 Oxygen-by-difference

Oxygen "by difference" is determined (ASTM D3176-85) from elemental analysis, i.e. as

$$[O] = 100 - ([C] + [H] + [N] + [S] + [H_2O] + [ASH])\%$$

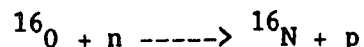
and on a dry, ash-free basis:

$$[O] = 100 - ([C] + [H] + [N] + [S])\%$$

This method is the most routinely used. However, its major drawback lies in the fact that all analytical errors accumulate in the oxygen value. Errors due to weight changes in the coal mineral matter are also included (Ode, 1963). However, this method is the least tedious.

2.2.1.2 Neutron Activation

The most direct method of oxygen determination is a Neutron Activation method (Ruberto & Cronauer, 1978; Berkowitz, 1985; Volborth et al., 1987), which involves



The oxygen concentration in the coal sample is obtained by counting the emitted beta or gamma radiation from $^{16}_7\text{N}$, and comparing the counts to standard samples of known oxygen content. Unfortunately, this is not the most convenient method as the short half life of $^{16}_7\text{N}$ (7s) may cause difficulty in collecting the data.

2.2.1.3 Pyrolysis

The coal samples can be pyrolyzed at 1100°C and the released volatile matter is passed over carbon at 1100°C - 1200°C to generate CO, which is then converted to CO₂ and quantitatively determined by adsorption on a bed of Ascarite or, more simply estimated by gas chromatography (Abernathy & Gibson, 1966).

2.2.2 Functional Group Analysis

Two approaches can be used for determination of O-bearing functional groups: wet chemical procedures and spectroscopic techniques. Used together, they can complement each other by confirming completion of reactions or by providing parallel sets of consistent, confirmatory data.

2.2.2.1 Instrumental Techniques

In the past several years, many spectroscopic techniques have become relatively commonplace for the study of bulk and surface oxygen in coals and solvent-refined coals. Fourier Transform Infrared Spectroscopy (FTIR) (which will be discussed later), X-ray Photoelectron Spectroscopy (XPS), sometimes also termed electron spectroscopy for chemical analysis or ESCA, and Nuclear Magnetic Resonance Spectroscopy (NMR) have all featured in the literature. Little or no sample preparation is necessary, but because all optics and data processing are computer controlled, the operations require great care.

Nuclear Magnetic Resonance (NMR)

In its most general definition, the NMR spectrum of a compound is the resultant of the interactions between the magnetic field of electromagnetic radiation at specific frequencies and the magnetic moment of nuclei of the element of interest which has positive or negative spin numbers (Dyer, 1965). Data are processed in the later versions by Fourier transform.

Variants of NMR spectroscopy are used in the study of coal structure. The determination of the relative concentrations of aromatic and aliphatic components is often done by both NMR (using ^{13}C NMR) and FTIR. However, oxygen determination by NMR is not simple, and the only form of NMR which can be used successfully for oxygen determination in coal is ^{17}O -NMR. This has been successfully applied to determine [O] in alcohols, phenols, ethers, carboxylic acids, furans, ketones and aldehydes in coal liquids (Grandy et al., 1984a). This technique has found limited use in the study of natural substances because of the low abundance of ^{17}O and because line broadening in the spectrum associated makes resolution difficult. Materials of low oxygen content require about 16hr of spectrometer time. For example, in an analysis of heavy distillate, 2.7 million scans are used. The method is specific to one element, and the signal area is directly proportional to the concentration of the functional group. Although quantitative analysis of O-functional groups appears promising, it so far proved useful only in liquids (Grandy et al., 1984b).

The use of solid state NMR in the study of oxygen in coal has been useful but controversial to date (Snape et al., 1989). There is still uncertainty as to whether all oxygen groups are sampled during analysis.

Fourier Transform Infrared Spectroscopy(FTIR)

Historically, the use of KBr discs of coal with transmission spectroscopy was improved by Fourier transform. Later, diffuse reflectance spectroscopy, a technique in which fine powdered mixtures are ground in KCl or KBr to cause dispersion of infrared radiation, was enhanced by FTIR. Most recently, FTIR in Fourier Transform Infrared Photoacoustic Spectroscopy (FTIR-PAS) has been used in coal structure analysis. The method uses about 25mg of the unmodified sample powder. Infrared radiation is absorbed by the sample which reflects the radiation in the form of heat. Heat causes pressure waves in a contacting gas in a frequency range which can be detected by a microphone. Since absorption intensities are dependent on the surface areas of the particles, it is important for comparative purposes, to use samples of the same size range (Rosencwaig, 1980). Statistical averaging of the hundreds of spectra has become a way of overcoming sampling difficulties.

Each of these methods can address specific aspects of coal functionalities as long as the bonding of atoms permits detectable infrared energy of absorption in stretching or bending vibrations. The most commonly used of these techniques to date

has been FTIR. The FTIR-PAS technique was used in this work for checking on completion of the reactions used in wet chemistry.

There have been characteristic wavelengths of absorption assigned to specific O-bearing functional groups. Protonated carboxyl has been identified with the 1700cm^{-1} band, and in salt form with bands at $1560\text{--}1590\text{ cm}^{-1}$. The 3300 cm^{-1} band is identified with -OH stretch. (Osawa & Shih, 1971). There is still some controversy about the assignment of the 1600cm^{-1} band to carbonyl. There is also some contribution to this band by -COOH as discussed before (Painter et al., 1983). Overtones and overlaps of bands become a problem. There is difficulty in getting good quantitative data because of different absorption coefficients of the various bonds and band overlap. Often derivitization is required to overcome this. In addition, the 3300cm^{-1} band is significantly affected by moisture and N-H stretching. The quantitative use of FTIR is not simple, and has been thoroughly reviewed by Painter et al. (1985). Bands that are of unequivocal quantitative use are those in which vibrational motion is well defined. Since all coal spectra have similar general features, the major differences between coals are band intensities. It is highly unlikely that band intensities due to the concentration of the appropriate functional groups remain constant among similar samples. If indeed they do, then peak integration can be performed and the area calculated under a peak can be related to the concentration of the specie of interest.

X-ray Photoelectron Spectroscopy (XPS)

XPS is little used in coal science. It is worthy of discussion here since quantitative data on oxygen functionalities has been recently acquired by it (Perry & Grint, 1986). The technique measures the kinetic energies of core and valence electrons (which have characteristic binding energies). This energy is emitted from coal when it is irradiated by soft X-rays (Mg or AlK α). All elements except hydrogen and helium can be analysed by this method.

The method has high surface sensitivity and only 3-4nm of the outer surface layer is analysed. This means fine grinding would be required to determine the oxygen of the bulk of the coal. There is more sensitivity to specific elements than to the functional groups. Again quantitative analysis is dependent on computer programs designed to resolve peaks by deconvolution techniques and these also suffer from lack of definition of fundamental spectral lineshape.

Most of the chemical shifts in this method have been determined from model compounds; therefore, transfer of model character to real systems is a likely source of error. On the other hand, since quantitative determination of functional group and the element is done in the same experiment, changes in functional groups can be correlated with oxygen (Briggs & Seah, 1983; Perry & Grint, 1986).

2.2.2.2 Wet Chemical Methods

These methods have been extensively reviewed in the past (Blom et al., 1957; van Krevelen, 1961,1981; van Krevelen & Schuyer, 1961; Dryden, 1963; Ignasiak et al., 1972; Ruberto & Cronauer, 1978; Given & Yarzab, 1978; Wender et al., 1978; Abdel-Baset et al., 1978); and recently by Attar & Hendrikson (1982) and by Berkowitz (1988). Some instrumental methods were reviewed by Ignasiak et al. (1972) and by Berkowitz (1985).

The wet chemical methods are subject to the usual errors incurred in the performance of such techniques. The principal weakness is inability of the reagents to completely access the coal structures due to variable porosities, i.e. the macropores and micropores (Berkowitz, 1979). The question of completion of reaction, and therefore time of reaction, becomes important for diffusion of the chemicals to the reactive sites. Since the porosity of coal decreases with increasing rank, the question of reagent access is more problematic for higher rank coals in which the pore structures are finer and less open than in lower rank coals. These problems can be minimized by fine grinding. The -200 mesh particles are the largest convenient sizes for accurate determination of oxygen functional group concentration by these methods (Ruberto & Cronauer, 1978). Optimum reaction times must be determined for each of the functional groups that are analysed by a given method.

Carboxylic Oxygen

Carboxyl groups ($-COOH$) are found in all low rank coals, and are most easily and reliably determined by ion exchange which forms the basis for determining acidity in coals. Most methods reported are only minor modifications of the basic ion exchange experimental procedure. The powdered, protonated and preferably demineralized coal is treated with an excess of either barium or calcium acetate. The cations displace the exchangeable protons of carboxylic acids, and this liberates acetic acid which is determined by potentiometric titration. Accuracy depends on time of reaction, particle size and method of titration.

In the earliest studies, $[-COOH]$ was determined indirectly from the decrease in calcium ions. This method assumed one calcium was bound to two (adjacent) carboxylic groups as in $-COO-Ca-OOC-$, thus allowing only proximal accessible groups to interact (Blom et al., 1957). The results of this method were found to be higher than calculations derived from released acetic acid (Ihnatowicz, 1952). The assumption of two carboxyl per calcium ion was the source of error. Also, there was the possibility of phenolic groups interacting and adding to errors.

Schafer (1970a,1970b) compared several related ion exchange methods which included the exchange of calcium acetate. Among these methods were

i) exchange with barium acetate in which the pH was strictly controlled at 8.25 to eliminate possible exchange with phenolic protons. (The exchange reaction was also optimized by refluxing the protonated coals with barium acetate for 4hr, and

then titrating the released acetic acid against NaOH and an indicator dye);

ii) exchange with sodium or barium chloride, followed by titration; and

iii) exchange with mixtures of barium chloride and barium hydroxide, followed by titration;

Good reproducibility was obtained with low rank coals. The only complications that could arise from the latter two methods are the presence of ortho phenols which may exchange at pH less than 8.0. In this case strict pH control at 8.25 ensures complete exchange of carboxyl groups.

Participation of phenolic -OH could also be prevented by a methylation reaction which blocks -OH prior to ion exchange. However, there are more reaction steps and potential sources of error increase.

When sodium acetate was used by Brooks & Sternhill (1957) on low rank coals, the mixture was refluxed for 16-20 hrs. Lynch & Durie (1960) refluxed coal with sodium acetate for 4hrs. Sodium acetate, however, solubilized some of the components of the coal and produced a brown filtrate. This made detection difficult when using indicator dyes in titration.

Carboxylic acids can also be determined from the total acidity with a subsequent correction for the phenolic -OH contribution. Coal suspensions were titrated in ethylenediamine against sodium aminoethoxide (Brooks & Maher, 1957). Values were lower than those recorded by means of Ihnatowicz's and Schafer's methods. A comparison of ion exchange and titrimetry on five

coals from around the world showed higher results from nonaqueous titrimetry. Some phenolic -OH would titrate with carboxylic groups, and weaker, less accessible, phenolic -OH could be found (Maher & Schafer, 1976).

Another variation of Schafer's method entailed allowing the coal slurry to stand in the barium acetate for 70 hours for ion exchange under nitrogen, with gentle intermittent swirling by hand. Refluxing of the samples was compared to samples just standing. Optimised times were determined by Takeuchi & Berkowitz (1988) for low rank coals.

Determination of carboxylic acids by quantitative FTIR was attempted by Starsinic et al. (1983). They used least squares curve fitting routines and curve resolving procedures for elimination of band overlap of the 1700cm^{-1} peak. While they criticized Schafer's method on the grounds that it suffered from incompleteness of the reaction, they nevertheless adopted this method for calibration of this FTIR procedure in order to define extinction coefficients. They used difference spectroscopy and claimed both speed and accuracy. However, in the absence of depth profiling of the coal particles, the technique remains more surface than bulk oriented.

Hydroxyl Oxygen

Phenolic -OH is more thermally stable than -COOH, and is commonly found in coal extracts and liquefaction products. Its analysis has been studied more than other groups. The wet chemical methods have been reviewed by van Krevelen (1961) and,

more recently, by Attar & Hendrikson (1982). The analyses have been described under two categories:

i) total -OH determinations which include acetylation, trimethylsilylation and deuteration;

ii) total acid determination for which corrections must be made for [-COOH]; this category includes methylation, reaction with dinitrofluorobenzene, barium exchange, nonaqueous titration, and acetylation with ketene.

The most common method to date is acetylation of the powdered coal. The coal is suspended in pyridine, acetic anhydride is added and refluxed at 90°C for 20-24 hours. The acetylated coal is then hydrolysed with barium hydroxide to produce barium acetate and -OH is quantitatively determined by either acidifying with phosphoric acid and titrating this distilled acetic acid with a base (Blom et al., 1957), or releasing acetic acid by ion exchange and titrating it (Takeya et al., 1965).

In a modification of this technique, the acetic anhydride is radiochemically labelled with ^{14}C and counted by scintillation counter upon release (Hill & Given, 1969). Alternatively, the labelled coal can be combusted and the gas counted by a scintillation counter. Scintillation counting normally has very substantial experimental errors, especially when dealing with small amounts of -OH.

Alternative procedures involve forming the trimethylsilyl ether derivative by reacting -OH with hexamethyltrisilazane in pyridine. The modified coal can be then analysed

for increased silicon content (Friedman et al., 1961). Deuteration has been used to exchange H in -OH following which the deuterated coal is combusted. The condensed water can be measured by increased density and the [OH] determined indirectly (Yokoyama et al., 1967).

The nonaqueous potentiometric methods developed by Brooks & Maher (1957) determine total acidity. These procedures have been compared with total exchange against barium hydroxide and found to produce lower values (Maher & Schafer, 1976). Like thermometric titration with alcoholic alkali for determination of the total acids (Vaughan & Swithenbank, 1970), these methods must be complemented with a method for determining [-COOH] which is subtracted from the total acid concentration. Again, error minimization depends on the experimenter and on the porosity and size of the coal particles. Care must be taken to minimize oxidation of the samples during analysis.

The four major wet methods - ion exchange with $\text{Ba}(\text{OH})_2$, acetylation, acid-base titration and silyl-ether formation - were evaluated with model compounds and a standard vitrain sample by Halleux et al. (1959). Agreement between acetylation and trimethylsilyl-ether formation was found. However, with model compounds some side reactions were observed. Results of [OH] versus [C], (Blom et al., 1957; Ihnatowicz, 1952; Lahiri, 1957; Wyss, 1955) showed large differences. This seems to reflect not so much differences in methods as differences in coals, and perhaps differences in sample treatments.

Dutta & Holland (1983) compared nonaqueous titration with acetylation of a subbituminous and a bituminous coal. Both yielded similar results for the bituminous coal, but for the subbituminous coal nonaqueous titration values were only 30% of the concentrations found by acetylation. It was suggested that lower values for the subbituminous were due to proximal phenolic groups which were partially titratable, and alcoholic groups which were not titratable. Earlier, Dutta & Holland (1983) were of the opinion that the acetylation method was self consistent and reproducible. Abdel-Baset et al. (1978) analysed 37 US coals by using ^{14}C -acetic anhydride and found a linear correlation between vitrinite reflectance and $[\text{OH}]$. However, no correlation was observed when the analytical results were expressed as a fraction of total oxygen, ie. $[\text{O}_{\text{OH}}]/[\text{O}]$. For coals of the same rank, hydroxyl contents decreased in the order Interior Province > Eastern Province > Rocky Mountain coals.

Some attempt has been made to determine $[-\text{OH}]$ by quantitative FTIR, using pressed KBr discs. Using plots of extinction coefficients, it was claimed that, with care, correlations with rank can be reproduced within $\pm 5\%$ and with results of Abdel-Baset et al. within $\pm 10\%$ (Solomon & Carengelo, 1981, 1982, 1988). Snyder et al. (1983) did not find much variation in the ratios of intensities of the 1740 and 1770 cm^{-1} bands of acetylated coals. By choosing another band (such as the carbonyl difference bands of acetylated and original coals), and using linear correlations for fitting individual band intensity data, they found that the absolute intensities of the acetyl

bands decreased with increasing rank of coals. By diffuse reflectance FTIR, Fuller et al. (1982) showed broad phenolic bands to decrease with increasing coal ranks. As indicated earlier, moisture contributions to -OH band intensities can be reduced by using acetylated coals which show better defined and more pronounced peaks. However, incorrect determination of extinction coefficients can lead to errors.

Carbonyl Oxygen

Carbonyl is found in coal in several forms (viz. quinoid, ketonic, aldehyde) and estimation of this functional group in one analysis is difficult. The most commonly used method involves formation of an oxime with hydroxylamine hydrochloride.

90°C



The oxime is then acidified and the nitrogen increase is measured before and after oxime decomposition, which is accomplished by acetone and acid. $[\text{=CO}]$ is calculated from the difference. Saponification and reduction of the acetoxime produces ammonia, which can be determined by titrimetry, so that the results can be rechecked.

In some cases nitrogen in the coal-oxime is measured by the Kjeldahl nitrogen determination: the oximated coal is heated in concentrated sulfuric acid which converts nitrogen to ammonium acid sulfate $(\text{NH}_4)_2\text{SO}_4$; the solution is then made basic by

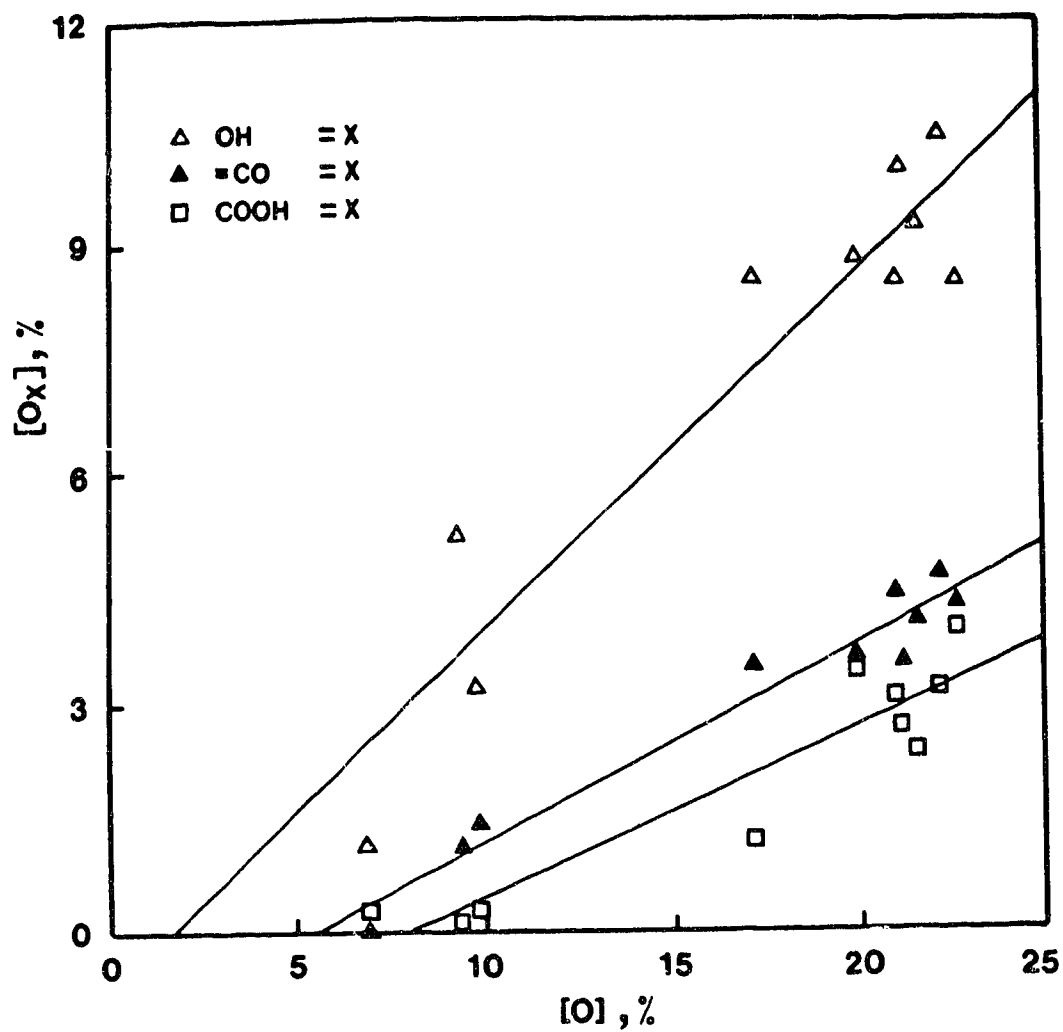


Fig. 3 Weight percentage of oxygen in O-bearing functional groups ($x = -OH, =CO, -COOH$) versus total oxygen $[O]$.

- (1) $[O_{OH}] = -0.971 + .488[O]$
- (2) $[O_{CO}] = -1.444 + .265[O]$
- (3) $[O_{COOH}] = -1.784 + .227[O]$

where, the correlation coefficients are 0.94, 0.98 and 0.92 for lines (1), (2), and (3) respectively. From the above equations, the ratio of oxygen in the O-bearing functional group to total oxygen $[O]$ can be defined in terms of $[O]$ by a simple transformation of these equations i.e. by dividing through by $[O]$. The solid lines in Fig.4 correspond to such transformations $f([O])$ plotted against $[O]$ e.g.

$$f([O]) = -0.971/[O] + .488 = [O_{OH}]/[O]$$

As $[O]$ becomes large, the ratio will approach a limiting value. Experimental data shown by the scatter symbols, fits this empirical function $f([O])$ plotted against $[O]$. However, the scatter increases for the ratio plots and especially in the case of $[O_{OH}]/[O]$ versus $[O]$. Again, the largest increases occur in $[O_{OH}]/[O]$, as $[O]$ is increased followed by $[O_{CO}]/[O]$, and $[O_{COOH}]/[O]$.

These trends should be regarded only as general indicators since the chemistry of the coals will influence their contents of O-bearing functional groups. For instance, if the data for Carboniferous coals #14 and #16 are removed from the

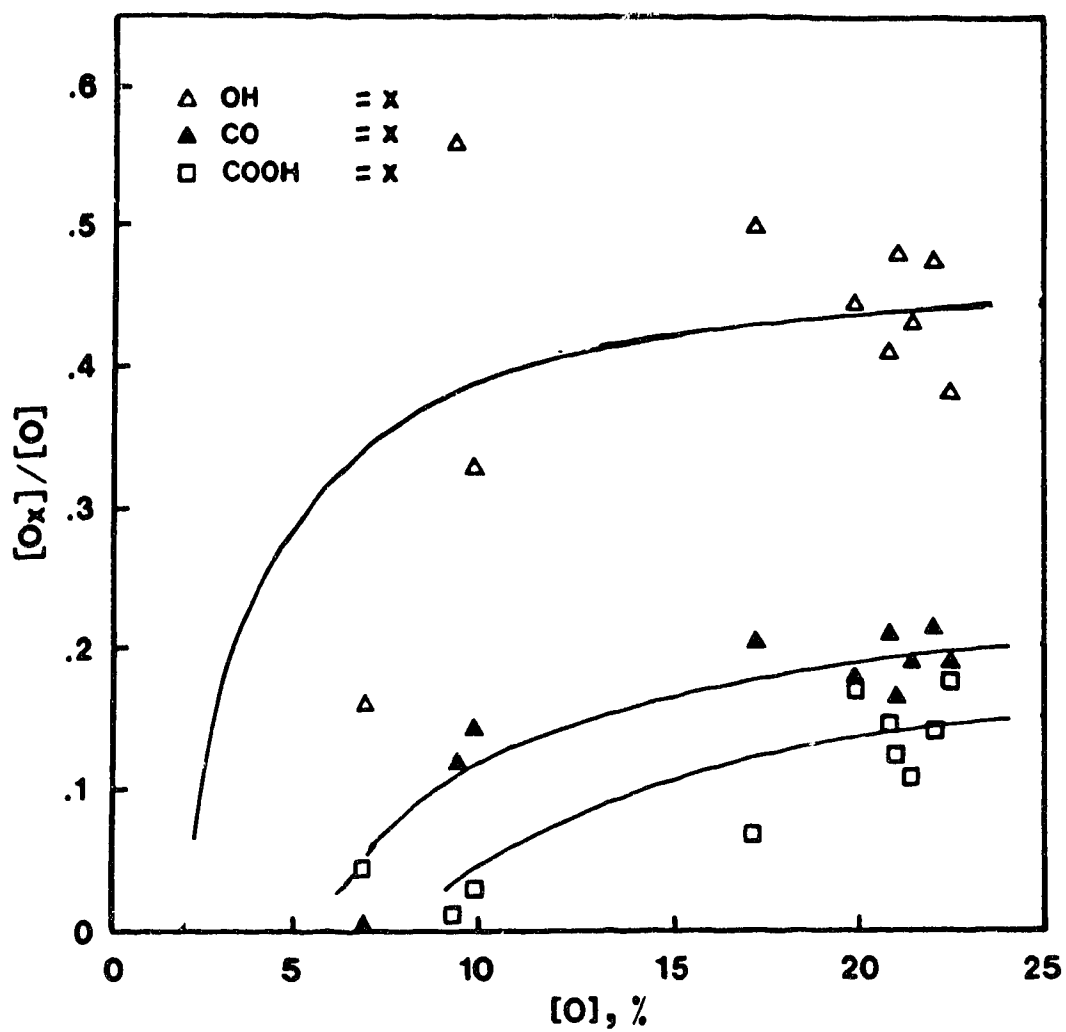


Fig. 4 Oxygen in O-bearing functional groups ($x = -OH, =CO, -COOH$) as a fraction of total oxygen $[O]$. Solid lines indicate the empirical $f([O])$ plotted against $[O]$.

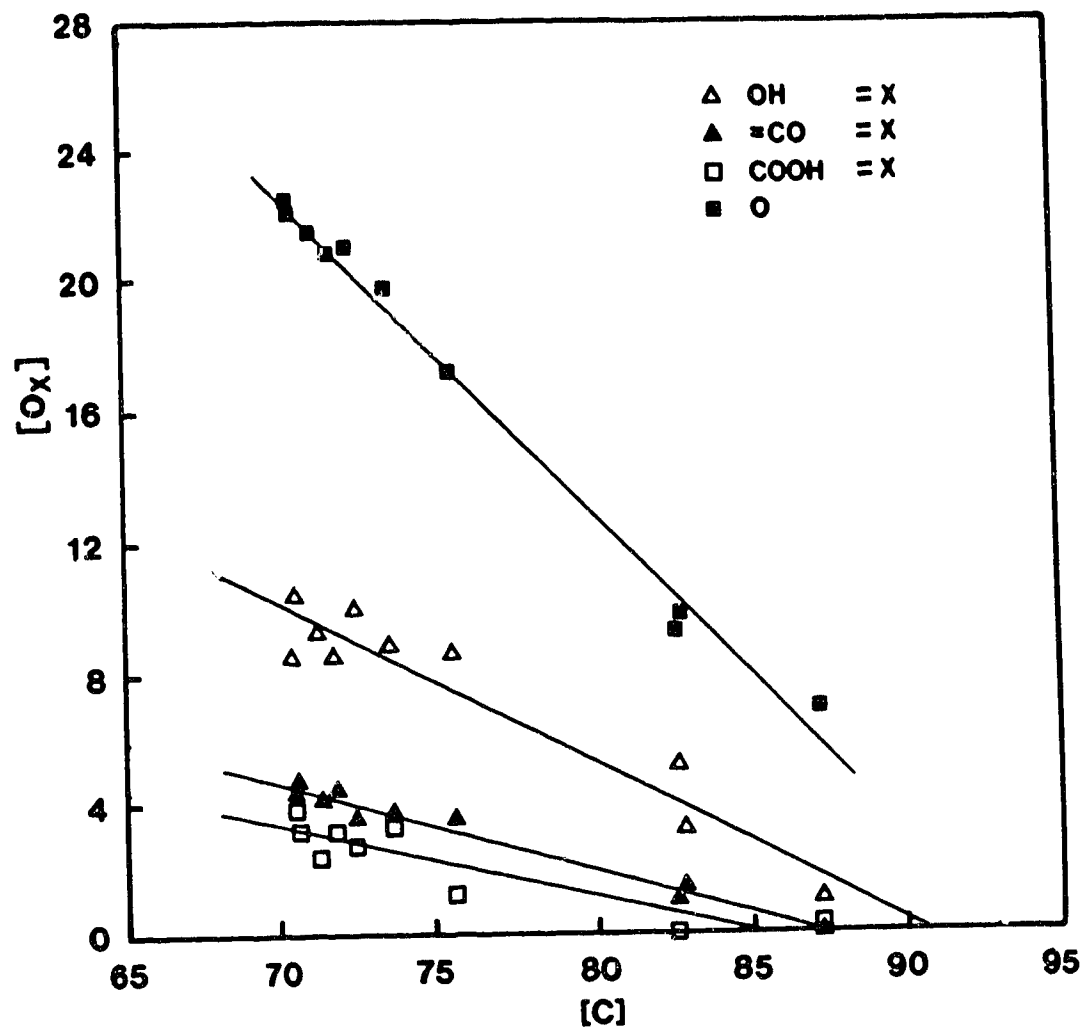


Fig. 5 Weight percentage of oxygen in O-bearing functional groups ($x = -OH, =CO, -COOH$) $[O_x]$ versus %C

graphs, there will be a shift in the slopes of the regression lines. On the other hand, a larger selection of coals including coals in the 76%C - 81%C range, will be more statistically significant.

Indian lignite (Iyengar & Ghosh, 1958) showed the same trends as the low rank Canadian coals, i.e.

$$[O_{OH}] > [O_{CO}] > [O_{COOH}] .$$

Similar studies have been performed on Japanese Cretaceous coals of comparable carbon contents, using identical experimental methods (Hatami et al., 1967). Their data sets for lower carbon coals follow the same pattern as the subbituminous coals used in this study. For coals from 72%C to 82%C the trend was similar to that shown above for Canadian coals. However above 85%C, no O_{COOH} was found, quite unlike the Canadian coals. On the other hand Takeya et al., (1965) found $[O_{COOH}]/[O]$ was greater than $[O_{CO}]/[O]$ in peat. No $[O_{COOH}]$ was reported for lignite but as the rank of the coals increased the trend became similar to that observed in Canadian coals. Unlike coal #20 (87%C) the higher carbon Japanese coals (>85%C) showed

$$[O_{OH}] > [O_{CO}], [O_{COOH}] = 0 .$$

The trend observed for Canadian Coals (Fig.5 & Fig.6b) is different from that reported by Blom et al. (1957) for a suite of European Carboniferous coals (Fig.6a). When total -OH oxygen is

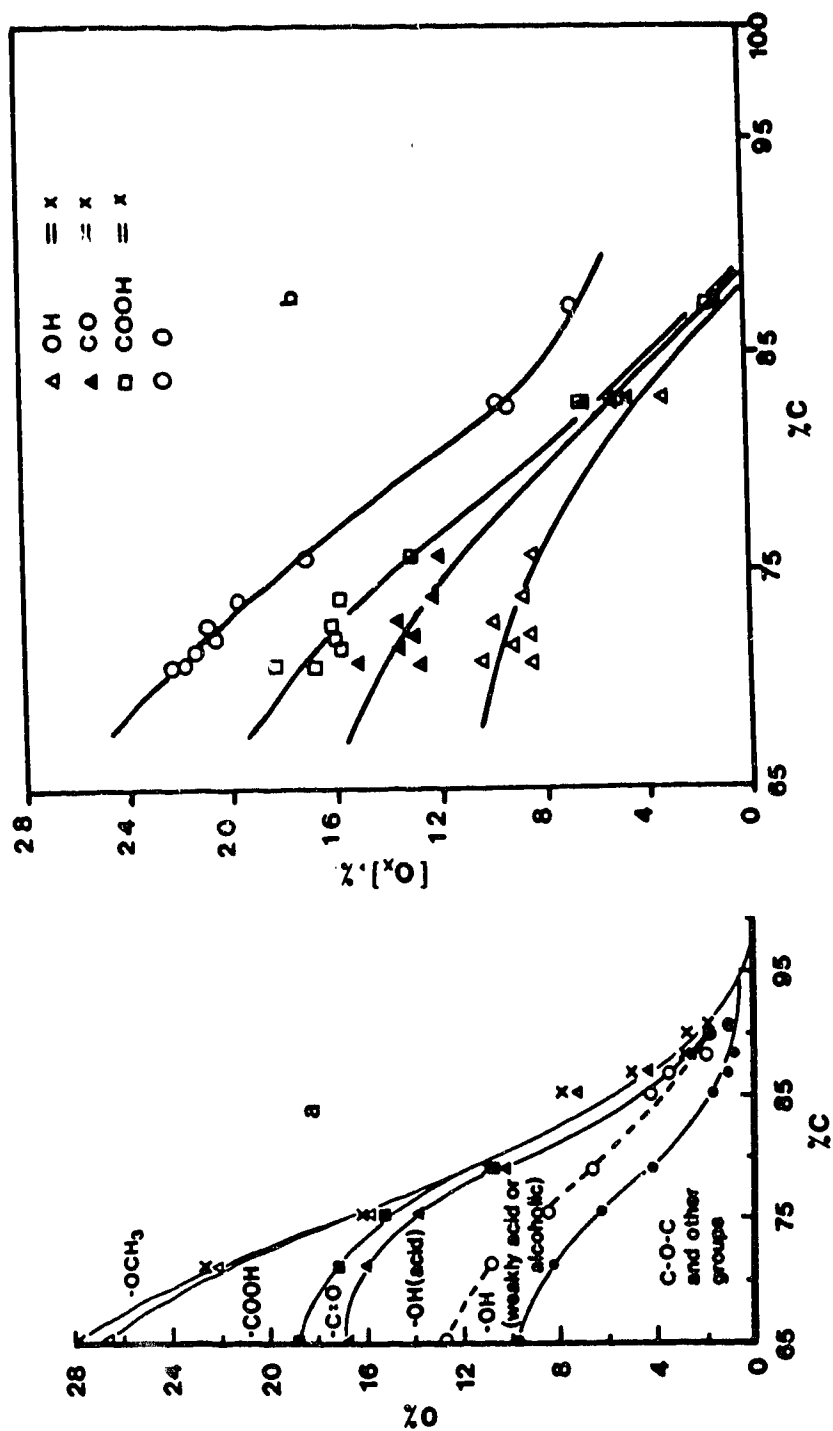


Fig. 6 Weight percentage of oxygen in O-bearing functional groups versus $\%C$ (a) after Blom et al., 1957, (b) Canadian coals (plotted cumulatively for direct comparison).

$$[O_{OH}] > [O_{COOH}] > [O_{CO}]$$

considered. Values were interpreted as a weight percentage of the coal. Coal #20 was in accord with this trend which was unlike the Canadian Carboniferous hvb coals #14 and #16. With Canadian coals, the decrease of O-bearing functional groups appear more linear with carbon content as compared with the coals reported by Blom et al. (Fig.5 and Fig.6b vs Fig.6a). By their data total oxygen was not accounted for, and in effect "residual" oxygen was ignored. Residual oxygen (see Tables 3 & 4), which carries the total errors of all other measurements, seems to depend on the particular coals and does not show any clear trend.

For Australian brown coals Given (1984) found

$$[O_{OH}] < [O_{COOH}]$$

based on total oxygen dmmf. He also reported that $[-COOH]$ in North Dakota lignites was even greater than in Australian brown coals, even though the latter were considered to be less mature lignites. Canadian lignite #1 did not rank highest in terms of $[O]$ or concentrations of all O-bearing functional groups as would be anticipated from established rank relationships. It had the greatest O_{COOH} concentration among the coals studied, but this concentration was lower than $[O_{OH}]$ and $[O_{CO}]$.

The results recorded in this work do not wholly conform with the generalizations in the literature. Given (1984) stated that among the O-bearing functional groups, carboxylic acids

would be of the maximum concentrations in subbituminous coals, as he found for brown coals (lignite). Berkowitz (1989) concluded from the available literature for low rank coals that oxygen is equally partitioned between functional groups.

4.3 Variations in Oxygen Distributions in Canadian Coals

In Fig.4 the coals are clustered depending on whether $[O]$ values are low or high. However, within the clusters there are wide variations among coals of similar rank. The hvb Cretaceous coal #10 groups neither with the hvb Carboniferous coals #14 and #16, nor with the mvb U.Cretaceous/Tertiary coal #20, but associates with low rank coals.

4.3.1 Low Rank U.Cretaceous/Tertiary Coals

For the five subbituminous coals studied, there is generally wide variation in partitioning of O-bearing functional group concentration among coals. For the four subbituminous C coals, $[O_{OH}]$ ranges between 8% and 10%, ($[O_{OH}]/[O]$ between 38% and 48%). Lowest $[O_{OH}]$ occurred in lignite #1. The subbituminous B coal #7 showed higher $[O_{OH}]$ than the lignite at 9% ($[O_{OH}]/[O] = 44\%$) but values were within those of its lower rank counterparts. Subbituminous C coal #2 showed the highest $[O_{OH}]$.

When data for $[O_{OH}]/[O]$ from this study were compared with data published by Abdel-Baset et al. (1978), close agreement with coals of the Rocky Mountain Province was observed (34% - 39% for subbit. B coals, and up to 46% for hvb coals).

Similarly good agreement was found with results recorded for low rank Japanese Cretaceous coals for which $[O_{OH}]/[O]$ ranged from 33% to 44%. Japanese lignites also has the lowest $[O_{OH}]/[O]$ at 33% (Takeya et al., 1965).

Data for $[O_{CO}]/[O]$ (17% - 21%) from this study were also comparable with data for Japanese low rank Cretaceous coals (16% - 21%). No $[=CO]$ was found in Japanese lignites (Takeya et al. 1965).

For subbituminous C coals (Tables 3 & 4), the concentrations of oxygen in $-COOH$ functional groups can be broadly described by noting that $[O_{COOH}]$ and $[O_{COOH}]/[O]$ were 2% - 3% and 11% - 15% respectively.

The highest $[O_{COOH}]$ and $[O_{COOH}]/[O]$ were found in lignite (#1) and the subbituminous B (#7) respectively (4.0% and 3.5% ; 17.9% and 17.7%). The subbituminous B coal #7, which is slightly higher in rank than the subbituminous C coals, contained higher $[O_{COOH}]$. This is contrary to rank expectations.

The carboxyl oxygen content of lignite, as compared to that of other coals is in keeping with what is conventionally expected for the least mature coals. The $[O_{COOH}]$ in lignite #1 was higher than in an Indian lignite (4.0% vs 2.2% dmmf; Iyengar & Ghosh, 1958). Although, previous work generally assumed that in lignites $[O_{COOH}]$ will predominate over the other oxygen-bearing functional groups, this was not the case.

4.3.2 High Ranked U.Cretaceous/Tertiary and Carboniferous Coals

A comparison of U. Cretaceous/Tertiary coals hvb #10 and mvb #20 with Carboniferous hvb #14 and hvb #16 is shown in Tables 3 & 4, and Figs. 3, 4, & 5. As expected, the mvb coal #20 displays the lowest concentrations of all O-bearing functional groups. Yet $[O_{COOH}]/[O]$ is higher (4.4%) than in the hvb Eastern Carboniferous coals #14 and #16 (3% and 1%). Most of the oxygen in coal #20 (79% of total oxygen) appears to be in unreactive forms which include ethers and heterocyclics.

The partitioning of O-bearing functional groups in the hvb coals were found to be as follows:

$[O_{OH}]/[O]$ accounts for 3% - 9% and $[O_{OH}]/[O]$ for 33% - 56%

$[O_{CO}]/[O]$ accounts for 1% - 4% and $[O_{CO}]/[O]$ for 12% - 20%

$[O_{COOH}]/[O]$ accounts for 0.1% - 1% and $[O_{COOH}]/[O]$ for 1% - 7%

Hvb coal #10 (Western Canadian U. Cret./Tert.) displayed the highest oxygen for all but the O-bearing functional groups. When $[O_{OH}]/[O]$ of Western coal is compared with the Eastern coals, values differ considerably (50% in coal #10, 33% in coal #14, and 56% in coal #16). Between the two Carboniferous coals #14 and #16 there are some differences in $[O_{CO}]/[O]$ and $[O_{COOH}]/[O]$. During proximate analyses of coals #14 and #16 it was observed that #14 formed a coke button in the thermogravimetric pan. It is conceivable that this reflects low porosity which in turn is associated with low bed moisture (Berkowitz, 1985, see note 1.). It is therefore possible that coal #14 was less completely accessible to the reagent than #16, resulting in lower $[O_{OH}]/[O]$.

Concentration of oxygen in phenolic -OH was generally higher than the 36% quoted by Brown & Wyss (1955) or the 40% generalised by Horton (1958) for the "bright" British coals.

All these differences may be conceivably due to differences in metamorphic histories.

4.4. Regional Metamorphic Effects

Coals of equal rank can possess diverse chemistries because of different formative histories. Coals of similar elemental composition, such as Eastern Carboniferous hvb #14 and #16 as well as the Western U. Cretaceous subbituminous C coals, were different in O-bearing functional group compositions. The higher concentrations of O-bearing functional groups in Western Canadian plains coals as compared to their Eastern counterparts could be attributed to diagenetic and metamorphic history in a broad sense. This idea was earlier put forward by Abdel-Baset et al. (1978) and Given (1984) when comparing populations of US coals.

The fact that coal #20 has more $[O_{COOH}]$ than $[O_{CO}]$ at 87% C may be a resultant of diagenetic and regional metamorphic effects, such as orogeny. However, the low concentrations of all O-bearing functional groups and disagreement with trends reported in the literature precludes firm conclusions. For such high carbon coals the reverse order or absence of $[-COOH]$ would be expected.

Variations in the compositions of the subbituminous coals and the lignite suggest differences in diagenetic conditions at

each location. However, it is difficult to prove any specific effects.

If one accepts the views of Raj (1976) that the phenol content is an indicator of diagenetic history, lignite #1 and subbituminous C coal #9, which have similar -OH contents, would originate from similar plant material. On the other hand, subbituminous C coals #2 and #9 have significantly different -OH concentrations despite originating from the same geological formation at separations of a few hundred kilometers. Perhaps small differences in environmental conditions, e.g. pH, temperature, seam depth and climatic changes, have influenced the compositions of the coals.

In light of the data presented here, variations in O-bearing functional group concentrations reflect considerable differences in the chemistry and reactivity of the coals. In these circumstances equivalent elemental compositions should not be expected to show the same chemical reactivity. Any reactions which are specific to a preferred oxygen site will be affected by such differences in oxygen partitioning. Some differences in reactivity are seen in conversion experiments with these coals (Berkowitz et al., 1988). Chemical variations will influence behaviour of both /b coals and subbituminous coals. Surface properties of coals and, consequently, processing of coals would be affected by variation in partitioning of oxygen.

4.5 Observations respecting Experimental Methods

Schafer (1970a, 1983) showed that carboxylic acids in subbituminous coals can be determined by ion exchange against barium acetate. Takeya et al. (1965) and Hatami et al. (1967) modified the methods by using specific equilibration times for ion exchange, then titrating the acetic acid back to pH 8.25, using a phenolphthalein indicator. In the current work, automated potentiometric titration did not involve an indicator. Fig.7 shows the titration plot of unbuffered acetic acid produced from hydrolysis of the acetylated coals, after passing through the ion exchange column. Fig.8 shows the titration curves of a buffered system for determination of carboxylic oxygen.

The standard method for preparation of a barium acetate solution of pH 8.25 involves dissolving 15.33g/l barium acetate and diluting this stock until pH 8.25 is achieved. It was found that the stock was already at pH 8.25 without dilution. Any dilution of the above stock changed the buffering capacity and the pH decreased. Dilution of the buffering capacity of the filtrate with de-ionized water caused barium hydroxide to precipitate when the filtrate was titrated with NaOH. This effect is clearly shown in the titration curve of Fig. 9. In the presence of an indicator dye, precipitation would not be observed and the data would be erroneous. To avoid precipitation, the exchanged coals were rinsed with a barium acetate solution, and dilution by water was thereby minimized.

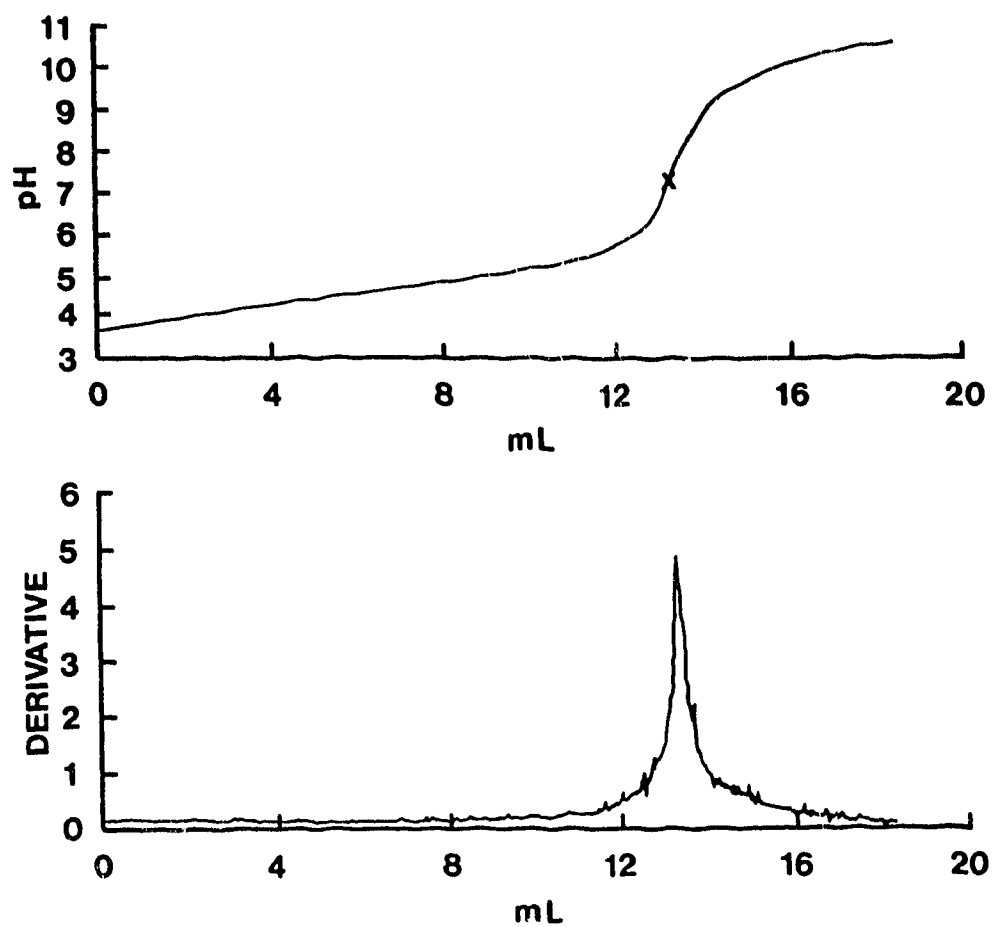


Fig. 7 Typical titration and derivative curves of unbuffered filtrate of ion exchanged hydrolysate of acetylated coal. Titrant is .05M NaOH.

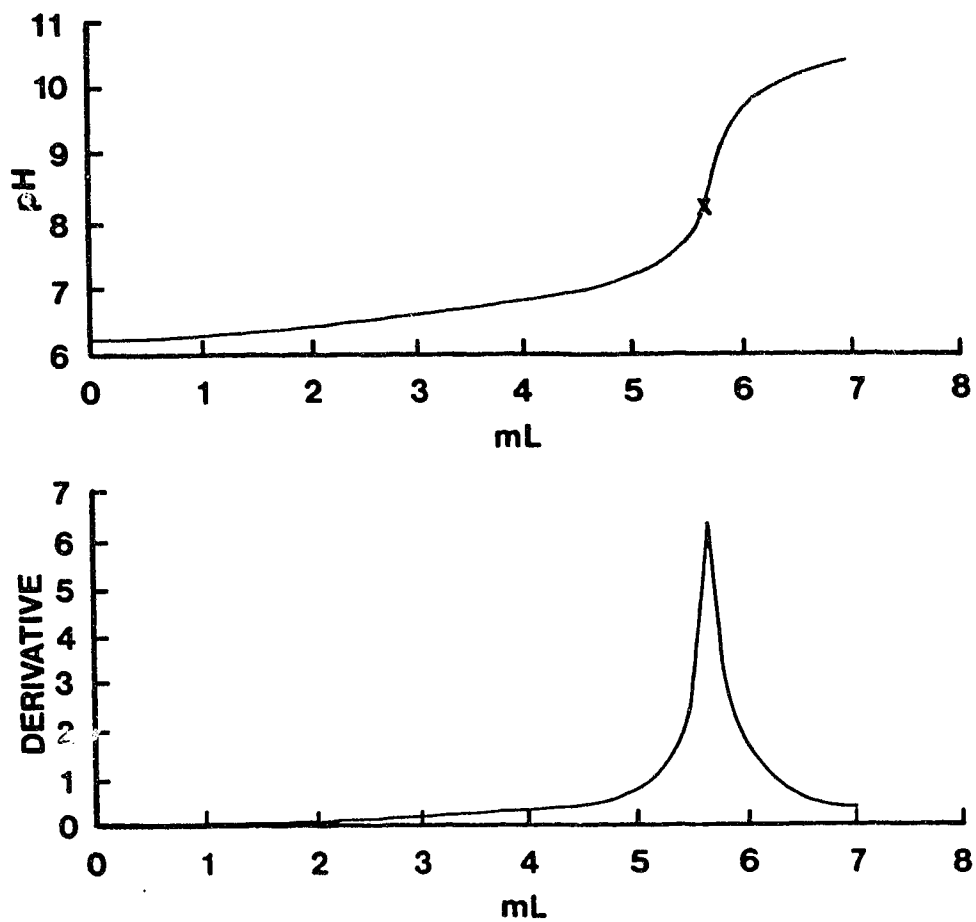


Fig. 8 Titration and derivative curves of filtrate from a coal exchanged against barium acetate and buffering capacity is undiluted. Titrant is .05M NaOH.

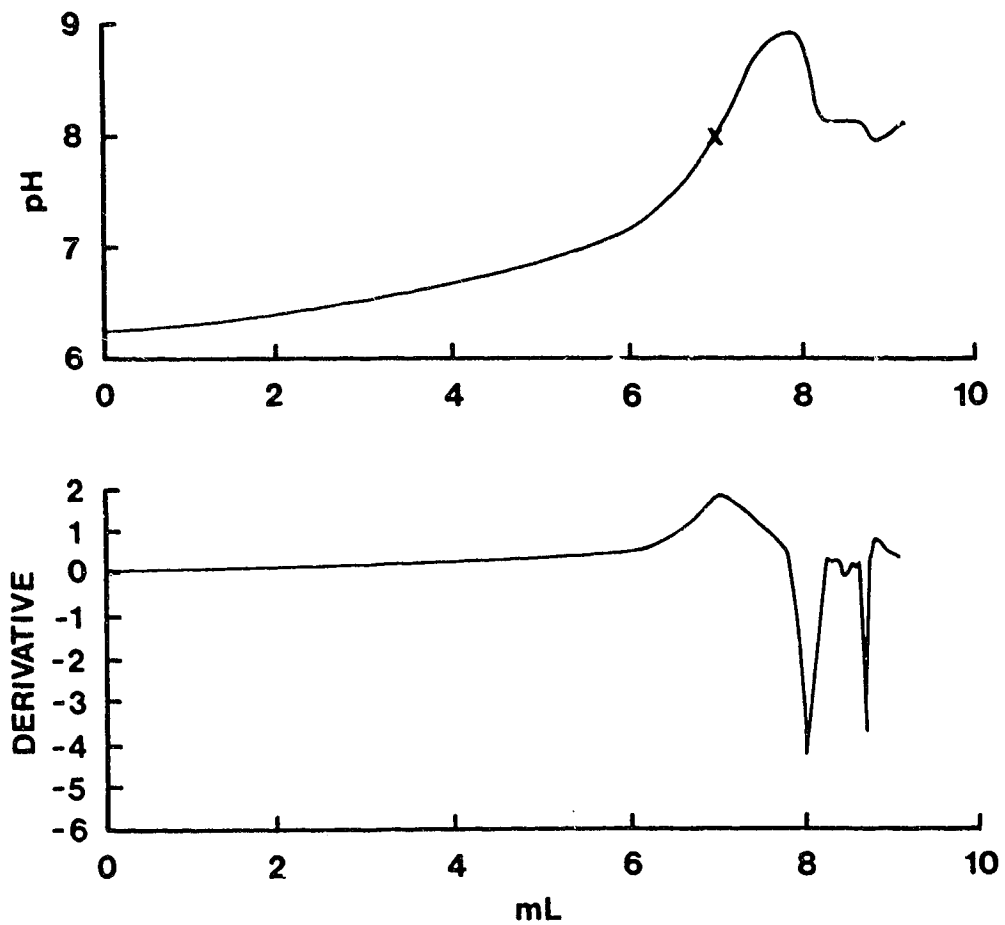


Fig. 9 Titration and derivative curves of filtrate from a coal exchanged against barium acetate. Buffering capacity is reduced and $\text{Ba}(\text{OH})_2$ precipitates. Titrant is .05M NaOH.

4.6 Qualitative Variations among Coals as detected by FTIR-PAS

It was intended that within the scope of this study FTIR-PAS would only be used in qualitative checks for the completion of chemical reactions. However, during the initial characterization of the protonated coals by FTIR-PAS, some differences were observed in the coal spectra. These spectra are included for the interested reader (Figs. 10 - 14e, Appendix 4).

The mid infrared region between 4000cm^{-1} and 400cm^{-1} of the coal spectra is shown in Appendix 4. The typical coal spectra show minor differences in the intensities of functional group bands. Fig. 10 shows typical superimposed spectra of coals #2, #1, #7, and #4 on the same scale. Despite wide differences in intensities of the peaks, intensities for the -OH stretch region (3300cm^{-1}) do not correspond to the actual -OH analysis, possibly because of the presence of moisture which influences these bands. The subbituminous coals and the lignite show little qualitative differences except for the 1700cm^{-1} region assigned to [-COOH]. Coal #1 has the most pronounced shoulder.

Variations in Alberta coals of different rank are shown in Fig. 11 where coals #11 (subbituminous C), #10 (hvb) and #20 (mvb) are compared. The mvb coal #20 shows aromatic CH stretch at 3030cm^{-1} . In coal #10 there is some evidence of aromatic CH stretch which is not as resolved in #11. Otherwise, little qualitative differences between coal #10 and coal #11 are observed except for the -OH region at 3300cm^{-1} . Different batches of #10 and #11 are compared in Fig. 12 (Appendix 4) but the differences between these coals seem negligible. The

apparently similar spectra of these coals may suggest that surface functional groups are nearly identical. The tendency of coal #10 to cluster with the lower rank coals shown previously in Figs. 3, 4 & 5. indicate a possible reason for such properties.

Differences between coal #10 and #14, which are U.Cret./Tert. and Carb. age but of similar rank, are shown in the 3030cm^{-1} aromatic CH stretch band, and 900cm^{-1} (fingerprint aromatic) region. Higher intensities are also observed for #14 as compared to #10 in the $1000 - 1500\text{cm}^{-1}$ region. The fingerprint region depicts stronger aromatic band intensities for #14 than #10 (Fig.13, Appendix 4). Also, a 1700cm^{-1} shoulder is noticeable in #10 and not in #14. This qualitative difference is corroborated by analytical data for $[-\text{COOH}]$.

The various derivatives of coal #4 are shown in Appendix 4 (Figs.14a-14e) as examples of completed reactions involved in the analysis of the oxygen functional groups. The most pronounced difference between the original and acetylated coals is the elimination of the $-\text{OH}$ band at 3300cm^{-1} . Spectra such as these verified that the reaction did indeed take place.

CHAPTER 5

RESULTS AND DISCUSSION II- THERMAL STABILITY

5.1 Introduction

Even relatively mild pyrolysis causes appreciable structural changes in coals. At temperatures below 600°C aliphatic and hydroaromatic moieties form primary tar and gases (Van Krevelen et al., 1957; Given, 1960; Mazumdar & Chatterjee, 1972). Some decarboxylation and dehydroxylation, with consequent condensation reactions are indicated as possible in the 175°C - 200°C range (Berkowitz, 1979). With structural changes in the coals during pyrolysis, it is expected that there will be appreciable changes in oxygen functional group distributions. However, the extent of structural rearrangements (which includes losses of functional groups) depend on the rate of heating, the atmosphere in which heating is conducted, and the temperature.

Heating rate effects have been thoroughly studied and reviewed by weight loss curves, using thermogravimetry (Howard, 1981), but there are few data for thermal stability of oxygen functional groups, particularly at temperatures below the nominal decomposition temperature (T_d) of coal.

The effects of mild thermal pretreatments on the distribution of O-bearing functional groups were studied in the early 1950s, but little information was then sought about the temperature-time relations. Data only covered oxygen functional groups of chars and semicokes from Carboniferous bituminous coals (Ihnatowicz, 1954; Uporova & Rafikov, 1956; Maher, 1957). The

general conclusion was that there were decreases in acidic functional groups. Stadnikov et al. (1936) had earlier concluded that while -OH was stable up to 350°C, decarboxylation was almost completed below 375°C. Kreulen & Kreulen van Selms (1957) noted the loss of carboxyl groups during prolonged heating of lignite and dopplerite at 150°C and 175°C.

Gradual elimination of -COOH around 200°C and almost complete elimination of -COOH at 300°C were reported for Australian brown coals (Brooks & Sternhill, 1957; Brooks et al., 1958). With these coals, pyrolysis was conducted at temperatures up to 600°C, but the heating rate was 5-7°C/min, and final temperatures were held for 2-5 hrs. Little change in =CO and only small decreases in -OH measured by infrared spectroscopy at 3300cm^{-1} were observed below 300°C.

There are large differences in the temperature at which -OH is reported to be lost. Brooks & Maher (1957) as well as Brown (1955b) found little loss of -OH from bituminous coals below 400°C, but Friedel & Queiser (1956) observed significant losses near 360°C. Even at low temperatures the complex structural changes in coal are expected to be influenced by heating rates and temperature-time histories.

The results presented here show the concentrations of oxygen in three O-bearing functional groups (-OH, =CO, -COOH) for a suite of coals which were mildly pyrolyzed in a stream of nitrogen at final temperatures of 200°C and 300°C. Target temperatures were reached by slow heating starting with coals which were initially dried in vacuo at 100°C for 20h (and in a

few cases at 70°C and 100°C sequentially, each for 20h in vacuo) then slowly cooled to room temperature. Selected low rank coals were heated rapidly, cooled rapidly and analyzed only for oxygen in -COOH functional groups. The results are separated into two categories:

(i) slow heating in nitrogen to the final temperature - (to reach 200°C the coals were heated at approximately 3.8°C/min and held at 200°C for 20h; Similarly, to reach 300°C the coals were heated at approximately 3.4°C/min and held for 0.5h);

(ii) fast heating at the desired temperature - (in this case the coals were placed in a furnace at 200°C or 300°C for 0.5h).

The purpose of these experiments was to determine whether the loss of O-bearing functional groups is affected by heating at the temperatures indicated above. The study of slow heating effects on reactive O-bearing functional groups of all coals, was designed to determine the extent of functional group redistribution or re-partitioning. Fast heating of low rank coals at 200°C and 300°C provides comparative data for testing temperature-time-heating rate effects on decarboxylation. 20h of slow heating is considered adequate for equilibrium.

Detailed data for concentrations of oxygen in O-bearing functional groups are given in the Appendix 1. $[O_{OH}]$, $[O_{CO}]$ and $[O_{COOH}]$ were determined for all coals except coal #4 (subbit.C) and coal #20 (mvb). After fast heating, only $[O_{COOH}]$ in coals #1, #2, #7 and #9 were measured.

Tables 5 & 6 summarize data for the absolute concentrations of oxygen in each O-bearing functional group, the total oxygen concentrations and the fraction of this total for each group after slow heating at 200°C and 300°C. Figures 5.1, 5.2, and 5.3 present graphs of $[O_{OH}]$, $[O_{CO}]$ and $[O_{COOH}]$ versus $[O]$ after heating at 100°C, 200°C and 300°C respectively.

Differences in $[O_{COOH}]$ between low rank coals after slow and fast heating at 200°C and 300°C are shown in Table 7, and linear regression plots of $[O_{COOH}]$ versus $[O]$ after fast heating at 300°C and 200°C respectively for the same coals are presented in Fig. 5.4. The results are discussed in terms of variations in coals of different rank and origin. Trends are derived from regression lines for absolute concentrations of oxygen in O-bearing functional groups versus total oxygen in the heated coals. For a pictorial representation of the coals before and after heat treatment, Figs. 5.8 to 5.15 show pie charts of O-bearing functional groups as fractions of total oxygen in the heat-treated coals. These diagrams illustrate redistribution of the O-bearing functional groups relative to each other after heat treatment.

The FTIR-PAS spectra of coals after slowly heating are presented in Figs. 5.5, 5.6, and 5.7, Appendix 4, and may be compared with the quantitative data presented in Tables 5 & 6. The FTIR-PAS technique is more surface- than bulk oriented- and therefore samples functional groups closer to the coals surface.

**Table 5 Oxygen distribution after slow heating (200°C, N₂ 8 cc/min, 20 h),
all concentrations in weight percentage daf coal.**

Coal	[O]	[O _{OH}]	$\frac{[O_{OH}]}{[O]}$	[O _{CO}]	$\frac{[O_{CO}]}{[O]}$	[O _{COOH}]	$\frac{[O_{COOH}]}{[O]}$	$\frac{[O_{res}]}{[O]}$
2	21.4 ± 0.0	9.5 ± 0.4	44.4 ± 2.0	5.3 ± 0.3	24.6 ± 1.5	2.8 ± 0.3	13.0 ± 0.8	18.0 ± 0.8
9	21.4 ± 1.0	9.5 ± 0.1	44.5 ± 2.0	4.3 ± 0.1	20.0 ± 1.0	2.4 ± 0.0	11.3 ± 0.6	24.2 ± 0.8
11	19.7 ± 0.4	9.9 ± 0.1	50.4 ± 1.0	3.8 ± 0.1	19.5 ± 0.6	2.2 ± 0.0	11.2 ± 0.3	18.9 ± 2.2
1	20.7 ± 0.4	8.5 ± 0.2	40.9 ± 1.5	4.0 ± 0.1	19.1 ± 0.8	3.2 ± 0.1	15.3 ± 0.6	24.7 ± 1.7
10	16.6 ± 0.6	8.2 ± 0.0	49.1 ± 1.5	3.0 ± 0.0	18.5 ± 0.7	1.1 ± 0.0	6.7 ± 0.3	25.6 ± 3.4
14	7.2 ± 0.0	3.9 ± 0.1	53.8 ± 1.1	1.4 ± 0.2	20.0 ± 2.1	0.3 ± 0.1	3.8 ± 1.1	22.4 ± 0.1
16	8.8 ± 0.2	5.4 ± 0.4	61.8 ± 4.3	1.3 ± 0.1	15.2 ± 1.1	0.1 ± 0.0	0.9 ± 0.1	22.1 ± 0.6

Standard deviations less than ± 0.05 are rounded to ± 0.0 .
Ratios are multiplied by 100.

**Table 6 Oxygen distribution after slow heating (300°C, N₂ 8 cc/min, 0.5 h),
all concentrations in weight percentage daf coal.**

Coal	[O]	[O _{OH}]	$\frac{[O_{OH}]}{[O]}$	[O _{CO}]	$\frac{[O_{CO}]}{[O]}$	[O _{COOH}]	$\frac{[O_{COOH}]}{[O]}$	$\frac{[O_{res}]}{[O]}$
2	19.7 ± 0.5	11.0 ± 0.1	56.3 ± 1.7	5.6 ± 0.4	28.5 ± 2.0	1.3 ± 0.1	6.6 ± 0.4	8.7 ± 0.2
9	24.0 ± 0.4	9.8 ± 0.1	40.9 ± 0.8	4.3 ± 0.3	17.8 ± 1.3	2.3 ± 0.0	9.6 ± 0.0	31.7 ± 1.4
11	18.5 ± 0.3	10.4 ± 0.4	55.9 ± 1.1	3.0 ± 0.1	16.2 ± 0.5	1.4 ± 0.2	7.3 ± 0.9	20.6 ± 0.0
7	16.0 ± 0.9	8.7 ± 0.0	54.6 ± 3.1	4.1 ± 0.2	25.7 ± 0.1	2.5 ± 0.2	15.5 ± 1.0	4.4 ± 0.2
1	19.8 ± 0.5	9.4 ± 0.0	47.7 ± 1.0	3.4 ± 0.1	16.9 ± 0.8	1.4 ± 0.2	7.1 ± 0.8	28.3 ± 2.2
10	16.7 ± 0.5	8.6 ± 0.1	51.6 ± 1.6	3.0 ± 0.2	17.9 ± 0.4	0.5 ± 0.0	2.9 ± 0.1	26.8 ± 7.7
14	7.5 ± 0.1	3.6 ± 0.1	47.5 ± 1.0	1.1 ± 0.4	15.0 ± 5.1	0.2 ± 0.0	3.2 ± 0.5	34.4 ± 0.3
16	9.2 ± 0.5	4.9 ± 0.1	53.4 ± 2.7	1.8 ± 0.2	19.5 ± 1.9	0.1 ± 0.0	0.6 ± 0.1	26.8 ± 4.8

Standard deviations less than ± 0.05 are rounded to ± 0.0 .

Ratios are multiplied by 100.

Table 7 Comparison of carboxyl oxygen for low rank coals, rapidly heated in N₂ (12 cc/min).

T = 200 °C (0.5 h)				T = 300 °C (0.5 h)		
Coal	[O]	[O _{COOH}]	$\frac{[O_{COOH}]}{[O]}$	[O]	[O _{COOH}]	$\frac{[O_{COOH}]}{[O]}$
1	20.0 ± 0.3	3.1 ± 0.1	15.7 ± 0.7	16.9 ± 0.2	0.5 ± 0.0	3.1 ± 0.1
2	22.2 ± 0.3	2.9 ± 0.1	13.2 ± 0.4	19.2 ± 1.5	0.7 ± 0.0	3.7 ± 0.3
7	21.9 ± 1.4	2.6 ± 0.0	12.1 ± 0.8	17.1 ± 0.6	0.5 ± 0.0	3.1 ± 0.3
9	16.9 ± 0.7	2.4 ± 0.2	14.4 ± 1.3	15.8 ± 1.0	0.4 ± 0.0	2.8 ± 0.2

Standard deviations less than ± 0.05 are rounded to ± 0.0 .

Concentration in % daf coal.

Ratios are multiplied by 100.

Pyrolytically generated differences as shown by wet analytical techniques may not be shown in the FTIR-PAS spectra.

5.2 Slow Heating

5.2.1 Thermal Stability of Hydroxyl Oxygen

It has been shown in chapter 4 that concentrations of oxygen in O-bearing functional groups were clustered into distinct populations when plotted against corresponding total oxygen. Fig. 5.1 illustrates that this pattern is maintained for $[O_{OH}]$ versus $[O]$ after heating at 200°C and 300°C. From the regression lines, the general trend of behaviour in slow heat treatment emerges.

High rank coals (low total oxygen) respond differently towards slow heating than low rank coals (high total oxygen). Among the Carboniferous hvb coals $[O_{OH}]$ increases after 200°C whereas the U.Cretaceous/Tertiary hvb coal #10 associates with the lower rank coals and displays little change in $[O_{OH}]$ even though there is a general decrease in total oxygen. This is shown by the decreasing slope of the trend line at 200°C in Fig. 5.1 which is heavily influenced by the Carboniferous hvb coals. There is only slight decrease in total oxygen for all coals (Table 5). Among the low rank coals there is wide scatter in $[O_{OH}]$ versus $[O]$ at 200°C, quite similar to the distribution of $[O_{OH}]$ among the original coals after drying at 100°C. Varied chemistries of individual coals are maintained. However coals #2 and #9 (subbit. C) which are elementally similar yet widely different in

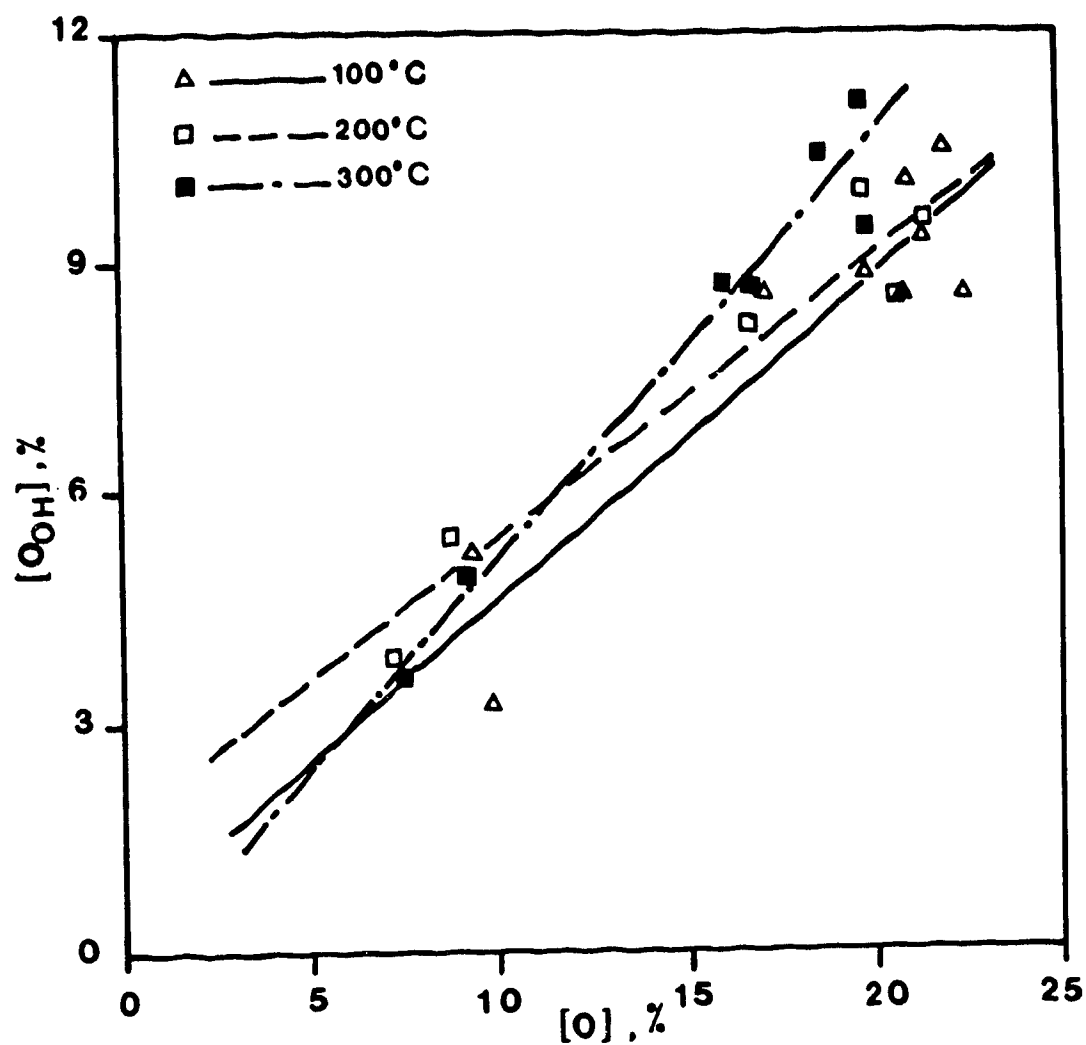


Fig. 5.1 Linear regression plots of $[O_{OH}]$ versus $[O]$ for low and high rank coals after slow heating at (i) 100°C (20h) in vacuo, (ii) 200°C (20h) and (iii) 300°C (0.5h) in N_2 (8cc/min).

O-bearing functional group distribution are becoming closer in total oxygen content as well as in $[O_{OH}]$ after slow heating at 200°C.

After heating at 300°C (0.5h) the trend lines for $[O_{OH}]$ versus $[O]$ appear to deviate from the original data of 100°C. In general, only minor changes occur in Carboniferous hvb coals #14 & #16 as well as in the Cretaceous hvb coal #10. Both #16 and #10 appear to decrease slightly in $[O_{OH}]$, indicating less thermal stability when slowly heated at 300°C.

On the other hand, after heating at 300°C most of the low rank coals show a marked increase in $[O_{OH}]$ with slight decrease in $[O]$. This effect is shown by the shift of the 300°C line towards higher $[O_{OH}]$. The slope of this line indicates that minor decreases occur in total oxygen content of the coals as $[O_{OH}]$ increases absolutely. Coal #9 which showed anomalous behaviour after heating at 300°C was excluded from the 300°C plot as an outlier.

Among the low rank coals the wide scatter in $[O_{OH}]$ indicates once more differences in partitioning of this functional group after 300°C. It would appear that $[-OH]$ in the low rank coals is thermally quite stable at 200°C. But at 300°C the increase in $[O_{OH}]$ may be explained by a conversion of other oxygen forms to $-OH$ groups. Such increases might reflect scission of ether linkages (Fisher & Eisner, 1937). Varying $[O_{OH}]$ among low rank coals indicates varied coal reactivities when slowly heated to 300°C. In some, but not all instances,

time and temperature-dependent molecular rearrangements seem to occur.

Qualitative data from the FTIR-PAS spectra of individual coals (e.g. subbit. C #9 at 200°C, Fig. 5.7 Appendix 4) showed decreased intensity of the 3300cm^{-1} region. Since infrared quantitative data reportedly (Solomon, 1981) have an accuracy of $\pm 10\%$ for any functional group, the decrease in the spectral intensity could be attributed to loss of moisture. On the other hand, the subbit. C coal #11 showed no change in $[\text{O}_{\text{OH}}]$ at 200°C and a decrease at 300°C (Tables 5 & 6). These changes were qualitatively corroborated by the FTIR-PAS spectra only at 200°C. This indicates that the sensitivity of the technique is limited to large changes at coal surfaces.

The comparative FTIR-PAS spectra of coal #14 shown in Fig. 5.6 (Appendix 4) exhibit the opposite effect to the quantitative data. In this case, the differences in the loss of water are greater than the increase of -OH groups at 200°C, and so this effect dominates in the 3300cm^{-1} spectra. Little change in the intensity of the 3300cm^{-1} band is observed between 200°C and 300°C.

It would not be surprising, however, if increases in the intensities of 3300cm^{-1} bands are a result of internal condensation reactions. It has been confirmed that -OH is one of the more stable reactive oxygen functional groups (Attar & Hendrikson, 1982). In studies of liquefaction and pyrolysis it has been found that -OH disappears only at temperatures above 400°C, i.e. during active decomposition of the coal.

5.2.2 Thermal Stability of Carbonyl Oxygen

In Fig. 5.2 the $[O_{CO}]$ versus $[O]$ regression lines at 200°C and 300°C show $[O_{CO}]$ to increase with temperature when coal is slowly heated. The difference between lines for 200°C and 300°C is not significant. Since total oxygen decreases only slightly, the increase in $[O_{CO}]$ after heating at 200°C and 300°C is not reflected in changes of slopes (slopes at 100°C = 0.24, at 200°C = 0.23 and at 300°C = 0.24), but a shift in the y axis direction.

The scatter of data at both temperatures suggests different chemistries of the individual high rank coals. The Carboniferous hvb coals show opposite responses with respect to $[O_{CO}]$ after slow heating at 200°C. While #14 shows an increase, #16 shows a decrease. At 300°C $[O_{CO}]$ in #16 increases whereas #14 shows little or no change from data for the original coal. The Cretaceous/Tertiary hvb #10, however, shows decreases in $[O_{CO}]$ at both temperatures, with the larger decrease appearing after heating at 300°C.

The chemistries of the individual low rank coals with respect to carbonyl oxygen also vary after slow heating at 200°C and 300°C. Some increases in $[O_{CO}]$ are observed after slow heating to higher temperatures. For example, in subbit. coal #2, $[O_{CO}]$ changed from 4.7% to 5.3% after 20h at 200°C, and more significantly to 5.6% after 0.5h at 300°C. The scatter in $[O_{CO}]$ versus $[O]$ is larger after heating at 300°C, again suggesting varying response of the coals to temperature. The fractions of $[O_{CO}]/[O]$ appears pictorially in Figs. 5.8 -5.13.

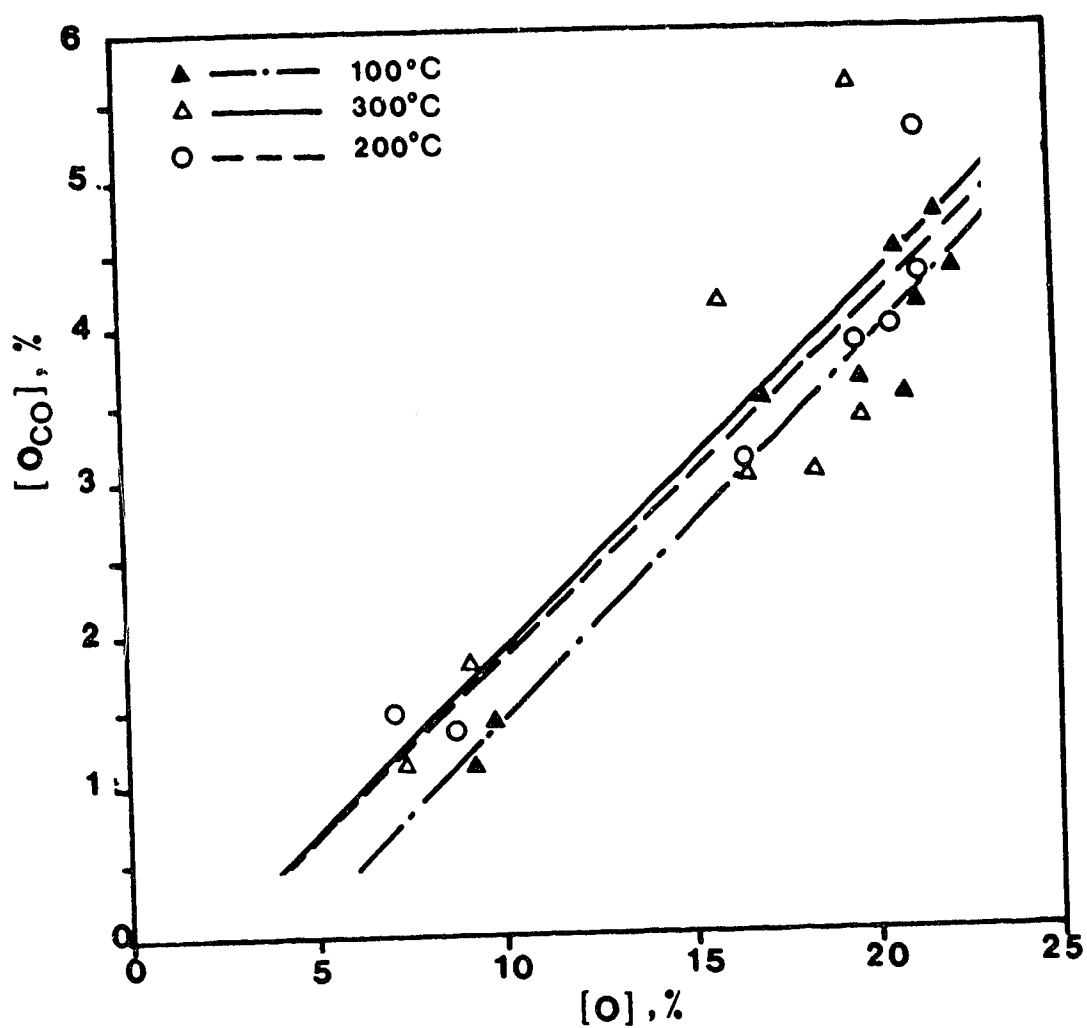


Fig. 5.2 Linear regression plots of $[O_{CO}]$ versus $[O]$ for low and high rank coals after slow heating at (i) 100°C (20h) in vacuo, (ii) 200°C (20h) and (iii) 300°C (0.5h) in N_2 (8cc/min).

The FTIR-PAS spectra for coal #11 in Fig. 5.5 (Appendix 4) show that the 1600cm^{-1} region, identified in part with =CO stretch, increased in intensity as the temperature increased. This qualitatively corroborates the 200°C , data but not the 300°C data. For coal #9 at 200°C a small intensity decrease of the 1600cm^{-1} band is observed (Fig. 5.7 in Appendix 4); and for the higher rank Carboniferous coal #14, the FTIR-PAS spectra at three temperatures (Fig. 5.6 in Appendix 4) showed no obvious differences in relative intensity between 200°C and 300°C in the 1600cm^{-1} region. These results cannot be conclusive as there is much controversy about the assignment of the 1600cm^{-1} band and other functional groups may be influencing the intensities by band overlap.

Where there are little changes in total oxygen and increases in $[\text{O}_{\text{CO}}]$, there is reasonable inference that =CO is formed from other forms of oxygen in the coal. A possible chemical reaction path is offered in section 5.4.

Japanese coals are reported to show increase in $[\text{O}_{\text{CO}}]$ only when bituminous coals with 86%C-88%C were heated at 200°C and 300°C (Hatami et al., 1967). This is in agreement with Fig. 5.2 for Carboniferous coals and some of the lower rank coals (#2, #11, #7). Others (Lynch et al., 1985) have observed increases in $[\text{O}_{\text{CO}}]$ when a Western Canadian mhb coal and an Eastern Canadian hvb coal were heated in nitrogen at 150°C - 200°C , and explained this by postulating conversion of peroxides to carbonyl structures. Peroxides are short lived, and known to develop during atmospheric oxidation of coals (Berkowitz, 1989). However,

Lynch et al. relied entirely on FTIR-PAS spectra, and in such spectra there is still controversy about the ν_{COOH} assignment (Painter et al., 1981a).

5.2.3 Thermal Stability of Carboxyl Oxygen

In the case of the U.Cretaceous/Tertiary hvb coal #10 significant decreases in $[O_{\text{COOH}}]$ were observed at both 200°C and 300°C (Table 5 & 6, Fig. 5.13), but the Carboniferous counterparts #14 and #16 showed only insignificant changes at these temperatures (Figs. 5.3 and Figs. 5.14 - 5.15). Even after long hours of heating, $[O_{\text{COOH}}]$ in these coals did not approach zero. According to the literature, coals of such high carbon content should be devoid of $[O_{\text{COOH}}]$. The refinement in the method of analysis (see chapter 3) is probably responsible for this apparent difference.

For all low rank coals, $[O_{\text{COOH}}]$ decreased significantly when slowly heated to 300°C (Tables 5 & 6, Fig. 5.3). Decrease in $[O_{\text{COOH}}]$ is more pronounced at 300°C than at 200°C. The larger decrease after slowly heating to 300°C is accompanied by a small decrease in total oxygen $[O]$. However, the regression trend lines in Fig. 5.3 show decreasing slopes as temperatures increased, suggesting a greater decrease in $[O_{\text{COOH}}]$ relative to $[O]$ (slopes at 100°C = .23, at 200°C = .19 and at 300°C = .12 respectively).

The low rank coals show a great deal of scatter in $[O_{\text{COOH}}]$ after slowly heating at both temperatures (Figs. 5.3, 5.4). However, less scatter is observed after slowly heating at

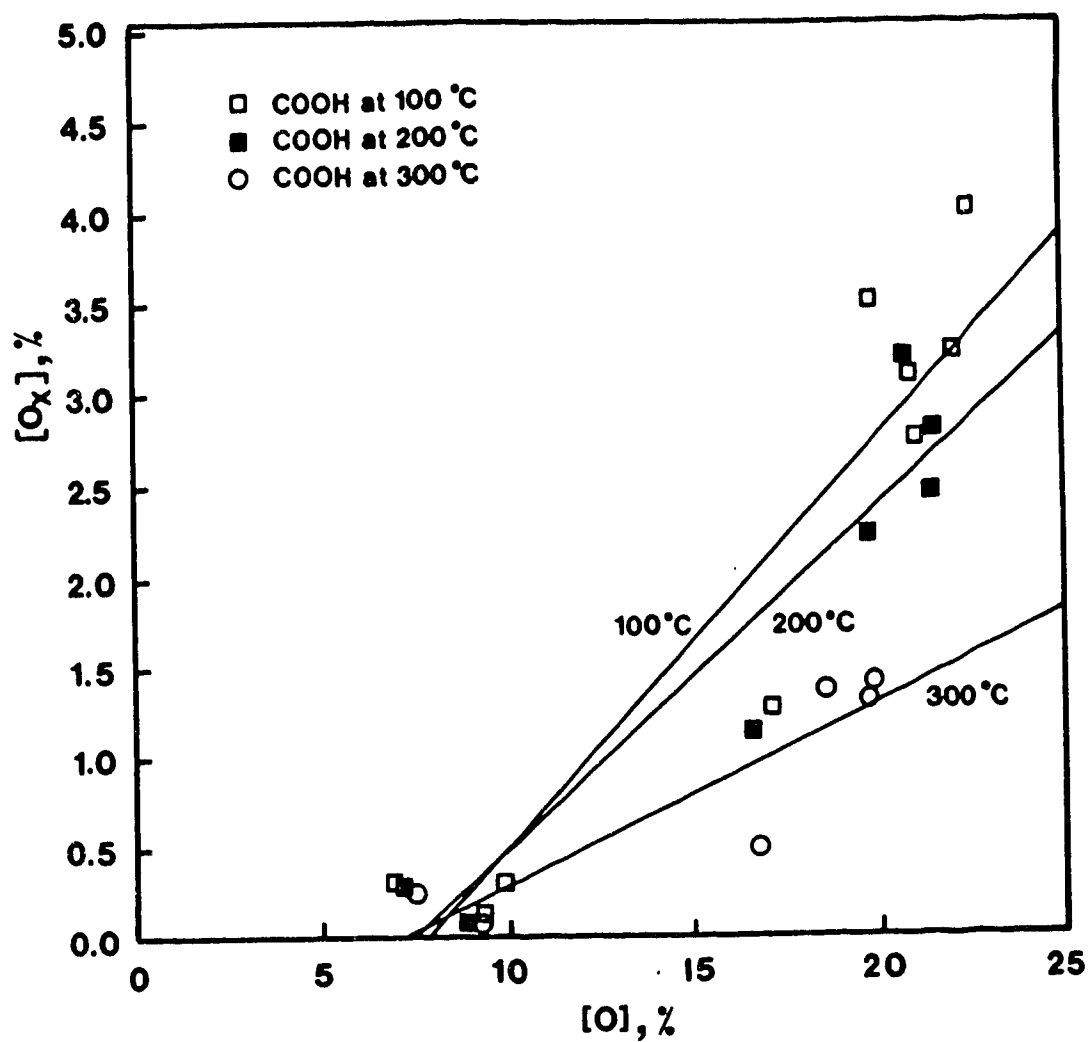


Fig. 5.3 Linear regression plots of $[O_{\text{COOH}}]$ versus $[O]$ for low and high rank coals after slow heating at (i) 100°C (20h) in vacuo, (ii) 200°C (20h) and (iii) 300°C (0.5h) in N_2 8cc/min.

300°C. The temperature effect is more marked than the time effect, since longer times of heating at 200°C (20h) still produced higher $[O_{COOH}]$ than heating at 300°C (0.5h).

Decreases in $[O_{COOH}]$ are consistent with observations reported elsewhere for Texas lignites and Australian brown coals (Schafer, 1979a; 1979b). Schafer found the rate of elimination of carboxylic acids depended on the cation attached to the COO-group. In the early 1950s coals were mildly pyrolyzed and functional groups were analysed and in most instances, decreases in $[O_{COOH}]$ with increasing temperature were noted. The extent of decarboxylation often varied widely, (Ihnatowicz, 1952; Maher, 1957; Uporova & Rafikov, 1956; Brooks & Maher, 1958; Brooks & Sternhill, 1957). Gradual elimination of $[O_{COOH}]$ was observed at 200°C and complete elimination at 300°C (Brooks & Maher, 1958; Brooks & Sternhill, 1957). However, rates of heating were rarely specified.

5.3 Effects of Rapid Heating on Carboxyl oxygen

5.3.1 Comparison of Slow and Fast Heating

Effects of slow and fast heating on $[O_{COOH}]$ versus $[O]$, are shown in the scatter about the lines in Fig. 5.4. Values of $[O_{COOH}]/[O]$ for low rank coals are also shown in the pie charts (Figs. 5.8 - 5.12a). Fig. 5.4 demonstrates that the data for slow and fast heating at 200°C show generally little differences in $[O_{COOH}]$ between slowly and rapidly heated coal in

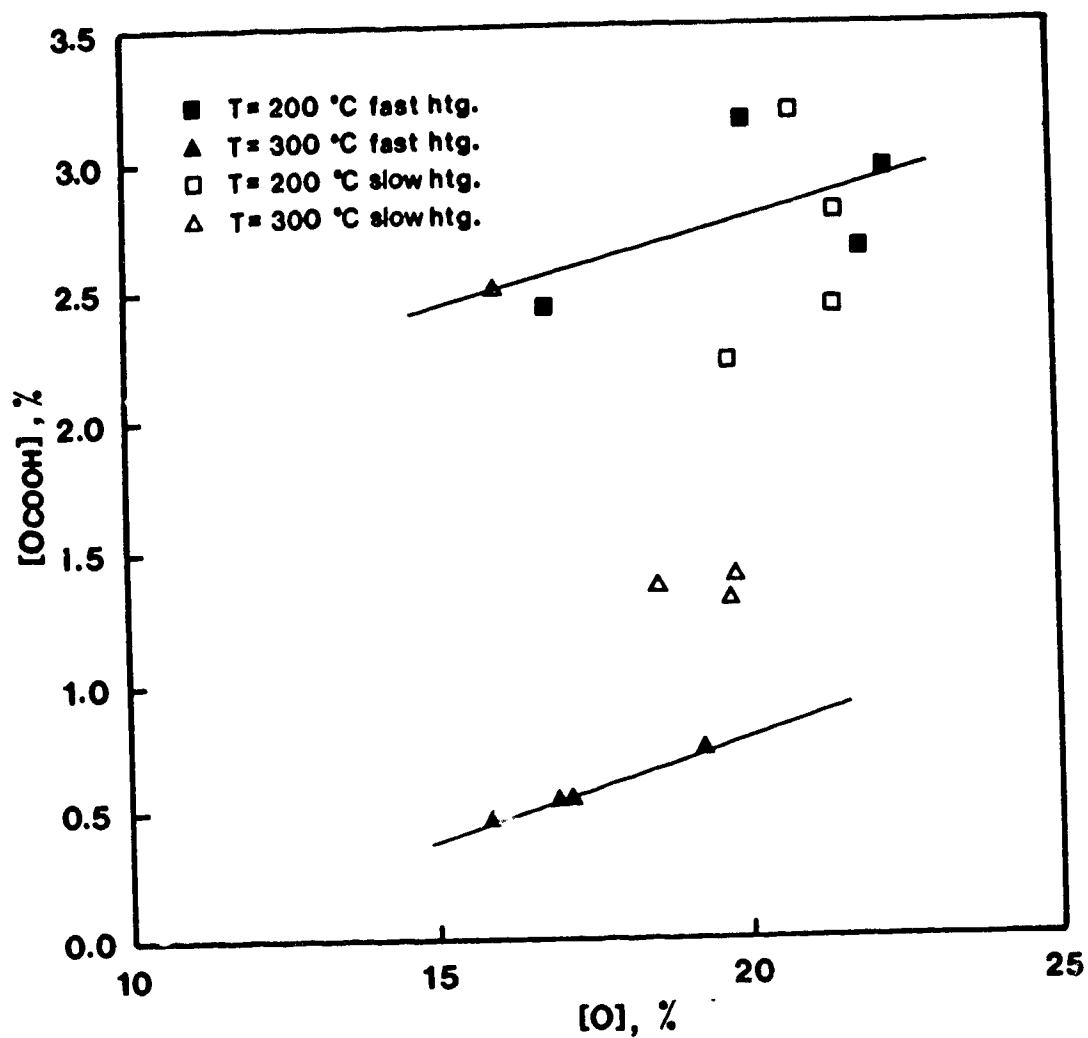


Fig. 5.4 Comparison of $[O_{COOH}]$ versus $[O]$ for low rank coals after slow and fast heating at (i) 200°C (0.5h) and (ii) 300°C (0.5h). Solid lines are linear regression plots for fast heated coals.

3 out of 4 cases. Small differences were not in proportion to the times of heating, since fast heating to 200°C was for only 0.5h as compared to 20h for slow heating. This suggests that at slow heating, time is not as important a factor as temperature. However, some internal molecular rearrangements are taking place since decreases in $[O]$ are minimal and other functional groups are increasing (for a pictorial representation of the chars, see pie charts). At fast heating, the temperature seems more important.

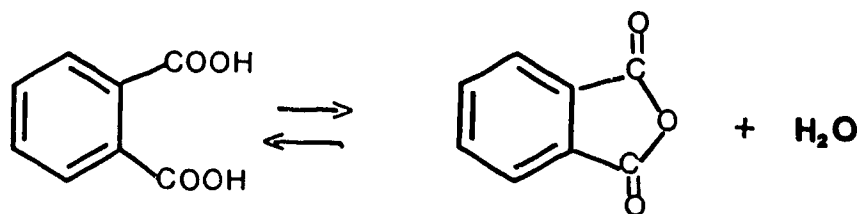
At 300°C fast heating always resulted in larger decreases in $[O_{COOH}]$ and less data scatter than slow heating (Fig. 5.4, Table 7, Figs. 5.8 - 5.12a). Since time was constant at 0.5h for both slow and fast heated coals, the large difference is directly attributable to the heating rate.

5.4 Inferences and Explanations of Observed Trends.

The redistribution of O-bearing functional groups after mild pyrolysis allows several inferences. Slow heating at 200°C and 300°C indicates several molecular rearrangements with $[O_{CO}]$ changing in two ways. In most instances it increased while total oxygen decreased, thus raising $[O_{CO}]/[O]$ in some coals. In other instances, $[O_{CO}]$ decreased slightly. This leads one to suspect complex conversion of other O-bearing groups to carbonyl entities. At 200°C, $[O_{OH}]$ increases in high rank coals but hardly changes in low rank coals. At 300°C an increase in $[O_{OH}]$ in low rank coals is noted, but in some high rank coals there is a tendency of $[O_{OH}]$ to decrease.

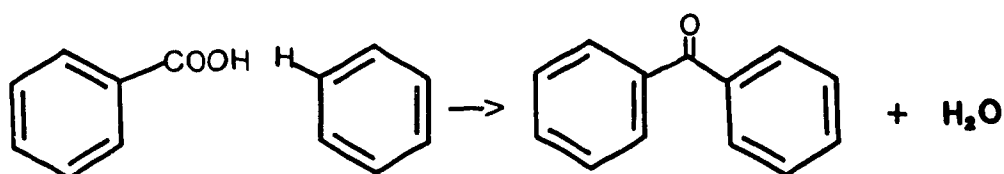
It is also noted that $[O_{COOH}]$ decreased by different amounts depending on the temperature and rate of heating. Since $-COOH$ may be lost via elimination of CO_2 , CO and/or H_2O and free radicals may form at peripheral functional groups, one can only speculate. However, two reaction paths are plausible for some of the observations respecting decarboxylation.

The first involves anhydride formation i.e



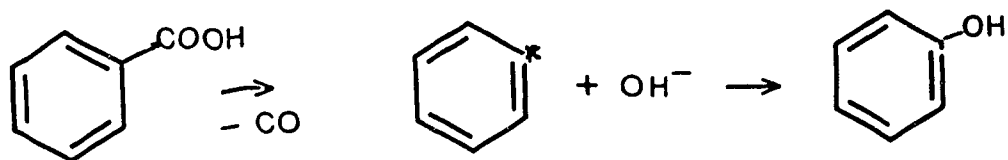
and rehydration when moisture is not quickly evolved. There are perhaps two rates of reaction R_1 and R_2 (reverse). At high heating rates H_2O leaves quickly, and $R_1 > R_2$. Rehydration is more likely to occur with slow heating (which changes the internal structure of the coal, and perhaps traps water in pockets). Thus smaller decreases in $[O_{COOH}]$ are then observed.

A second mechanism involves a condensation reaction of this type



which would lead to high $[\text{O}_{\text{CO}}]$ and large decreases in $[\text{O}_{\text{COOH}}]$. Since nothing is definitely known about the thermal stability of the residual O-bearing functional groups or the exact pathway of decarboxylation, material balances are not possible.

If, however, $[\text{O}_{\text{COOH}}]$ is lost via elimination of carbon monoxide, the following



may account for observed increases in $[O_{OH}]$ in low and high rank coals after slow heating.

5.5 Qualitative Observations on Coal Chemistry after Pyrolysis.

For most coals, the pyridine extracts of acetylated heat-treated coals were far darker than those of the original coals. It was also observed that in some instances (e.g. #7) heating conferred greater hydrophobicities on the coal surface. This became apparent when the coals were more attracted to plastic surfaces than to the aqueous phase. For all heat-treated coals, wetting was more difficult than before heating to 200°C or 300°C. This indicates some changes in macropore network of the coals as well as conversion to greater hydrophobicity. This is not surprising as hydrophilicity is associated with the carboxyl groups which are lost during pyrolysis. Thus, surface properties of coals change with thermal history and processing of coals would be affected by these properties.

5.6 Ramifications of Heating rate Effects

Few mild pyrolysis experiments reported in the literature give heating rates. The conclusions drawn in some of these studies may not be as general as heretofore believed. The thermal history of the coals has an important bearing on the distribution of oxygen in functional groups and needs to be considered in interpretation of experimental results.

Although the making and breaking of bonds must be thermodynamically feasible, in many instances chemical changes

are kinetically governed. Each coal must be considered as an assembly of functional groups or bonds with a given initial distribution of oxygen functional groups which is specific to that coal. In many instances the rate of heating influences the kinetics of reactions in the coal. This was earlier suggested with reference to liquefaction kinetics (Attar, 1978; Messenger & Attar, 1979).

The data reported here clearly indicate that the rate of heating is important in structural changes and may, indeed, influence the preferred reaction pathways.

Maher, T.P., and Schafer, H.N.S. "Determination of acidic functional groups in low-rank coals: comparison of ion-exchange and non-aqueous titration methods." *Fuel* 55(2), 138-140, 1976.

Mazumdar, B.K., Bhangale, P.H. and Lahiri, A. "Further studies on the relative oxygen groups in coal." *Fuel* 36, p. 307-312, 1957.

Mazumdar, B.K., Bhangale, P.H. and Lahiri, A. *J.Sci. Indust. Res.*, B. 15, 44, 1956.

Mazumdar, B.K., and Chatterjee, N.N. "Mechanism of coal pyrolysis in relation to industrial practice", *Fuel* 52(1), 11-19, 1973.

Messenger, L. and Attar, A. "Thermodynamics of the transformations of oxygen and sulfur containing functional groups during coal liquefaction in hydrogen donor solvents." *Fuel* 58(9), 655-666, 1979.

Mrazikova, J., Stanislav, S., Ververka, L., Makak, J., "Evolution of organic oxygen bonds during pyrolysis of coal." *Fuel* 65 (3), 342-345, 1986.

Murata, T., "Deoxidizing, reforming and wettability of the oxygen containing functional groups in coal(III). A study of the wetting of coal." *Nippon Kogyo Kaishi*, 98(1131), 417-422, 1982.

Nandi, B.N., Brown, T.D. and Lee, G.K. "Inert coal macerals in combustion." *Fuel* 56(2), 125-130, 1977.

Nandi, S.P., Kim, R.A., Lahiri, A. "Die reaktivitat von tieftemperatur-verkokungsruckstanden" *Brennst. Chemie* 60, 85, 1959.

Neavel, R.C. "Coal Structure and Coal Science - Overview and Recommendations." in Coal Structure, ACS Adv. Chem. Ser. 192, M.L. Gorbaty and K. Ouchi, eds., p. 1, 1981.

Neavel, R.C., "Origin, Petrography and Classification of Coal" in Chemistry of Coal Utilization, 2nd Suppl. Vol., Elliot, M.A., ed., chapt.3, p. 148, 1981.

Nurkowski, John R. "Coal quality, coal rank variation and its relation to reconstructed overburden, Upper Cretaceous and Tertiary Plains Coals, Alberta, Canada." M.Sc. Thesis, University of Alberta, 1984.

Ode, W.H. "Chemistry of Coal Utilization." Suppl. Vol., Wiley, H.H. Lowry, ed., ch. 5, 1963.

Ouchi, K., Imuta, K. "New oxygen-containing compound isolated from coal." Fuel 52(3), 171-173, 1973.

Painter, P. C., Starsinic, M., and Coleman, M.M. "Determination of functional groups in coal by fourier transform interferometry." Academic Press, John R. Ferraro and Louis J. Basile, eds., Vol. 4, Chapter 5, 1985.

Painter, P.C., Coleman, M.M., Snyder, R.W., Mahajan, O., Komatsu, M. and Walker Jr., P.L., "Low temperature air oxidation of caking coals FTIR studies." Appl. Spectrosc. 35, 106, 1981.

Painter, P.C., Snyder, R.W., Starsinic, M., Coleman, M.M., Kuehn, D.W., Davis, A., "Concerning the application of FTIR to the study of coal: A critical assessment of band assignment and application of spectral analysis programs." Appl. Spectrosc. 35(5), 475-485, 1981.

Perkin Elmer TGS-2/Thermal Analysis Data Station (TADS) System. Norwalk, Connecticut, 1983.

Perkin Elmer TGS-2 Thermogravimetric System. Norwalk, Connecticut, 1981.

Perry, David L., and Grint, A. "Functional group analysis of coal and coal products by x-ray photoelectron spectroscopy." CISTI 31(1), 107-15, 1986.

Perry, D.L., Grint, A., "Functional group analysis of coal products by xray photoelectron spectroscopy." ACS Div. Fuel Chem. Prepr. 31(11), 107-115, 1986.

Plessis, H.G., Reinecke, C.F., Van Nierop, J.G., "The influence of Oxygen containing Surface Functional Groups on Selective Oil Agglomeration Properties of Coal." Proc. Int. Conf. Coal Science, Sydney, Australia, 521-524, 1985.

Raj, Swadesh. "Study of the Chemical Structural Parameters of Coals." PhD. Thesis, The Pennsylvania State University, 1976.

Rosencwaig, A. "Photoacoustics and Photoacoustics Spectroscopy." Wiley-Interscience Publication, John Wiley & Sons, N.Y., 1980.

Ruberto, R.G. and Cronauer, D.C. "Oxygen and Oxygen Functionalities in Coal and Coal Liquids." ACS Symposium Series, CISTI 71 (Org. Chem. Coal), 50-70, 1978.

Schafer, H.N.S. "Determination of carboxyl groups in low rank coals." Fuel 63(5), 723-725, 1984.

Schafer, H.N.S., "Pyrolysis of brown coals. 1. decomposition of acidic groups in coals containing carboxylic groups in the acid and cation forms." Fuel 58(9), 625-667, 1979.

Schafer, H.N.S. "Pyrolysis of brown coals. 2. decomposition of acidic groups on heating in the range 100 -900 C." Fuel 58(9), 673-678, 1979.

Schafer, H.N.S. "Factors affecting the equilibrium moisture contents of low rank coals." Fuel 51(1), 4-9, 1972.

Schafer, H.N.S. "Carboxyl groups and ion exchange in low rank coals." Fuel 49(2), 197-213, 1970.

Schafer, H.N.S. "Determination of total acidity of low rank coals ." Fuel 49(3), 271-280, 1970.

Schwager, I., Yen, T.F. "Determination of nitrogen and oxygen functional groups in coal-derived asphaltenes." Analytical Chemistry 51(4), 1979.

Selvig, W.A. and Ode, W.H. U.S. Bureau Mines Bull. No. 571, 1957.

Sindler, S., Macak, J., Buryan, P., Kohl, M. "Analysis of functional oxygen groups in coal and coal pyrolysis products." Freiburger Forschungsh A., 636, 21-29, 1980.

Smith, G.G. "Coal Resources of Canada", Geological Survey of Canada, Paper 89-4, 1989.

Snape, C.F., Axelson, D.E., Botto, R.E., Delpuech, J.J., Tekely, P., Gerstein, B.C., Pruski, M., Maciel, G.E. and Wilson, M.A. " Quantitative reliability of aromaticity and related measurements on coals by ^{13}C NMR - A debate." Fuel 68(5), 547, 1989.

Snyder, R.W., Painter, P.C., Havens, Koenig, J.L. "The Determination of hydroxyl groups in coal by FTIR and ^{13}C NMR spectroscopy." Appl. Spectros. 37(6), 497-502, 1983.

Solomon, P.R. "Relation Between Coal Structure and Thermal Decomposition Products." in Coal Structure, Am. Chem. Soc., M.L. Gorbaty and K. Ouchi, eds., Chapter 7, 1981.

Solomon, P.R. and Carangelo, R.M. "FT-ir analysis of coal, 2. aliphatic and aromatic hydrogen concentration." Fuel 67(7), 949-959, 1988.

Solomon, P.R. and Carangelo, R. M. "FTIR analysis of coal I. Techniques and determination of hydroxyl concentration." Fuel 61, 663, 1982.

Solomon, P.R. and Carangelo, R.M. "Characterization of Wyoming Subbituminous Coals and Liquefaction Products by Fourier Transform Infrared Spectrometry". EPRI Final Report, Project No. 1604-2, 1981.

Somasundaran, P. "Flotation and Flocculation Chemistry of coal and oxidized coal." Technical Progress Report Sept 15 1987-1988, Columbia Univ., DOE PC79919-5, 1988.

Stadnikov, G., Suiskov, K., and Ushakova, A. "Uber die thermische zersetzung der huminsauren." Brennst. Chem. 17, 381, 1936.

Starsinic, M., Y. Otake, P.L. Walker Jr., and P.C. Painter. "Application of FTIR spectroscopy to the determination of COOH groups in coal." Fuel 63(7), 1002-1007, 1984.

Szladow, A.J. and Given, P.H. "The Role of oxygen functional groups in the mechanism of coal liquefaction." ACS Div. Fuel Chem. Prepr. 23(4), 161-168, 1978.

Takegami, Y., Kajiyama, S. and Yokoyama, C., "Studies on the chemical structure of coal II - hydrogenolysis of bituminous coal and humic acid in the presence of the Adkins copper-chromite catalyst." Fuel 42(7), 291-302, 1963.

Takeuchi, M. and Berkowitz, N. Unpublished data, 1988.

Takeya, G., Itoh, M., Makino, M., Yokoyama, S. "A Study on the Oxygen Containing Groups in Japanese Coals." Report of Hokkaido University No. 35, 1965.

Tartarelli, R., Belli, R. "The Functional oxygenated groups of carbon and their role in water adsorption process when preparing coal/water mixtures." Riv. Combust. 39(9), 241-253, 1985.

Teichmuller, M. and Teichmuller, R. in "Coal and Coal-Bearing Strata" Elsevier, Amsterdam, D. Murchison and T.S. Westoll, eds., 1968.

Tooke, P.B., and Grint, A. "Fourier transform infrared studies of coal." Fuel 62(9), 1003-1008, 1983.

Trevhella, M.J., and Grint, A. "Condensation of phenolic groups during coal liquefaction model compound." Fuel 67(8), 1135-1138, 1988.

Tyler, R.J., "Flash pyrolysis of coals. 1. devolatilization of a Victorian brown coal in a small fluidized reactor." Fuel 58(9), 680-686, 1979.

Uporova, E.P., and Rafikov, S.R., Bull. Acad. Sci. USSR 9:23 Chem Abstr. 50:8992, 1956.

Van der Flier-Keller, E., Fyfe, W.S. "Relationship between inorganic constituent and organic matter in a northern

Ontario lignite." ACS Div. Fuel Chem. Prepr. 32(1), 41-48, 1987.

Van Krevelen, D.W. "Coal: Functional Group Analysis." in Coal: Typology, Chemistry, Physics, Constitution, Elsevier, pp. 160-176, 1961.

Van Krevelen, D.W. "Coal as a Chemical Reactant. Model Compounds." in Coal: Typology, Chemistry, Physics, Constitution, Elsevier, Chapter VIII, 1961.

Van Krevelen, D. W. "Geochemistry of Coal," in Organic Geochemistry, Pergamon Press, N.Y., Irving A. Breger, ed., Chapter 6, 183, 1963.

Van Krevelen, D. W., Wolfs, P.M. and Waterman, H.I. Brennst. Chem. 40, 371, 1959.

Volborth, A., Dahy, J.P., Miller, G.E., "Organic Oxygen Determination in eleven Sulfur-Rich Coals by Fast Neutron Activation." Coal Science and Chemistry, Elsevier, A. Volborth, ed., 417, 1987.

Wachowska, H.M., Nandi, B.N. and Montgomery, D.S. "Oxidation studies on coking coal related to weathering. 4. oxygen linkages influencing the dilatometric properties and the effect of cleavage of ether linkages." Fuel 53(3), 212-219, 1974.

Wender, I., Heredy, L.A., Neuworth, M.B. and Dryden, I.G.C., Chemistry of Coal Utilization, 2nd Suppl. Vol., Wiley - Interscience, New York, M.A. Elliot, ed., 503-521, 1981.

Whitehurst, D.D. "A primer on the chemistry and constitution of coal." in Organic Chemistry of Coal, J.W. Larsen, ed., ACS Symp. Ser. 71, 1978.

Wiser, W.H., Proc. EPRI Conf. on Coal Catal., Santa Monica, CA, ACS Symp. Ser. 71, 29, 1978.

Wyss, W.F. "Hydroxyl groups in bright coals." Chem. and Ind. 34, 1095, 1956.

Yohe, G.R. and Blodgett, E.O. "Reaction of coal with oxygen in the presence of aqueous sodium hydroxide. Effect of methylation with dimethyl sulfate." J. Am. Chem. Soc. 69, 2646, 1947.

Zhou, P. Dermer O.C. and Crynes, B.L. "Oxygen in Coals and Coal Derived Liquids." in Coal Science, Vol. 3, Academic Press, N.Y., M. Gorbaty, J. Larsen and I. Wender, eds., 1984.

Appendix 1

Detailed Experimental Data on O-bearing Functional Groups in Protonated and Heat-treated Coals

Table 1: Oxygen in O-Bearing functional groups in coal #1 (lignite)
(a.) % in coal (daf)
(b.) fraction of total oxygen x 100

Sample Identifier	Thermal History Time (hrs) e Temp (C°)	(a) [O _{CO}]	(b) [O _{CO}]/[O]	(a) [O _{COOH}]	(b) [O _{COOH}]/[O]	(a) [O _{OH}]	(b) [O _{OH}]/[O]
1.H	20 70	4.3±0.3	20.0±1.4	4.0	18.9±0.3	8.5±0.1	40.0±0.9
1a.H	20 70	4.3±0.1	19.3±0.6	4.1±0.1	18.5±0.6	8.4±0.6	37.7±2.8
1ab.H	20 70 } + 20 100 }	4.3±0.1	19.5±0.7	3.9±0.2	17.8±1.2	8.5±0.5	39.2±2.5
1ac.H	20 100			3.9±0.1	16.2±0.3		

(*) after initial drying at 100°C, rapidly heated in a tube furnace under N₂ (12 cc/min)

(**) after initial drying at 100°C, slowly heated in a N₂ purged oven (8cc/min)

Table 1: Continued

Sample Identifier	Thermal History Time (hrs) e Temp (C°)	(a) [O _{CO}]	(b) [O _{CO}]/[O]	(a) [O _{COOH}]	(b) [O _{COOH}]/[O]	(a) [O _{OH}]	(b) [O _{OH}]/[O]
1acP.H (**) <u> </u>	20 100 } + 20 200 }	4.0±0.1	19.1±0.7	3.2±0.1	15.3±0.6	8.5±0.3	40.9±1.5
1acQ.H (**) <u> </u>	20 100 } + 0.5 300 }	3.4±0.1	16.9±0.8	1.4±0.2	7.1±0.8	9.4±0.0	47.7±1.2
1acPt.H (*) <u> </u>	20 100 } + 0.5 200 }			3.1±0.1	15.7±0.7		
1acQt.H (*) <u> </u>	20 100 } + 0.5 300 }			0.5±0.05	3.1±0.2		

(*) after initial drying at 100°C, rapidly heated in a tube furnace under N₂ (12 cc/min)(**) after initial drying at 100°C, slowly heated in a N₂ purged oven (8cc/min)

Table 2: Oxygen in O-bearing functional groups in coal #2 (subbituminous C)
(a.) % in coal (daf)
(b.) fraction of total oxygen x 100

Sample Identifier	Thermal History Time (hrs) Temp (C°)	(a) [O _{CO}]	(b) [O _{CO}]/[O]	(a) [O _{COOH}]	(b) [O _{COOH}]/[O]	(a) [O _{OH}]	(b) [O _{OH}]/[O]
2.H	20 70	4.7±0.3	22.9±2.0	3.0±0.01	14.6±0.9	10.8±0.7	52.8±4.6
2b.H	20 70 + 20 100	4.4±0.4	20.3±1.8	3.0±0.05	13.8±0.5	9.7±0.05	45.2±1.4
2b2.H	20 70	4.7±0.1	21.7±0.9	3.2±0.1	14.7±0.6	10.7±0.9	49.6±4.6
2c.H	20 100	5.1±0.3	21.4±1.4	3.7±0.01	15.4±0.4		

(*) after initial drying at 100°C, rapidly heated in a tube furnace under N₂ (12 cc/min)
(**) after initial drying at 100°C, slowly heated in a N₂ purged oven (8cc/min)

Table 2: Continued

Sample Identifier	Thermal History Time (hrs)	Temp (C°)	(a) [O _{CO}]	(b) [O _{CO}]/[O]	(a) [O _{COOH}]	(b) [O _{COOH}]/[O]	(a) [O _{OH}]	(b) [O _{OH}]/[O]
2cP.H (**)	20 + 20	100 200	5.3±0.3	24.6±1.4	2.8±0.2	13.0±0.8	9.5±0.4	44.4±2.0
2cPt.H (*)	20 + 0.5	100 200			2.9±0.1	13.2±0.4		
2cQt.H (*)	20 + 0.5	100 300			0.7±0.02	3.7±0.3		
2dQ.H (**)	20 + 0.5	100 300			1.2±0.1	6.4±0.5	11.1±0.02	59.2±0.9
2cQ.H (**)	20 + 0.5	100 300	5.6±0.4	27.2±0	1.4±0.5	6.7±0.3	11.1±0.1	53.5±1.6

(*) after initial drying at 100°C, rapidly heated in a tube furnace under N₂ (12 cc/min)(**) after initial drying at 100°C, slowly heated in a N₂ purged oven (8cc/min)

Table 3: Oxygen in O-bearing functional groups in coal #4 (subbituminous C)
(a.) % in coal (daf)
(b.) fraction of total oxygen x 100

Sample Identifier	Thermal History		(a)	(b)	(a)	(b)	(a)	(b)
	Time (hrs)	Temp (C°)	[OCO]	[OCO]/[O]	[OCO _{OH}]	[OCO _{OH}]/[O]	[OOH]	[OOH]/[O]
4.H	20	70	4.0±0.4	19.3±2.0	2.4±0.0	11.3±0.5	9.6±0.4	46.3±2.6
4a.H	20	100	4.1±0.2	18.61±0.7	2.3±0.0	10.6±0.1	8.7±0.0	39.7±0.2

Table 4: Oxygen in O-bearing functional groups in coal #7 (subbituminous B)
(a.) % in coal (daf)
(b.) fraction of total oxygen x 100

Sample Identifier	Thermal History		(a) [Oco]	(b) [Oco]/[O]	(a) [OcoOH]	(b) [OcoOH]/[O]	(a) [OOH]	(b) [OOH]/[O]
7.H	20	100	3.7±0.2	18.2±1.2	3.4±0.1	16.3±0.4	9.0±0.0	43.6±0.3
7a.H	20	100	3.5±0.5	18.2±2.7	3.6±0.1	18.3±0.8	8.7±0.2	45.8±1.4
7aPt.H(*)	20 + 0.5	100 200			2.6±0.0	12.1±0.1		
7aQt.H(*)	20 + 0.5	100 300			0.5±0.0	3.1±0.2		
7aQ.H(**)	20 + 0.5	100 300	4.1±0.2	25.7±1.8	2.5±0.2	15.5±1.3	8.7±0.0	54.4±3.0

(*) after initial drying at 100°C, rapidly heated in a tube furnace under N₂ (12 cc/min)
(**) after initial drying at 100°C, slowly heated in a N₂ purged oven (8cc/min)

Table 5: Oxygen in O-bearing functional groups in coal #9 (subbituminous C)
(a.) % in coal (daf)
(b.) fraction of total oxygen x 100

Sample Identifier	Thermal History Time (hrs) @ Temp (C°)	(a) [OCO]	(b) [OCO]/[O]	(a) [OCO _{OH}]	(b) [OCO _{OH}]/[O]	(a) [OOH]	(b) [OOH]/[O]
9.H	20 100	4.4±0.2	21.2±1.3	3.1±0.0	15.0±0.4	8.5±0.1	40.3±1.3
9b.H	20 100			3.1±0.0	14.9±0.9		
9P.H(**)	20 100 + 20 200	4.3±0.1	20.0±1.0	2.4±0.0	11.3±0.6	9.5±0.1	44.5±2.0
9bPt.H(*)	20 100 + 0.5 200			2.4±0.2	14.4±1.3		
9Q.H(**)	20 100 + 0.5 300	4.3±0.3	17.8±1.3	2.3±0.0	9.6±0.0	9.8±0.1	40.9±0.8
9bQt.H(*)	20 100 + 0.5 300			0.4±0.0	2.8±0.2		

(*) after initial drying at 100°C, rapidly heated in a tube furnace under N₂ (12 cc/min)

(**) after initial drying at 100°C, slowly heated in a N₂ purged oven (8cc/min)

Table 6: Oxygen in O-bearing functional groups in coal #10 (high volatile Bituminous)
(a.) % in coal (daf)
(b.) fraction of total oxygen x 100

Sample Identifier	Thermal History Time (hrs) e Temp (C°)	(a) [OCo]	(b) [OCo]/[O]	(a) [OCoOH]	(b) [OCoOH]/[O]	(a) [OH]	(b) [OH]/[O]
10.H	20 70	3.7±0.0	20.50±0.4	1.4±0.0	7.9±0.2	8.9±0.2	48.8±1.3
10a.H	20 100	3.2±0.1	19.2±0.8	1.4±0.1	8.5±0.9	8.2±0.9	48.8±1.3
10aP.H(**)	20 100 + 20 200	3.1±0.0	18.5±0.7	1.1±0.0	6.7±0.3	8.2±0.0	49.1±1.5
10aQ.H(**)	20 100 + 0.5 300	3.0±0.2	17.5±0.1	0.6±0.0	3.3±0.0	8.3±0.1	48.6±1.9
10bQ.H(**)	20 100 + 0.5 300			0.4±0.0	2.5±0.0	9.0±0.1	54.8±2.2

(*) after initial drying at 100°C, rapidly heated in a tube furnace under N₂ (12 cc/min)

(**) after initial drying at 100°C, slowly heated in a N₂ purged oven (8cc/min)

Table 7: Oxygen in O-bearing functional groups in coal #11 (subbituminous C)
(a.) % in coal (daf)
(b.) fraction of total oxygen x 100

Sample Identifier	Thermal History Time (hrs) @ Temp (C°)	(a) [CO]	(b) [CO]/[O]	(a) [COOH]	(b) [COOH]/[O]	(a) [OH]	(b) [OH]/[O]
11.H	20 70	3.5±0.0	17.8±0.1	3.2±0.0	16.1±0.1	9.9±0.0	50.9±0.2
11a.H	20 100	3.6±0.2	15.9±0.8	2.6±0.1	11.4±0.6	10.0±0.3	44.6±1.6
11b.H	20 70			2.5±0.0	14.72±0.3		
11aP.H(**)	20 100} + 20 200}	3.9±0.1	19.5±0.6	2.2±0.0	11.2±0.3	9.9±0.1	50.4±1.0
11aQ.H(**)	20 100} + 0.5 300}	3.0±0.1	16.20±0.5	1.4±0.2	7.3±0.9	10.4±0.4	55.9±1.1

(*) after initial drying at 100°C, rapidly heated in a tube furnace under N₂ (12 cc/min)
(**) after initial drying at 100°C, slowly heated in a N₂ purged oven (8cc/min)

Table 8: Oxygen in O-bearing functional groups coal #14 (hvCb, Carboniferous)
(a.) % in coal (daf)
(b.) fraction of total oxygen x 100

Sample Identifier	Thermal History		(a) [O _{CO}]	(b) [O _{CO}]/[O]	(a) [O _{COOH}]	(b) [O _{COOH}]/[O]	(a) [O _{OH}]	(b) [O _{OH}]/[O]
14.H	20	100	1.4±0.2	14.5±2.1	0.3±0.0	3.1±0.2	3.2±0.3	32.7±3.6
14P.H(**)	20 + 20	100 200	1.4±0.2	20.0±2.1	0.3±0.1	3.8±1.1	3.9±0.1	53.8±1.1
14Q.H(**)	20 + 0.5	100 300	1.1±0.4	15.0±5.1	0.2±0.0	3.2±0.5	3.6±0.1	47.5±1.0

(**)after initial drying at 100°C, slowly heated in a N₂ purged oven (8cc/min)

Table 9: Oxygen in O-bearing functional groups in coal #16 (hVCb, Carboniferous)
(a.) % in coal (daf)
(b.) fraction of total oxygen x 100

Sample Identifier	Thermal History		(a) [OCO]	(b) [OCO]/[O]	(a) [OCO ₂ H]	(b) [OCO ₂ H]/[O]	(a) [OOH]	(b) [OOH]/[O]
16.H	20	100	1.1±0.2	11.8±2.4	0.1±0.0	1.1±0.1	5.2±0.5	55.9±8.7
16P.H(**)	20 + 20	100 200	1.3±0.1	15.2±1.1	0.1±0.0	0.9±0.1	5.4±0.4	61.8±4.3
16Q.H(**)	20 + 0.5	100 300	1.8±0.2	19.5±1.9	0.1±0.0	0.6±0.1	4.9±0.1	53.4±2.7

(**)after initial drying at 100°C, slowly heated in a N₂ purged oven (8cc/min)

Table 10: Oxygen in O-bearing functional groups in coal #20 (mvb)
(a.) % in coal (daf)
(b.) fraction of total oxygen x 100

Sample Identifier	Thermal History		(a) [OCO]	(b) [OCO]/[O]	(a) [OCOOH]	(b) [OCOOH]/[O]	(a) [OOH]	(b) [OOH]/[O]
	Time (hrs)	Temp (C°)						
20.H	20	70	0.01±0.0	0.2±0.0	0.3±0.0	4.4±0.3	1.1±0.0	16.1±1.1

Appendix 2

Elemental Analyses of Protonated and Heat-treated Coals

Table 1: Ultimate analysis of protonated coal (daf) #1 (lignite)

Coal Identifier	Thermal History		$\%C$	$\%H$	$\%N$	$\%O^b$
	Time (hrs)	at Temp ($^{\circ}C$)				
1.H	20	70	71.68 \pm 0.25	5.18 \pm 0.13	1.78 \pm 0.11	23.14
1a.H	20	70	70.36 \pm 0.49	5.58 \pm 0.04	1.80 \pm 0.06	24.06
1ab.H	20 + 20	70 100	71.39 \pm 0.64	5.06 \pm 0.04	1.78 \pm 0.73	23.55
1ac.H	20	100	68.98 \pm 0.15	5.36 \pm 0.05	1.63 \pm 0.02	25.66
1acP.H	20 + 20	100 200	72.26 \pm 0.38	5.33 \pm 0.01	1.72 \pm 0.08	22.41
1acQ.H	20 + 0.5	100 300	74.23 \pm 0.48	4.50 \pm 0.04	1.49 \pm 0.08	20.85
1acPt*.H	20 0.5	100 200	73.91 \pm 0.2	4.98 \pm 0.06	1.49 \pm 0.10	21.11
1acQt*.H	20 + 0.5	100 300	77.06 \pm 0.18	4.59 \pm 0.06	1.49 \pm 0.05	18.35

b. $\%O \approx [100 - \%C - \%H - \%N]$, sulfur contents were considered small.

*. Heated rapidly in a tube furnace in N_2 (12cc/min), at higher temperature.

Table 2: Ultimate analysis of coal daf #2 (subbituminous c)

Coal Identifier	Thermal History		%C	%H	%N	%O ^b
2.H	20	70	71.65±1.0	5.72±0.14	2.14±0.11	20.49±1.22
2b.H	20 + 20	70 100	71.38±0.20	4.98±0.02	2.13±0.12	21.51±0.68
2c.H	20	100	68.93±0.48	5.30±0.04	1.91±0.08	23.86±0.54
2cP.H	20 + 20	100 200	71.41±1.2	5.24±0.09	1.90±0.03	21.45±0.03
2cQ.H	20 + 0.5	100 200	72.37±0.81	5.06±0.04	1.90±0.17	20.66±0.68
2dQ.H	20 + 0.5	100 300	74.15±1.2	5.17±0.01	1.99±0.12	18.68±0.28
2cPt*.H	20 + 0.5	100 200	71.33±0.12	4.75±0.19	1.73±0.01	22.25±0.33
2cQt*.H	20 + 0.5	100 300	74.52±1.4	4.58±0.04	1.69±0.17	19.21±1.5

b. %O = [100 - %C - %H - %N], sulfur contents were considered small.

(*) Heated rapidly in a tube furnace in N₂ (12 cc/min) at higher temperature.

Table 3: Ultimate analysis of coal daf #4 (Subbituminous C)

Coal Identifier	Thermal History		$\%C$	$\%H$	$\%N$	$\%O^b$
	Time (hrs)	at Temp ($^{\circ}C$)				
4.H	20	70	71.48 \pm 0.83	5.56 \pm 0.12	2.27 \pm 0.21	20.81 \pm 0.88
4a.H	20	100	71.19 \pm 0.43	5.22 \pm 0.02	1.56 \pm 0.01	22.03 \pm 0.05

b. $\%O = [100 - \%C - \%H - \%N]$, sulfur contents were considered small.

Table 4: Ultimate analysis of coal daf #7 (Subbituminous B)

Coal Identifier	Thermal History		$\bar{x}[C]$	$\bar{x}[H]$	$\bar{x}[N]$	$\bar{x}[O]^b$
	Time (hrs)	Temp (°C)				
7.H	20	100	72.87±0.99	4.95±0.08	1.59±0.09	20.60±0.10
7a.H	20	100	74.44±0.37	4.86±0.08	1.73±0.17	18.98±0.43
7aQ.H	20 + 0.5	100} 300}	78.29±0.79	4.71±0.04	1.05±0.01	15.95±0.89
7aPt*.H	20 + 0.5	100} 200}	72.82±0.36	4.30±0.06	1.0±0.13	21.86±1.4
7aQt*.H	20 + 0.5	100} 300}	77.85±0.65	4.02±0.06	1.01±0.01	17.11±0.62

b. $\bar{x}[O] = [100 - \bar{x}C - \bar{x}H - \bar{x}N]$, sulfur contents were considered small.

(*) Heated rapidly in a tube furnace in N₂ (12cc/min) at higher temperature.

Table 5: Ultimate analysis of coal (daf) #9 (subbituminous C)

Coal Identifier	Thermal History		$\%C$	$\%H$	$\%N$	$\%O$ ^b
	Time (hrs)	at Temp (°C)				
9.H	20	100	71.79±0.47	4.99±0.01	2.13±0.08	20.98±0.59
9P.H	20	100}	71.34±0.93	4.83±0.09	2.38±0.07	21.45±0.95
	+ 20	200}				
9Q.H	20	100}	69.28±0.23	4.54±0.04	2.21±0.18	23.96±0.41
	+ 0.5	300}				
9b.H	20	100	71.93±0.83	4.99±0.11	2.24±0.07	20.61±1.2
9bQ.H	20	100}	74.25±0.74	4.54±0.16	2.51±0.30	18.65±0.92
	+ 0.5	300}				
9bPt*.H	20	100}	76.79±0.54	4.63±0.13	1.72±0.16	16.86±0.71
	+ 0.5	200}				
9bQt*.H	20	100}	77.82±0.84	4.52±0.04	1.83±0.01	15.84±0.97
	+ 0.5	300}				

b. $\%O = [100 - \%C - \%H - \%N]$, sulfur contents were considered small.

* Heated rapidly in a tube furnace in N_2 (12cc/min) at higher temperature.

Table 6: Ultimate analysis of coal (daf) #10 (hvCb)

Coal Identifier	Thermal History		$\bar{x}[C]$	$\bar{x}[H]$	$\bar{x}[N]$	$\bar{x}[O]^b$
	Time (hrs)	at Temp ($^{\circ}C$)				
10.H	20	70	75.32 ± 0.34	5.52 ± 0.08	1.30 ± 0.01	18.19 ± 0.32
10a.H	20	100	75.33 ± 0.72	5.41 ± 0.36	2.48 ± 0.36	16.79 ± 0.44
10aP.H	20 + 20	100} 200}	75.49 ± 0.05	5.33 ± 0.07	2.58 ± 0.06	16.61 ± 0.55
10aQ.H	20 + 0.5	100} 300}	75.49 ± 0.06	5.08 ± 0.12	2.39 ± 0.18	17.05 ± 0.65
10b.H	20	100	75.87 ± 0.34	5.52 ± 0.04	2.28 ± 0.06	16.34 ± 0.03
10bQ.H	20 + 0.5	100} 300}	77.031 ± 0.5	5.096 ± 0.0	2.51 ± 0.32	15.37 ± 0.77

b. $\bar{x}[O] \approx [100 - \bar{x}C - \bar{x}H - \bar{x}N]$ sulfur contents were considered small.

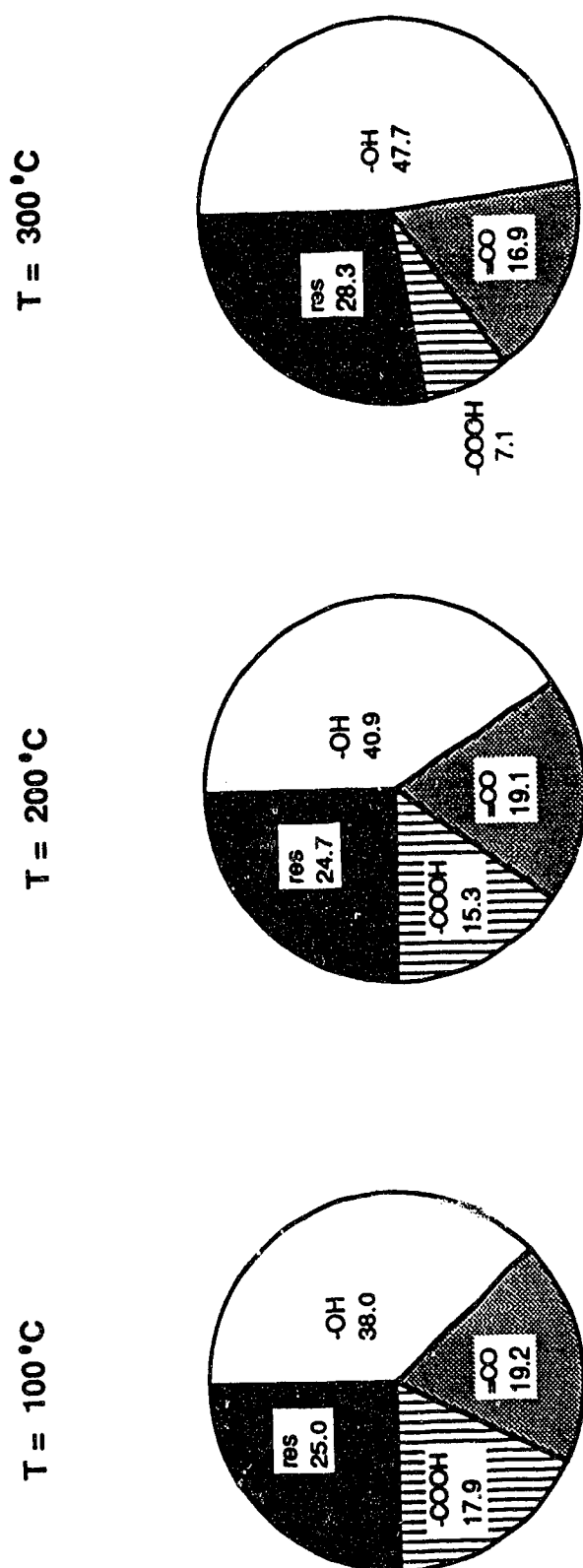


Fig. 5.8 Fraction of total oxygen in O-bearing functional groups of protonated lignite #1 dried at (i) 100°C (20h), and after slow heating in N_2 8cc/min, at (ii) 200°C (20h), (iii) 300°C (0.5h).

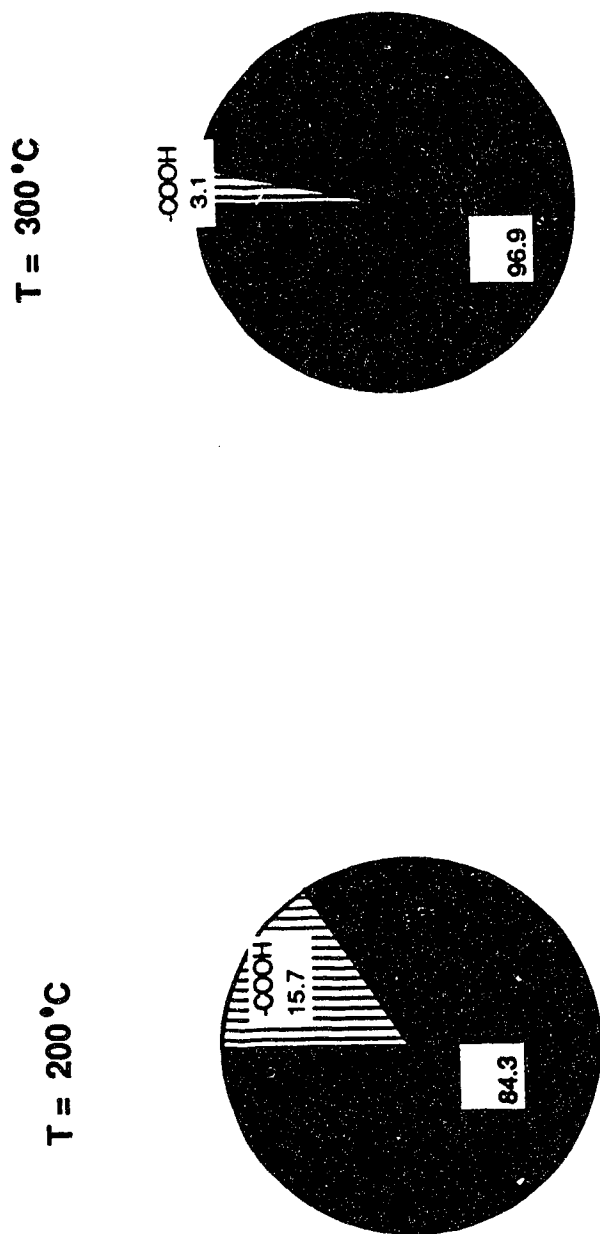


Fig. 5.8a Fraction of total oxygen in carboxyl group of protonated lignite #1 after fast heating in N₂, 12cc/min., 0.5h, at 200°C and 300°C.

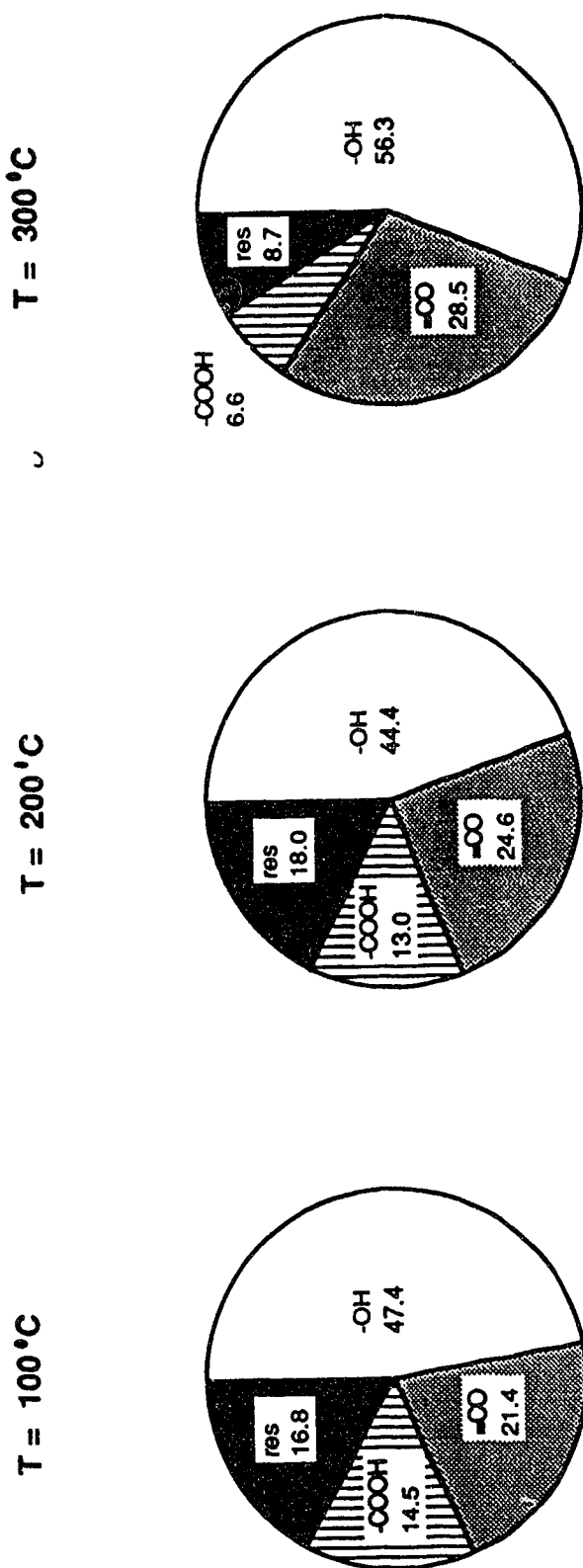
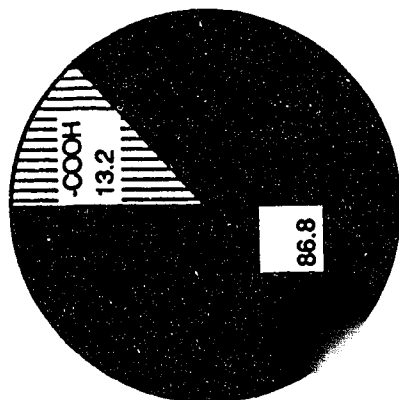


Fig. 5.9 Fraction of total oxygen in O-bearing functional groups of protonated subbit. C #2 dried at (i) 100°C (20h) in vacuo and after slow heating in N_2 8cc/min, at (ii) 200°C (20h), (iii) 300°C (0.5h).

T = 200 °C



T = 300 °C

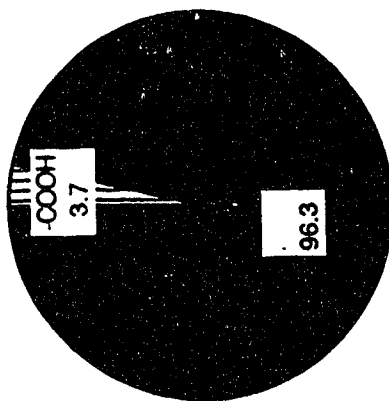


Fig. 5.9a Fraction of total oxygen in carboxyl group for protonated subbit. C #2 dried at (i) 100°C (20h) in vacuo and after fast heating in N₂ 12cc/min for 0.5h at (ii) 200°C (iii) 300°C.

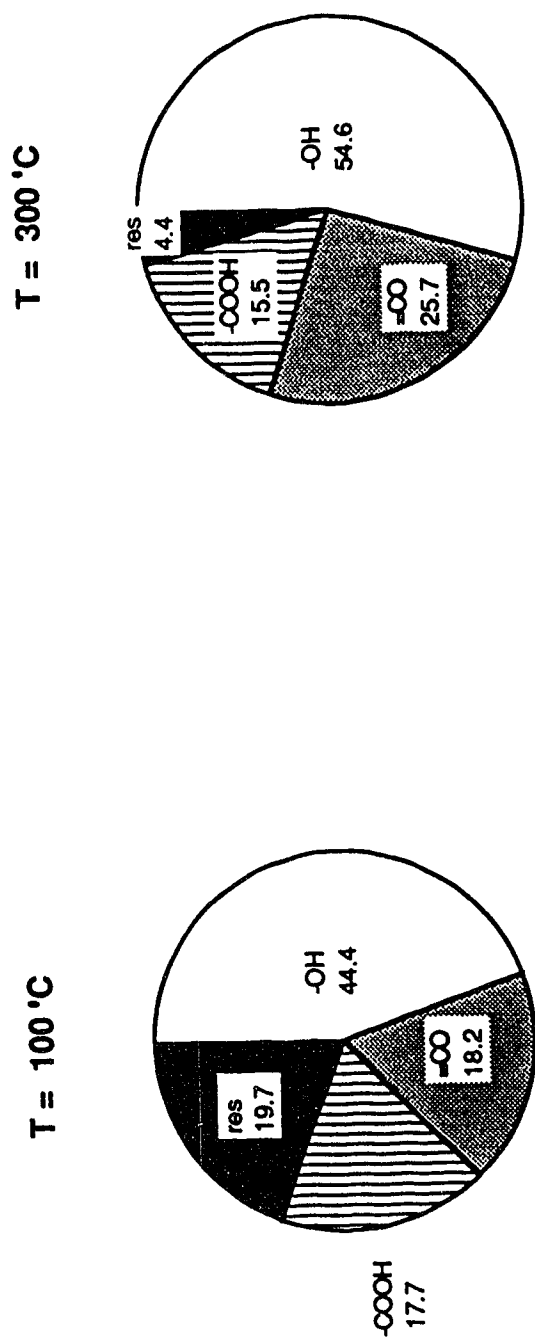
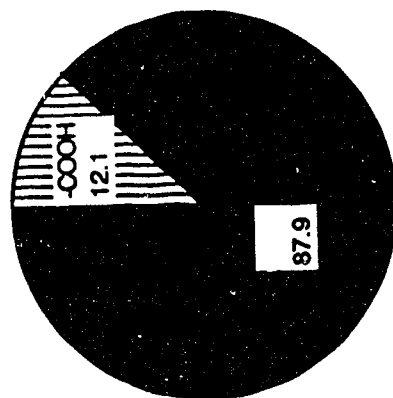


Fig. 5.10 Fraction of total oxygen in O-bearing functional groups of protonated subbit. B #7 dried at (i) 100°C (20h) in vacuo and after slow heating in N₂ 8cc/min for 0.5h at (ii) 300°C.

T = 200 °C



T = 300 °C

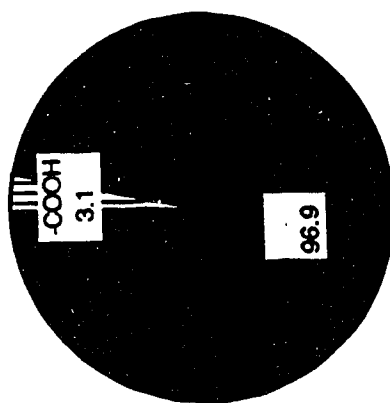


Fig. 5.10a Fraction of total oxygen in carboxyl group for protonated subbit. B #7 dried at (i) 100°C (20h) in vacuo and after fast heating in N₂ 12cc/min for 0.5h, at (ii) 200°C and (iii) 300°C.

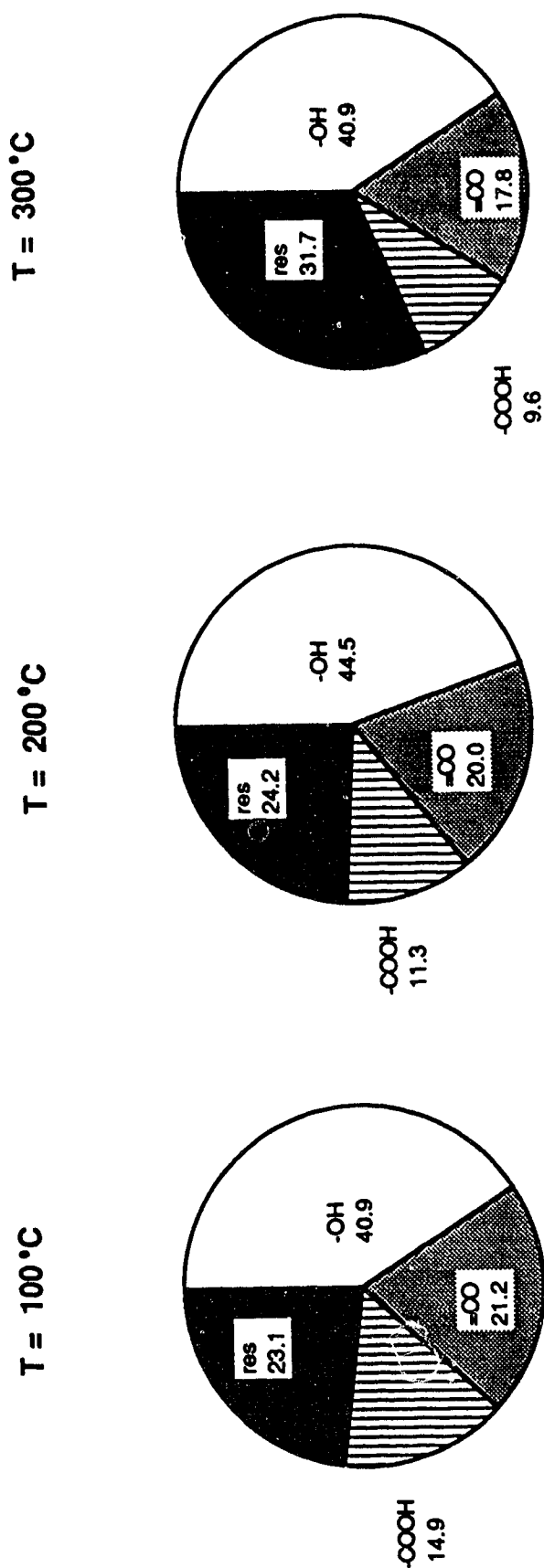
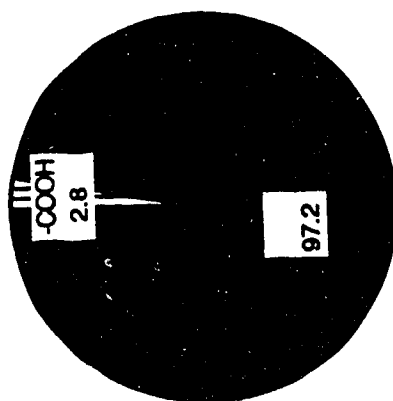


Fig. 5.11 Fraction of total oxygen in O-bearing functional groups of protonated subbit. C #9 dried at (i) 100°C (20h) in vacuo and after slow heating in N₂ 8cc/min, at (ii) 200°C (20h) (iii) 300°C (0.5h).

T = 300 °C



T = 200 °C

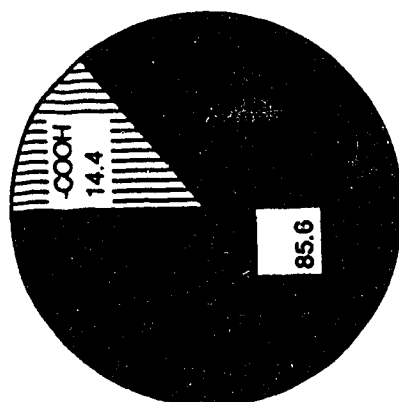


Fig. 5.11a Fraction of total oxygen in carboxyl group for protonated subbit.B #9 dried at (i) 100°C (20h) in vacuo and after fast heating in N₂ 12cc/min for 0.5h, at (ii) 200°C (iii) 300°C

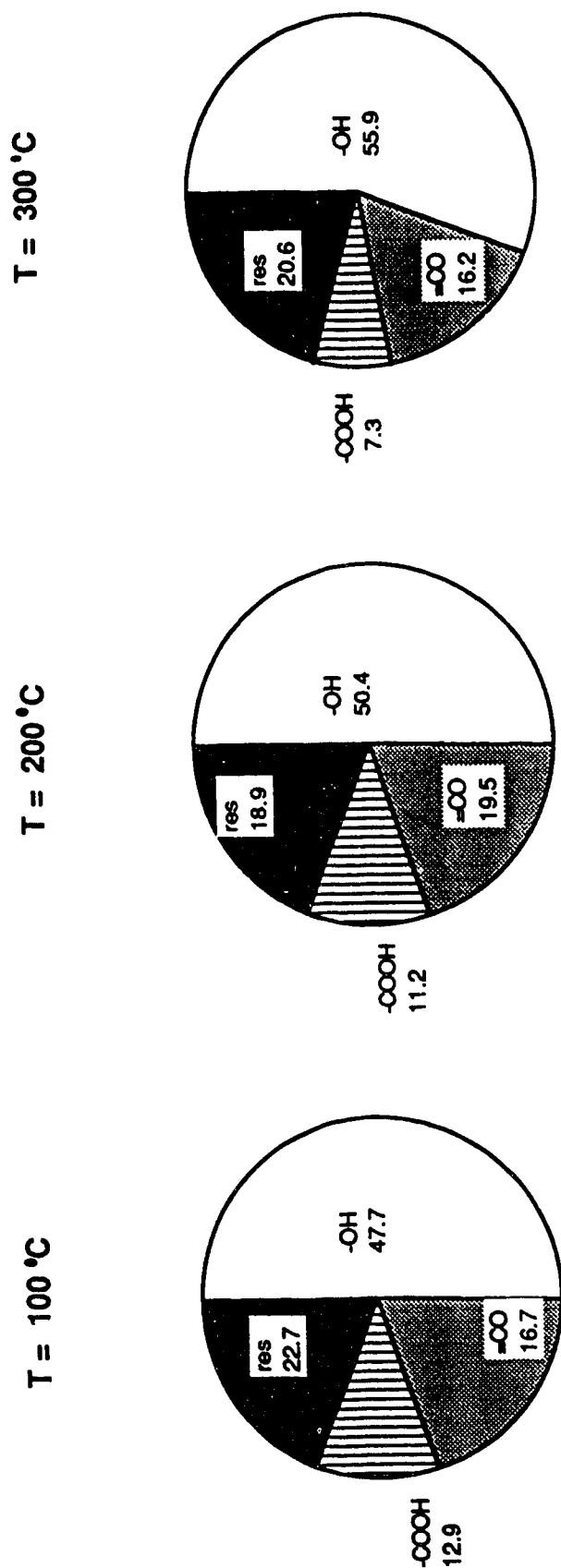


Fig. 5.12 Fraction of total oxygen in O-bearing functional groups of protonated subbit. C #11 dried at (i) 100°C (20h) in vacuo and after slow heating in N_2 8cc/min, at (ii) 200°C (20h), (iii) 300°C (0.5h).

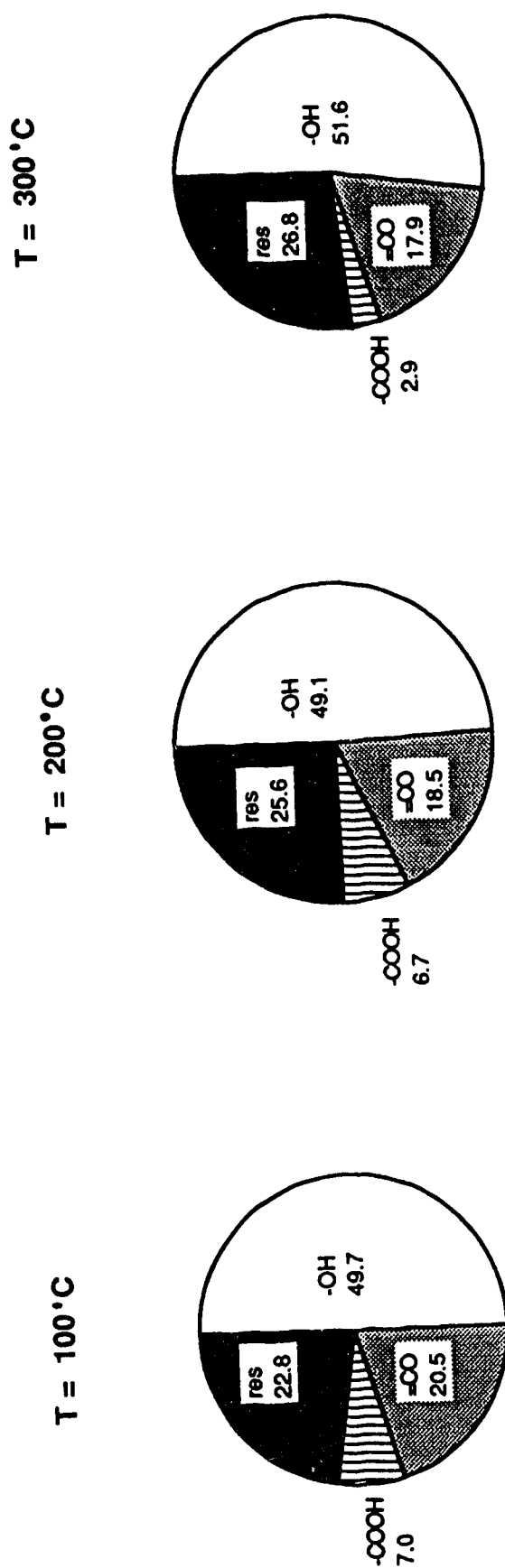


Fig. 5.13 Fraction of total oxygen in O-bearing functional groups of protonated hvb #10 dried at (i) 100°C (20h) in vacuo and after slow heating in N₂ 8cc/min, at (ii) 200°C (20h) (iii) 300°C (0.5h)

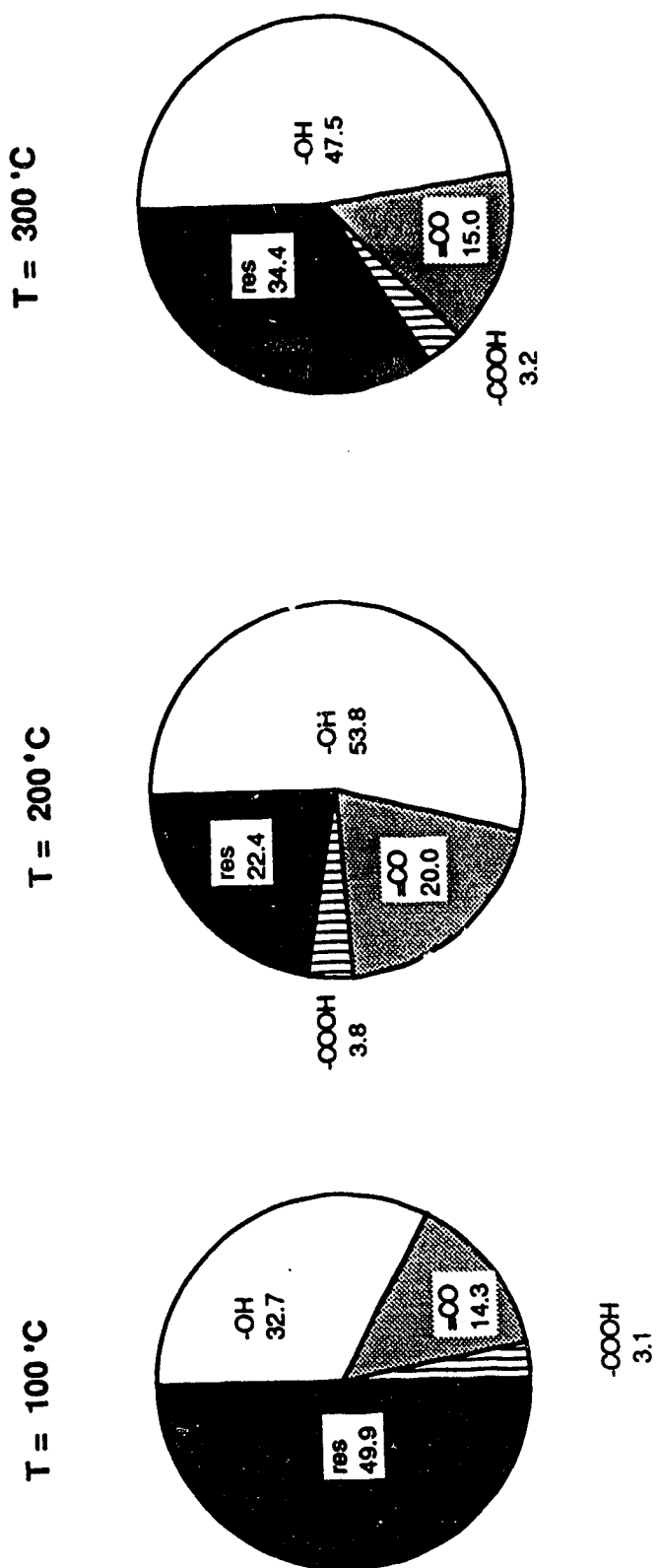


Fig. 5.14 Fraction of total oxygen in O-bearing functional groups of protonated hvb Carboniferous #14 dried at (i) 100°C (20h) in vacuo and after slow heating in N₂ 8cc/min, at (ii) 200°C (20h) (ii) 300°C (0.5h).

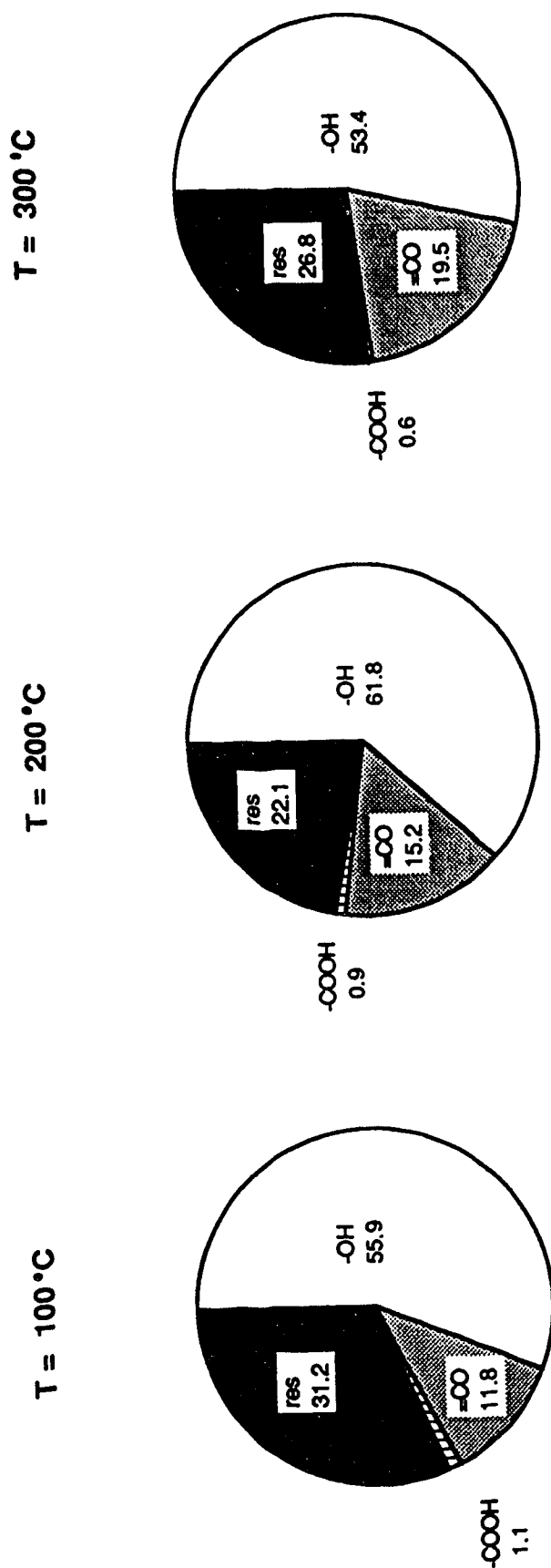


Fig. 5.15 Fraction of total oxygen in O-bearing functional groups of protonated hvb Carboniferous #16 dried at (i) 100°C (20h) in vacuo and after slow heating in N₂ 8cc/min, at (ii) 200°C (20h) (iii) 300°C (0.5h).

CHAPTER 6

CONCLUSIONS

The conclusions are divided into two parts. The first part covers the distribution of O-bearing functional groups and the second part covers thermal stability. Recommendations are given at the end of this chapter.

6.1 The distribution of oxygen in functional groups

Automatic Potentiometric Titrimetry (APT) is a demonstrable improvement of classical techniques for the determination of $[O_{OH}]$ and $[O_{COOH}]$. It is more sensitive than visual methods and facilitates close control of the buffering capacity of barium acetate/acetic acid. This avoids premature hydroxide precipitation which would not be observable with colored indicator dyes. APT is sensitive in detecting traces of $-COOH$.

In nine cases out of ten, both the concentrations of O-bearing functional groups and the fraction of total oxygen in these groups were in the order

$$O_{OH} > O_{CO} > O_{COOH}$$

This result conforms with results reported for Japanese Cretaceous coals. The sole exception was the U. Cret./L. Tert. mvb coal for which :

$$O_{OH} > O_{COOH} > O_{CO}$$

The sequence agreed with data for European Carboniferous coals in which $[O_{COOH}] > [O_{CO}]$.

Oxygen concentrations in the functional groups increased linearly with total oxygen, and the fraction of total oxygen in each group approached a limiting value as total oxygen increased.

Unlike European Carboniferous coals, concentrations of oxygen in each functional group decrease more linearly with increasing %C (with interpolations in the 76%C - 80%C range) and are comparable with data reported for Japanese Cretaceous coals and Indian lignites. Residual oxygen, which is not generally reported in the literature, ranged from 17% to 79% of total oxygen.

Large variations in concentrations of O-bearing functional groups among coals with quite similar elemental compositions emphasize the fact that coals which are compositionally equivalent are not necessarily equivalent in their chemistries. These variabilities will affect coal behaviour in conversion and processes influenced by surface properties.

The wide variations are likely due to environmental influences during diagenesis. The lignite, however, did not have the highest concentrations of either $[O_{OH}]$ or $[O_{CO}]$ as might be expected from established rank correlations, and subbituminous B coal did not conform to conventional rank correlations in terms of total oxygen and O-bearing functional group concentrations.

According to the literature, $[O_{COOH}]$ should be higher than other groups in low rank coals, but this is not the case for Canadian coals.

Differences in concentrations of O-bearing functional groups in the two U. Cret./Tert. coals, hvb #10 and mvb #20, suggest regional metamorphic effects. In accord with rank correlations, coal #20 (mvb) contained lower concentrations of all O-bearing functional groups. However, in this coal, $[O_{COOH}]$ was unexpectedly higher than $[O_{CO}]$ (which was negligible).

-COOH is the first group to be lost in normal metamorphism, and is virtually absent in most normally metamorphosed coals with greater than 85°C.

Tertiary and Carboniferous coals of similar rank differed significantly in concentrations of O-bearing functional groups. These differences may be attributed in part, to the impact of dissimilar diagenetic and metamorphic histories of the coals. One of the Carboniferous Eastern Canadian coals (#14) formed a coke button on heating during TGA, suggesting lower porosity and perhaps limited reagent access, thus lower measured $[O_{OH}]$.

The FTIR-PAS aromatic bands were more intensified in the coals of Carboniferous age as compared to the Tertiary age of similar rank. No aromatic CH stretch bands were seen in the spectra of subbituminous coals. This technique appears to have limited applicability in studies of oxygen functionalities at concentrations typical of this work.

6.2 Thermal Stability of Canadian Coals

Decarboxylation of coals is affected significantly by heating rates. When heated rapidly at 200°C or 300°C, the coals lost more O_{COOH} than when heated slowly for a longer time. The loss of $-COOH$ was greater at 300°C than at 200°C for slow or fast heating. Temperature is an important factor for decarboxylation even at slow heating rates. Heating rates should be reported with experimental results because they affect reactivity and hence the processability of coals.

For slowly heated samples the effects on redistribution and loss of O-bearing functional groups were more pronounced at 300°C (0.5Hr) than at 200°C (20hr). Although $[O_{OH}]$ and $[O_{CO}]$ sometimes decreased in the low rank coals, the general trend was for both $[O_{OH}]$ and $[O_{CO}]$ to increase and $[O_{COOH}]$ to decrease. At slow heating, these changes were accompanied by a small loss of total oxygen. Changes in $[O_{OH}]$ and $[O_{CO}]$ accompanied by a loss of $[O_{COOH}]$ and, in addition, larger losses in $[O_{COOH}]$ after fast heating, may be explained by:

- (i) a reaction in which formation of an anhydride from proximal carboxylic groups liberates H_2O . If this is not removed, as in slow heating, the reaction is reversible.
- (ii) the reaction of proximal $COOH$ with H on aromatic species to form a $-CO-$ bridged product complex.
- (iii) the loss of CO from $COOH$ generating a free radical which is stabilized by $-OH$ to form phenolic $-OH$.

Pyridine extracts during acetylation of pyrolyzed coals were darker than non-pyrolyzed coals, suggesting molecular rearrangements occur in the coals during pyrolysis. The variation in chemical composition, and hence reactivity, after pyrolysis would influence the processing of even mildly pyrolyzed coals.

Molecular rearrangements caused by mild pyrolysis may not be observable directly by FTIR-PAS. This method for studying oxygen functionality on coals was not sensitive to concentration differences found in the samples, probably because it measures more from the surface than the bulk of coal particles.

6.3 Recommendations

The errors common to most wet analytical methods can be minimized by proper sampling and allowing enough time for reagents to access the inner surfaces of coals. Most research done in this area is partial to one method or another, but because sample treatments are not uniform, it is difficult to compare results. Therefore it is recommended that standard methods be established for the determination of oxygen functional group distributions to allow global comparisons. All results should also be reported with standard deviations or error analysis.

The surface-sensitive techniques of FTIR-PAS need to be further explored for quantitative data. Detection of -OH groups is subject to many interferences from water and N-H stretch and cannot be used for correlation with quantitative data. The 1700cm^{-1} band is more promising for correlations, but measures

must be taken to avoid or resolve band overlaps. Peak to peak ratioing for analysis should be explored.

For thermal pretreatments it is recommended that, at temperatures below T_d , further experiments be performed to establish the influence of faster heating rates on O-bearing functional groups. Perhaps this can be followed by experiments in processing of the coals.

In this work the emphasis was on low rank coals. A larger number of coals of other ranks should be studied to verify the trends indicated by this suite of coals. Surface properties should also be studied for correlation with this data.

REFERENCES

Abdel-Baset, Z., Given, P.H. and Yarzab, R.F. "Re-examination of the phenolic hydroxyl contents of coals." Fuel, 57 (2) 95-99, 1978.

Abdel-Baset, Z., Yarzab, R.F., and Given, P.H. "Dependence of coal liquefaction behaviour on coal characteristics. 3. Statistical Correlations of conversions in coal tetralin mixtures." Fuel 57(2) 89-94, 1978.

Abernathy, R.F., and Gibson, F.H. US Bureau of Mines Rept. Invest., 1966.

Angelova, G., and Lazarova, L. "Functional O groups in the thermal treatment of hard coal." Brennst. Chemie 46(7), 204-206, 1965.

Angle, C.W., Donini, J.C.D., and Hamza, H.A. "The Effects of ultrasonication on the surface properties, ionic composition and electrophoretic mobility of an aqueous coal suspension." Colloids and Surfaces, 30, 373-385, 1988.

Angle, C.W. and Hamza, H.A. "The effects of selected polymers on the electrokinetic properties of fine coal particles and silica in washery water." in Flocculation in Biotechnology and Separation Systems, Elsevier, Y.A. Attia, ed., 75-93, 1987.

Angle, C.W., and Hamza, H.A. "Electrokinetic behaviour of a relatively unoxidized coal." Paper presented at ACS 57th Colloid and Interface Science Symposium, Toronto, Canada, June 1983.

Angle, C.W., Leung, W.M., Mikula, R.J. and Hamza, H.A. "Sulfur characterization of Eastern Canadian coals for

optimization of beneficiation processes." in Processing and Utilization of High Sulfur coals, Elsevier, A. Attia, ed., 67-88, 1985.

Angle, C.W. and Mo, A.W., "Novel automatic titration system for research on solids/liquids systems." Can. patent application, 1988.

Angle, C.W. , Mo, A.W. and Furman, S. "Use of automatic titrimetry in fossil fuel research". CANMET Div. Report, 1988.

ASTM Standard D3176-84. Petroleum Products, Lubricants and Fossil Fuels. 05.05, 1985.

ASTM Standard D3172-73. Proximate-Analysis of Coal and Coke Combustion. 05.05, 1984.

ASTM Standard D4239-83. Description of Tube Furnace. 05.05, 1984.

Attar, A. "The Kinetics of coal liquefaction in hydrogen donor solvents." ACS Div. Fuel Chem. Prepr., 23(4), 169-180, 1978.

Attar, A. and Hendrikson, G. "Functional groups and heteroatoms in coal." in 'Coal Structure', Academic Press, R.A. Meyers, ed., pp. 131-198, 1982.

Banks, H.P. "Evolution and Plants of the Past." Wadsworth Publishing Co., Inc., Belmon, California, U.S.A., 1970.

Berkowitz, N. "Atmospheric Oxidation of Coal." in "Sample Selection, Aging, and Reactivity of Coal". John Wiley, Klein, ed., chapter 5, 1989.

Berkowitz, N. Course Notes in Coal Chemistry given at CANMET labs, Devon, Alberta, Canada, Aug. 1987.

Berkowitz, N. "The Chemistry of Coal." chapter 3, Elsevier, 1985.

Berkowitz, N., "Introduction to Coal Technology.", Academic Press, 1979.

Berkowitz, N. "Relationship between chemical structure and technological behaviour of coal." The Robert A. Welch Foundation Conferences on Chemical Research XXII: Chemistry of Future Energy Resources, November 6-8, Houston, Texas, U.S.A., 1978.

Berkowitz, N., Calderon, J., Liron, A. "Some observations respecting reaction paths in coal liquefaction." Fuel, 67(5), 626-631, 1988.

Bhaumik, M.N., Mukherjee, A.K., Mukherjee, P.N. and Lahiri, A. "Ether Oxygen in Coal." Fuel, 41, 443-446. 1962.

Biner, J. , Given, P.H., Raj, S. "Phenols as Chemical Fossils in Coal" in Organic Chemistry of Coal, ACS Symposium Ser. 174, J.W. Larsen, ed., 86-99. 1977.

Blom, L., Edelhausen, L. and Van Krevelen, D.W. "Chemical structure of and properties of coal XVIII - oxygen groups in coal and related products." Fuel, 36, 135-153, 1957.

Bouwman, R., and Freriks, I.L.C. "Low temperature oxidation of a bituminous coal. infrared spectroscopic study of samples from a coal pile." Fuel, 59(5), 315-322, 1980.

Briggs, P., Seah, M.P., eds. "Practical Surface Analysis by Auger, and X-Ray photoelectron Spectroscopy." John Wiley, 1983.

Brooks, J.D., Durie, R.A., and Sternhill, S., " Chemistry of brown coals - III Pyrolytic reactions." Aust. J. Appl. Sci. 9(9), 303-320, 1958.

Brooks, J.D., Durie, R.A., and Sternhill, S., "Chemistry of brown coals II." Aust. J. Appl. Sci. 9(9), 63-113, 1958,

Brooks, J.D., and Maher, T.P. "Acidic oxygen-containing groups in coal." Fuel 36. p. 51-63, 1957.

Brooks, J.D., and Sternhill, S., Aust. J. Appl. Sci. 8, 206, 1957.

Brown, J.K., "The infrared spectra of coals."J. Chem. Soc. London, 744-752, 1955.

Brown, J.K., "The infrared spectra of carbonized coals."J. Chem. Soc. London, 752-757, 1955.

Brown, J.K. and Wyss, W.F. "Oxygen in bright coals." Commun. Chem. and Ind. 33, 1118, 1955.

Bruker IFS User's Manual ATS 87G, 1987.

Chaffee, A.L., Perry, G.J., Johns, R.B. George, A.M. "Carboxylic Acids and Coal Structure." in Coal Structure, M. Gorbati and K. Ouchi, eds., Chapter 8, 1981.

Coal Directory of the Coal Association of Canada, 1988.

Collins, C.J., Hagaman, E.W. and Raaen, V.I. Coal Tech. Q. Rep. ORNL 5252 Dec. 31, 1976.

Dryden, I.G. "Chemical Constitution and Reaction of Coal" in "Chemistry of Coal Utilization", Suppl. Vol. John Wiley, H.H. Lowry, ed., chapt. 6, p.263, 1963.

Du Plessis, H.G., Reinecke, C.F., van Nierop, J.G. "The Influence of oxygen Containing surface Functional Groups on the Selective Oil Agglomeration properties of coal." in Proc. Int. Conf. on Coal Science. Sydney, Australia. Pergamon Press, 521-524, 1985.

Dutta, P.K. and Holland, R.J. "Acidic groups in coal and coal-derived materials." Fuel, 62, 732-737, 1983.

Dyer, J.R., "Applications of Absorption Spectroscopy of Organic Compounds." Foundations of Modern Organic Chemistry Series, Prentice Hall, K.L. Rinehart Jr., ed., Chapt.4, 54-132, 1965.

Elliot, M.A. and Yohe, R.G. "The Coal Industry and Coal Research and Development and Perspective", in Chemistry of Coal Utilization, 2nd Suppl. Vol., Wiley, Elliot, M.A., ed., chap.1, 34, 1981.

Franz, J.A., Camaioni, D.M., Skiens, W.E. "Application of ^{13}C , ^2H , ^1H , NMR and GPC to the Study of Structural Evolution of Sub-bituminous Coal in Tetralin at 427 C." in Coal Structure, M.L. Gorbaty and K. Ouchi, eds., ACS Adv. Chem. Ser. 192, 1981.

Friedman, S., Kaufman, M.L., Steiner, W.A. and Wender, I. "Determination of hydroxyl content of vitrains by formation of trimethylsilyl ethers." Fuel 40, 33 1961.

Friedel, R.A., and Queiser, J.A., "Infrared analysis of bituminous coal and other carbonaceous materials." Anal. Chem. 28:22, 1956.

Furimsky, E., Macphee, J.A., Vancea, L., Ciavaglia, L.A., Nandi, B.N. "Effect of oxidation on the chemical nature and distribution of low temperature pyrolysis products from bituminous coals." Fuel 62, 395-400, 1983.

Georgiadis, C. "Contribution a l'etude chimique et physiochimique des houilles Durant: Lille. Thesis 1946.

Given, P.H. "Essay on the Organic Geochemistry of Coal." in Coal Science, Academic Press, Inc., M. Gorbaty, J. Larsen and I. Wender, Eds., pp. 63-252, 1984.

Given, P.H. "Dehydrogenation of coals and its relation to coal structure." Fuel 40, 427-431, 1961.

Given, P.H. "The Distribution of hydrogen in coals and its relation to coal structure." Fuel 39, 147-153, 1960.

Graham, J.A., Grim, W.M., Fateley, W.G. "Fourier Transform Infrared Photoacoustic Applications to Chemical Systems." Academic Press, John R. Ferraro and Louis J. Basile, Ed., Vol. 4, Chapter 9. 1985.

Grandy, D.W., Petrakis, L., Young, D.C., Gates, B.C., "On O - NMR to determine O-functional groups in coals and coal liquids." Nature 308(5955), 175-177. 1984.

Grandy, D.W., Petrakis, L., Young, D.C., Gates, B.C., "Naturally abundant Oxygen-17 Nuclear Magnetic Resonance and the Determination of Oxygen Functionalities in Synthetic Fuels." Nato ASI Series C. Mathematical and Physical Sciences 124, Magn. Reson. 689-698, 1984.

Halleux, A., Delavarenne, S. and Tschamler, C.T. "Determination of hydroxyl groups in model compounds, coal and coal extracts." Fuel 38, 283-290, 1959.

Hara, T. "Structural Analysis of Oxygen and Nitrogen Containing Compounds Involved in Coal Derived Liquids and their Reactions - Studies on Utilization of Coal Through Conversion." Ministry of Education, Science and Culture, Tokyo, Japan, 59-64, 1987.

Harris, W.E. and Kratochvil, B. "Introduction to Chemical Analysis." Saunders College Publishing, Philadelphia, Penn., Chapter 2, 1981.

Hatami, M., Osawa, Y. Sugimura, H. "Chemical structure and properties of heat treated coal on the early state of carbonization (VIII) - behaviour of oxygen containing functional groups." Japan Fuel 46, 819, 1967.

Hayatsu, R., Winans, R.E., Mcbeth, R.L., Scott, R.G., Moore, L.P., Studier, M.H. "A structural characterization of coal:Lignin-like polymers in coals." in Coal Structure, M. Gorbaty and K. Ouchi, eds., ch.9, 1979.

Horton, L. "The Chemical Constitution of Coal." Proc. Conf. on Science on the Use of Coal, Sheffield, Inst. Fuel, London A-24 - A28, 1958.

Howard, J.B. "Fundamentals of Coal Pyrolysis and Hydropyrolysis." Chemistry of Coal Utilization -2nd Suppl., Wiley, M.A. Elliot, ed., chapt. 12, 1981.

Ignasiak, B.S., Ignasiak, T.M. and Berkowitz, N. "Advances in Coal Analysis." Rev. Anal. Chem. 2, p. 278, 1975.

Ignasiak, B.S. and Berkowitz, N. "Studies on coal blends: preparation and mechanical strengths of some experimental cokes." Bull. Can. Inst. Min. 67(747), 72-76, 1974.

Ignasiak, B.S. Clugston, D.M., and Montgomery, P.S. "Oxidation studies on coking coal related to weathering; Part 2. the distribution of absorbed oxygen in the products resulting from pyrolysis of the slightly oxidising coking coal." Fuel 51, 76 1972.

Ihnatowicz, A. Prace Głównego Inst. Gorn. Komun. No.125, 39, 1952.

Instruction Manual CHN-600 Elemental Analyzer for Macrosamples 785-500 System. LECO Corporation, 1984.

Instruction Manual Fisher Model 490 Coal Analyzer. Fisher Scientific, an Allied Company, 1984.

Iyengar, M.S., and Ghosh, R.S. "Factors influencing carbonization of south arcot lignites briquettes." Proc. Conf. on Science in the Use of Coal, Sheffield, Inst. Fuel Paper 25, C-49, 1958.

Iyengar, M.S., Sibal, D.N., and Lahiri, A., "Role of hydrogen bonds in the briquetting of lignite." Fuel 36, 76, 1957.

Jones, Kenneth Lee. "Methods for the Characterization of the Acidic and Basic Surface Sites of Coal." Ph.D. Thesis, Lehigh University, 1985.

Kamiya, Y., Nagai, S. and Oikawa, S., "Effect of coal minerals on the thermal treatment of aromatic ethers and carbonyl compounds." Fuel 62(1), 30-33, 1983.

Kamiya, Y., Yao, T., and Oikawa, S., Prepr. Am. Chem. Soc. 24(2), 116, 1979.

Kini, K.A., Nandi, S.P., Sharma, J.N., Iyengar, M.S., and Lahiri, A., "Surface area of coal." Fuel 35, 71, 1956.

Kreulen, D.J.W., and Kreulen van Selms, F.G., "Thermische zersetzung von lignin und huminsäuren bei relativ niedrigen temperaturen." Brennst. Chem. 38, 49, 1957.

Kroger, C., Fuhr, K. and Darsow, G. "Physikalisch-chemische eigenschaften von braunkohlen und braunkohlenkomponenten V. Die carbonylgruppen- und Athersauerstoffbestimmung." Erdol Kohle 18, 36- 70, 1965.

Kroger, C., and Darsow, G. "Physikalisch-chemische eigenschaften von braunkohlen und braunkohlenkomponenten III. Hydroxylgruppenbestimmung durch saurekatalysierte acetylierung." Erdol Kohle 17, 88, 1964.

Ladner, W.R. "The Products of coal pyrolysis: properties, conversion, and reactivity." Fuel Processing Tech. 20, 207-222, 1988.

Landais, P. and Monthieux, M.B. "Closed system pyrolysis: an efficient technique for simulating natural coal maturation." Fuel Processing Technology 20, 123-132, 1988.

Larsen, J.W. "Macromolecular structure and coal pyrolysis." Fuel Processing Technology 20, 13-22, 1988.

Larsen, J.W., Nader, P.A., Mohammadi, M. and Montano, P.A., "Spatial distribution of oxygen in coals. Development of a tin labeling reaction and Mossbauer studies." Fuel 61, 889-893, 1982.

Lazarov, L., and Angelova, G. "Treatment of coals with sodium in liquid ammonia solution." Fuel 47(5), 333-341, 1968.

Liotta, R., "Effect of O-alkylation on caking properties of coal." Letters to the editor, Fuel 60(5), 453-455, 1981.

Liotta, R., "Selective alkylation of acidic hydroxyl groups in coal." Fuel 58(9), 724-728, 1979.

Liotta, R., Brons, G., and Isaacs, J. "Oxidative weathering of Illinois No. 6 coal." Fuel 62(7), 781-791, 1983.

Lucht, L.M.H. "Macromolecules Network Structure of Coals: Interpretation of Equilibrium and Dynamic Swelling Experiments." PhD. Thesis, Purdue University, 1983.

Ludvig, M.M., Gard, G.L., Emmet, P.H., "Use of acontrolled oxidation to increase the surface area of coal: application to a bituminous and a semi-anthracite coal." Fuel 62(12), 1393-1395, 1983.

Lynch, B.M., Lancaster, L., MacPhee, J.A., "Characterization of surface functionality of coals by photoacoustic FTIR spectroscopy, reflectance infrared microspectrometry, and Xray photoelectron spectroscopy." ACS Div. Fuel Chem. Prepr. 32(1), 138-145, 1987.

Lynch B.M., Lancaster, L., MacPhee, J.A., "Carbonyl groups from chemically and thermally promoted decomposition of peroxides on coal surfaces." Fuel 66(7), 979- 983, 1987.

Lynch, B.M., Lancaster, L., Fahey, J.T., "Detection by photoacoustic infrared Fourier transform spectroscopy of surface peroxide species in chemically and thermally modified coals." ACS Div. Fuel Chem. Prepr. 31(1), 43-48, 1986.

Maher, T.P., and O'Shea, J.M. "Phenolic groups in coal extracts and residues." Fuel 46, 283-287, 1967.

Table 7: Ultimate analysis of coal (daf) #11 (subbituminous C)

Coal Identifier	Thermal History		$\%C$	$\%H$	$\%N$	$\%O$ ^b
	Time (hrs)	at Temp (°C)				
11.H	20	70	72.85±0.22	5.44±0.21	2.2±0.07	19.51±0.07
11a.H	20	100	70.19±0.18	5.11±0.14	2.27±0.25	22.42±0.48
11aP.H	20 + 20	100} 200}	72.72±0.28	5.02±0.25	2.55±0.14	19.71±0.45
11aQ.H	20 + 0.5	100} 300}	73.68±0.23	4.89±0.11	2.92±0.36	18.52±0.34
11b.H	20	70	74.35±0.34	5.48±0.04	2.26±0.06	16.91±0.30
11bQ.H	20 + 0.5	70} 300}	72.79±0.26	4.96±0.03	2.12±0.07	20.13±0.38

b. $\%O = [100 - \%C - \%H - \%N]$ sulfur contents were considered small.

Table 8: Ultimate analysis of coal (daf) #14 (hvCb)

Coal Identifier	Thermal History		$\%C$	$\%H$	$\%N$	$\%O$ ^b
	Time (hrs)	Temp (°C)				
14.H	20	100	82.66±0.53	5.35±0.03	2.20±0.05	9.78±0.52
14P.H	20	100	84.92±0.09	5.49±0.01	2.40±0.11	7.19±0.04
	20	200				
14Q.H	20	100}	84.54±0.02	5.38±0.06	2.60±0.11	7.48±0.06
	+ 0.5	300}				
14b.H	20	70	85.14±0.99	5.56±0.29	2.74±0.57	6.56±0.79
14bQ.H	20	70}	85.74±1.3	5.48±0.05	2.51±0.13	6.24±1.45
	+ 0.5	300}				

b. $\%O = [100 - \%C - \%H - \%N]$

Table 9: Ultimate analysis of coal (daf) #16 (hvCb)

Coal Identifier	Thermal History		$\%C$	$\%H$	$\%N$	$\%O^b$
	Time (hrs)	at Temp ($^{\circ}C$)				
16.H	20	100	82.49 ± 0.22	5.51 ± 0.06	2.35 ± 0.16	9.29 ± 0.71
16P.H	20 + 20	$\begin{matrix} 100 \\ 200 \end{matrix}$	$\begin{matrix} 83.56 \pm 0.18 \\ 83.56 \pm 0.18 \end{matrix}$	$\begin{matrix} 8.44 \pm 0.01 \\ 8.44 \pm 0.01 \end{matrix}$	$\begin{matrix} 2.20 \pm 0.13 \\ 2.20 \pm 0.13 \end{matrix}$	$\begin{matrix} 8.79 \pm 0.22 \\ 8.79 \pm 0.22 \end{matrix}$
16Q.H	20 0.5	$\begin{matrix} 100 \\ 300 \end{matrix}$	$\begin{matrix} 83.60 \pm 0.52 \\ 83.60 \pm 0.52 \end{matrix}$	$\begin{matrix} 5.44 \pm 0.06 \\ 5.44 \pm 0.06 \end{matrix}$	$\begin{matrix} 1.87 \pm 0.06 \\ 1.87 \pm 0.06 \end{matrix}$	$\begin{matrix} 9.2 \pm 0.47 \\ 9.2 \pm 0.47 \end{matrix}$

b. $\%O = [100 - \%C - \%H - \%N]$

Table 10: Ultimate analysis of coal (daf) #20 (mvb)

Coal Identifier	Thermal History		%C	%H	%N	%O ^b
	Time at (hrs)	Temp (°C)				
20.H	20	70	87.17±1.34	4.37±0.17	1.61±0.14	6.85±0.5

b. %O = [100 - %C - %H - %N] sulfur contents were considered small.

Appendix 3

Proximate Analyses of Protonated and Heat-treated Coals

Table 1: Proximate analysis of protonated coal #1 (Lignite)

Coal Identifier	Thermal History		# RUNS	ASTM ^a Method of Analysis	% H ₂ O	% Vol	% Ash	DAF ^b Factor
	Time (hrs)	Temp (°C)						
1.H	20	70	2	CA	4.99±0.06	46.86±0.40	3.46±0.01	1.092
1a.H	20	70	4	CA	6.83±0.13	45.18±1.08	2.96±0.08	1.109
1ab.H	20 +20	70 100	2	CA	3.80±0.03	45.11±0.73	3.04±0.10	1.073
1ac.H	20	100	2	CA	0.57±0.05	48.86±0.36	2.95±0.05	1.036
1acP.H	20 +20	100 200	2	TGA	2.41±0.24	50.32±6.50	2.85±0.06	1.056
1acQ.H	20 + 0.5	100 300	2	TGA	2.44±0.06	45.10±0.66	2.84±0.00	1.056
1acPt.H(*)	20 + 0.5	100 200	1	TGA	2.30	50.24	2.89	1.055
1acQt.H(*)	20 + 0.5	100 300	1	TGA	2.17	49.25	2.93	1.054

a. CA = Fisher Coal Analyser TGA = Perkin Elmer Thermogravimetry

b. DAF FACTOR = $1/(100 - \%H_2O - \%Ash)$ (*) Heated rapidly in a tube furnace at higher temperature in N₂ (12cc/min)

Table 2: Proximate analysis of protonated coal #2 (Subbituminous C)

Coal Identifier	Thermal History		# RUNS	ASTM ^a Method of Analysis	% H ₂ O	% Vol	% Ash	DAF ^b Factor
	Time (hrs)	Temp (°C)						
2.H	20	70	4	CA	8.64±0.65	36.74±0.88	14.55±0.58	1.302
2c.H	20	100	2	CA	0.86±0.02	39.98±0.34	20.81±0.12	1.223
2b.H	20 +20	70 100	3	TGA	4.33±0.07	43.10±4.84	13.88±0.70	1.223
2cP.H	20 +20	100 200	2	TGA	2.33±0.06	38.99±6.00	20.93±0.80	1.310
2cQ.H	20 + 0.5	100 300	2	TGA	1.84±0.01	55.86±0.08	21.04±0.80	1.297
2cPt.H	20 + 0.5	100 200	2	TGA	2.85±0.13	36.31	20.07±1.40	1.298
2cQt.H	20 + 0.5	100 300	2	TGA	2.24±0.16	37.08±6.60	21.53±0.14	1.321
2cPQ.H	20 + 0.5	100 300	2	TGA	2.68±0.12	38.68±3.85	23.14±0.02	1.330

a. CA = Fisher Coal Analyser

TGA = Perkin Elmer Thermogravimetry

b. DAF factor = $1/(100-\%H_2O-\%Ash)$ (*) Heated rapidly in a tube furnace at higher temperature in N₂(12cc/min)

Table 3: Proximate analysis of protonated coal #4 (Subbituminous C)

Coal Identifier	Thermal History		# RUNS	ASTM ^a Method of Analysis	% H ₂ O	% Vol	% Ash	DAFb Factor
	Time (hrs)	Temp (°C)						
4.H	20	70	2	CA	5.88±.01	41.02±.76	6.22±.76	1.138
4a.H	20	100	2	CA	0.9±0.04	41.05±.39	7.62±.002	1.093

a. CA = Fisher Coal Analyser

b. D F factor = $1/(100-\%H_2O-\%Ash)$

Table 4: Proximate analysis of protonated coal #7 (Subbituminous B)

Coal Identifier	Thermal History		# RUNS	ASTM ^a Method of Analysis	% H ₂ O	% Vol	% Ash	DAF ^b Factor
	Time (hrs)	Temp (°C)						
7.H	20	100	2	CA	7.54±0.04	34.72±0.07	8.91±0.02	1.197
7a.H	20	100	1	TGA	3.97±0.24	38.12±0.89	9.28±0.07	1.153
7aPt.H(*)	20 + 0.5	100 200	3	TGA	0.95±0.087	36.96±2.07	8.41±0.22	1.103
7aQt.H(*)	20 + 0.5	100 300	3	TGA	2.39±0.21	60.38±0.11	9.92±0.22	1.140
7aQ.H	20 + 0.5	100 300	2	TGA	2.04±0.01	35.8±1.75	10.25±0.07	1.140

a. CA = Fisher Coal Analyser

TGA = Perkin Elmer Thermogravimetry

b. DAF factor = $1/(100-\%H_2O-\%Ash)$ (*) Heated rapidly in a tube furnace at higher temperature in N₂ (12cc/min)

Table 5: Proximate analysis of protonated coal #9 (Subbituminous C)

Coal Identifier	Thermal History		# RUNS	ASTM ^a Method of Analysis	% H ₂ O	% Vol	% Ash	DAF ^b Factor
	Time (hrs)	Temp (°C)						
9.H	20	100	2	CA	2.79±0.01	35.32±0.23	17.73±0.07	1.258
9P.H	20 +20	100 200	2	TGA	3.01±0.0	35.82±1.82	16.44±0.23	1.241
9Q.H	20 + 0.5	100 300	2	TGA	3.06±0.25	41.82±4.10	16.84±0.62	1.248
9bQ.H	20 + 0.5	100 300	2	TGA	1.78±0.10	47.52±7.70	15.34±0.45	1.207
9b.H	20	100	2	TGA	3.46±0.08	55.34	14.32±0.39	1.216
9bPt.H(*)	20 + 0.5	100 200	2	TGA	2.34±0.15	39.15±7.10	16.09±2.35	1.226
9bQt.H(*)	20 + 0.5	100 300	2	TGA	2.09±0.18	35.98±5.70	15.96±0.78	1.220

a. CA = Fisher Coal Analyser

TGA = Perkin Elmer Thermogravimetry

b. DAF factor = $1/(100 - \%H_2O - \%Ash)$ (*) Heated rapidly in a tube furnace at higher temperature in N₂(12cc/min)

Table 6: Proximate analysis of protonated coal #10 (hvCb, U. Cretaceous/Tertiary)

Coal Identifier	Thermal History		# RUNS	ASTM ^a Method of Analysis	% H ₂ O	% Vol	% Ash	DAF ^b Factor
	Time (hrs)	Temp (°C)						
10.H	20	70	2	CA	4.33±0.03	38.80±0.70	12.36±0.08	1.200
10.H	20	70	2	TGA	3.67±0.04	35.24±0.08	11.83±0.06	1.183
10a.H	20	100	2	CA	5.06±0.01	37.28±0.54	10.81±0.07	1.189
10aP.H	20 +20	100 200	3	TGA	3.65±0.263	41.88±5.1	11.05±0.38	1.172
10aQ.H	20 + 0.5	100 300	2	TGA	2.45±0.02	38.70±0.66	12.08±0.01	1.170
10b.H	20	100	2	TGA	3.42±0.06	40.58±0.71	10.91±0.23	1.167
10bQ.H	20 + 0.5	100 300	2	TGA	1.74±0.18	40.37	11.98±0.31	1.159

TGA = Perkin Elmer Thermogravimetry

a. CA = Fisher Coal Analyser

b. DAF factor = $1/(100-\%H_2O-\%Ash)$

Table 7: Proximate analysis of protonated coal #11 (Subbituminous C)

Coal Identifier	Thermal History		# RUNS	ASTM ^a Method of Analysis	%H ₂ O	% Vol	% Ash	DAF ^b Factor
	Time (hrs)	Temp (°C)						
11.H	20	70	2	TGA	5.33±0.07	36.02±0.28	10.62±0.10	1.190
11.H	20	70	2	CA	6.98±0.014	41.70±0.93	11.20±0.01	1.222
11a.H	20	100	2	CA	2.91±0.05	38.84±0.19	9.86±0.22	1.146
11aP.H	20 +20	100 200	2	TGA	3.58±0.14	48.2±7.72	9.26±0.21	1.147
11aQ.H	20 + 0.5	100 300	2	TGA	2.66±0.49	59.97±3.40	10.48±0.29	1.151
11b.H	20	70	2	TGA	3.69±0.40	40.62±0.76	10.07±0.59	1.159
11bQ.H	20 + 0.5	100 300	2	TGA	1.68±0.04	37.36±0.42	9.58±0.88	1.127

TGA = Perkin Elmer Thermogravimetry

a. CA = Fisher Coal Analyser

b. DAF factor = $1/(100-\%H_2O-\%Ash)$

Table 8: Proximate analysis of protonated coal #14 (hvCb, Carboniferous)

Coal Identifier	Thermal History		# RUNS	ASTM ^a Method of Analysis	% H ₂ O	% Vol	% Ash	DAF ^b Factor
	Time (hrs)	Temp (°C)						
14.H	20	100	2	CA	0.43±0.00	36.24±1.5	4.78±0.04	1.055
14P.H	20 +20	100 200	2	CA	0.60±0.02	34.94±1.37	5.70±0.92	1.067
14Q.H	20 + 0.5	100 300	3	TGA	0.69±0.038	39.75	4.31±0.14	1.053
14b.H	20	70	2	TGA	0.66±0.08	37.71±0.00	4.43	1.054
14bQ.H	20 + 0.5	70 300	2	TGA	0.56±0.02	31.94±0.06	4.60±0.10	1.054

a. CA = Fisher Coal Analyser

TGA = Perkin Elmer Thermogravimetry

b. DAF factor = $1/(100-\%H_2O-\%Ash)$

Table 9: Proximate analysis of protonated coal #16 (hvCb, Carboniferous)

Coal Identifier	Thermal History		# RUNS	ASTM ^a Method of Analysis	% H ₂ O	% Vol	% Ash	DAF ^b Factor
	Time (hrs)	Temp (°C)						
16.H	20	100	2	CA	0.88±0.00	35.60±0.04	2.68±0.01	1.037
16.H	20	100	2	TGA	1.24±0.12	30.78±1.58	2.67±0.07	1.040
16P.H	20 +20	100 200	3	TGA	1.18±0.15	36.4±5.30	2.66±0.13	1.040
16Q.H	20 + 0.5	100 300	2	TGA	1.127±0.14	34.46±2.73	2.73±0.03	1.040

TGA = Perkin Elmer Thermogravimetry

a. CA = Fisher Coal Analyser

b. DAF factor = $1/(100-\%H_2O-\%Ash)$

Table 10: Proximate analysis of protonated coal #20 (mvb, Tertiary)

Coal Identifier	Thermal History		# RUNS	ASTM ^a Method of Analysis	% H ₂ O	% Vol	% Ash	DAF ^b Factor
	Time (hrs)	Temp (°C)						
20.H	20	70	2	CA	1.12±0.00	20.86±0.65	9.55±0.01	1.111

a. CA = Fisher Coal Analyser

b. DAF factor = $1/(100-\%H_2O-\%Ash)$

Appendix 4

FTIR-PAS Spectra of Protonated, Chemically modified and Heat-treated coals

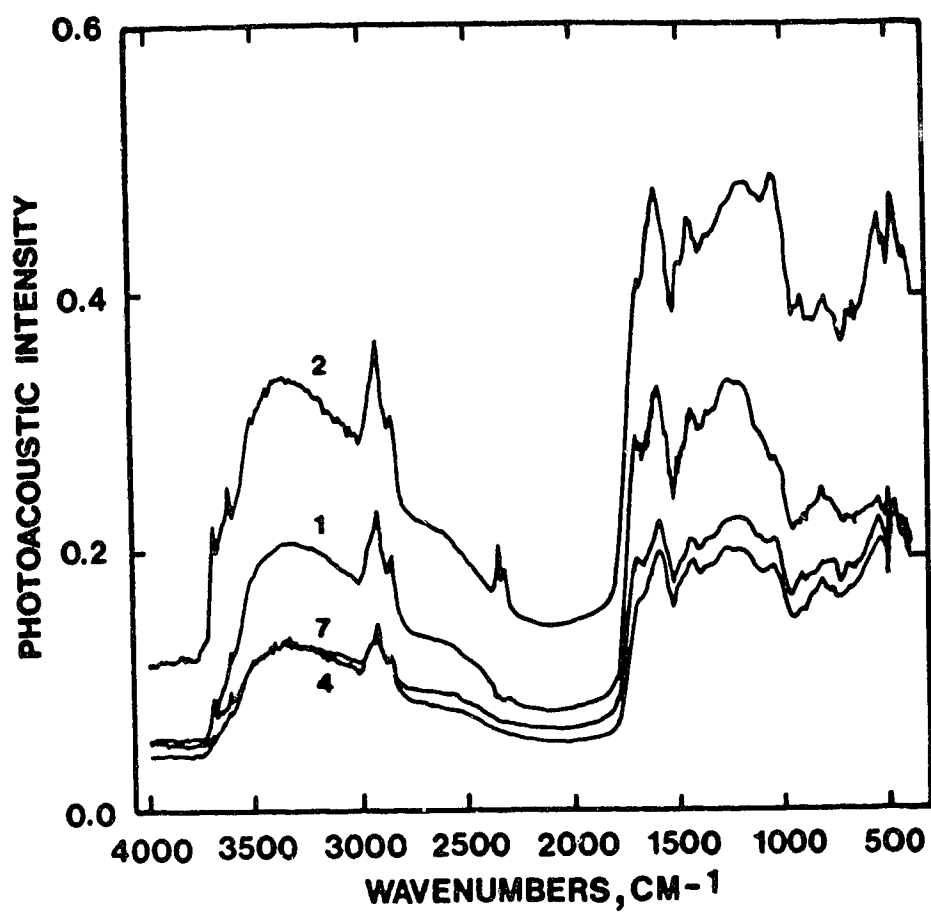


Fig.10 Typical FTIR-PAS spectra for low rank coals (#2, #4 subbit. C, #1 lignite, #7 subbit. B)

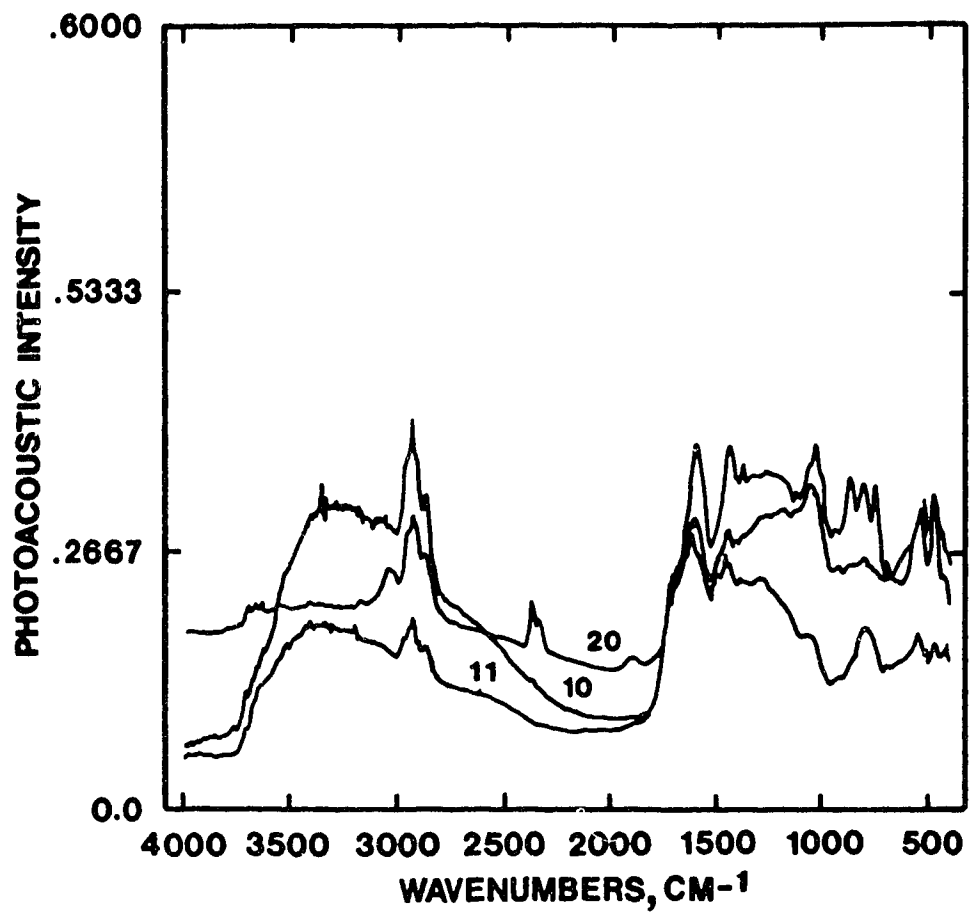


Fig. 11 FTIR-PAS spectra of different rank Western Canadian coals
#11 (subbit. C.,), #10 (hvb) and #20 (mvb).

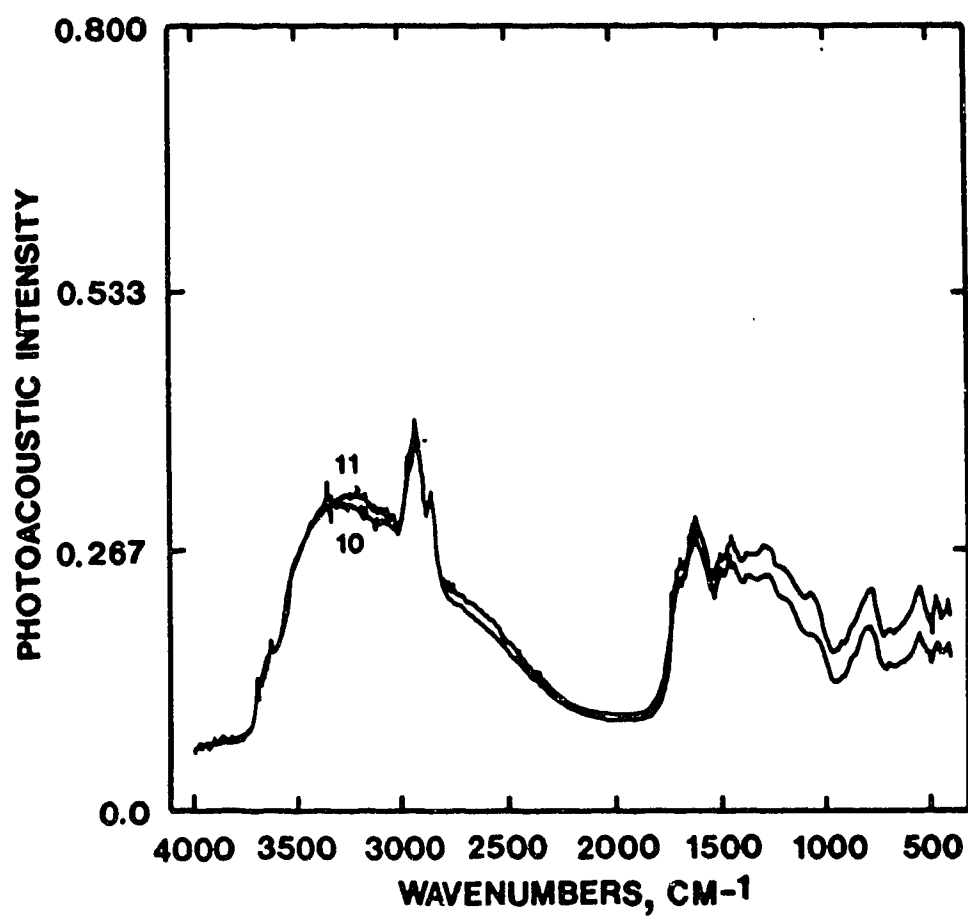


Fig.12 FTIR-PAS spectra of U.Cretaceous coals #11 (subbit. C)
and #10 (hvb)

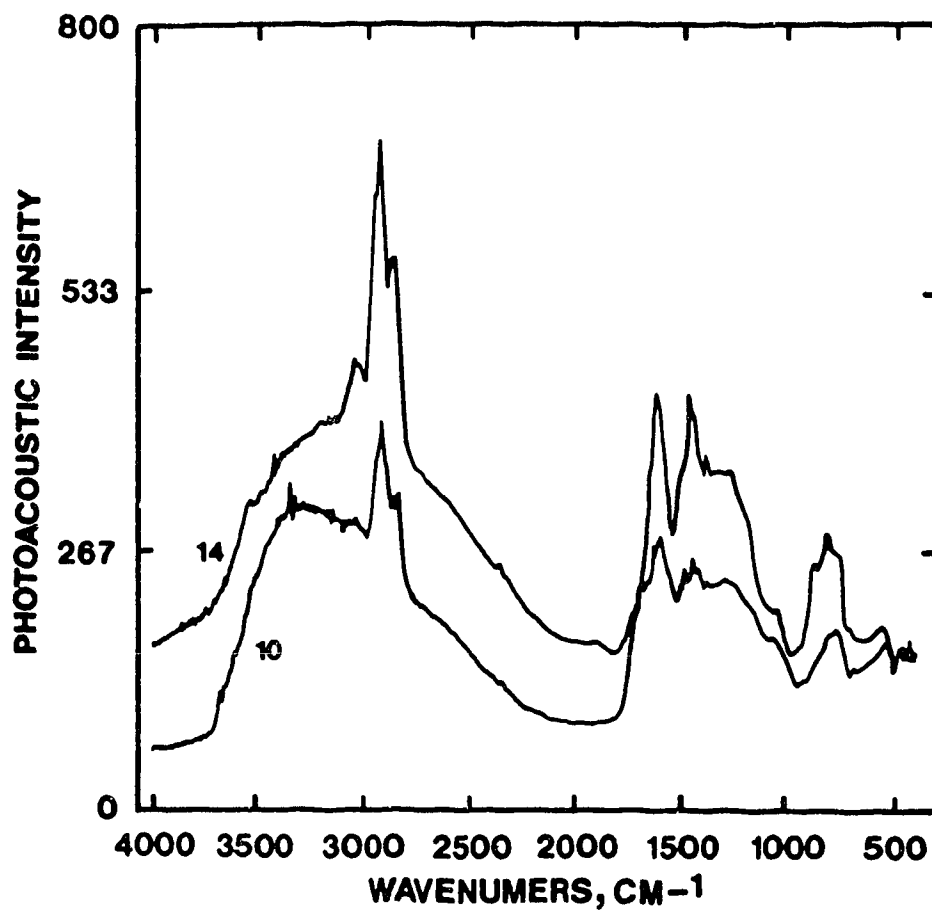


Fig.13 FTIR-PAS spectra of similar rank (hvb) coals which differ in Geological age (#10 is U.Cretaceous /Tertiary, #14 is Carboniferous).

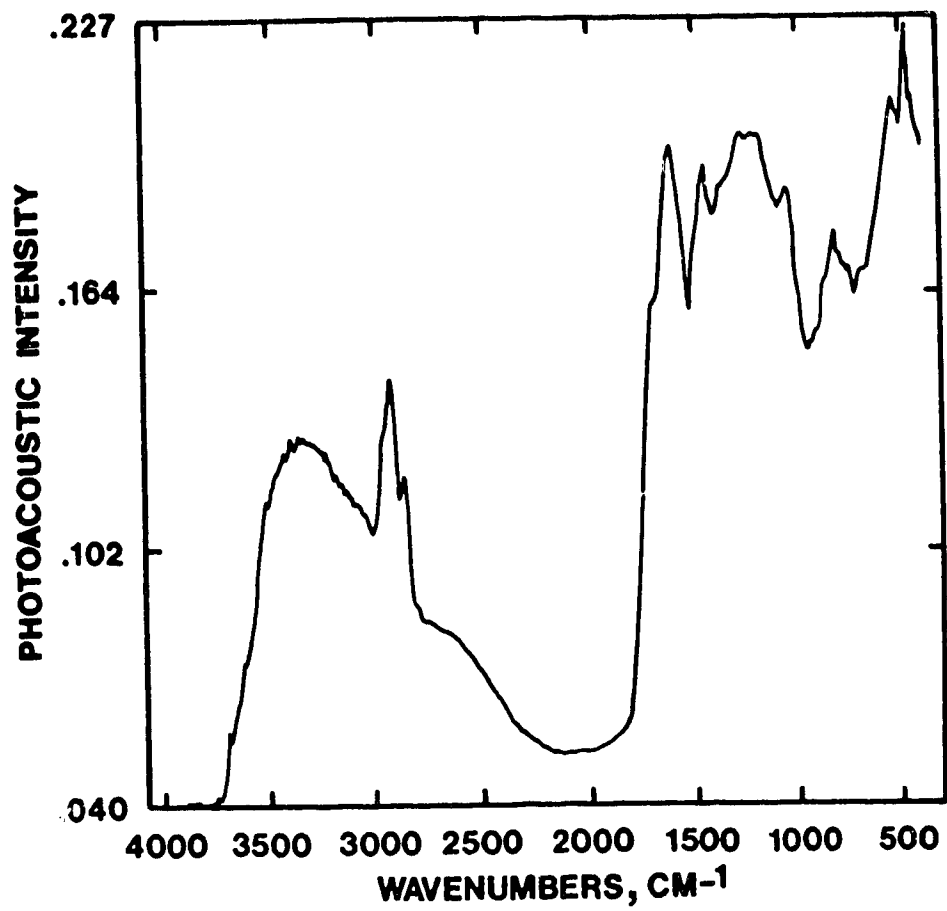


Fig.14a Typical FTIR-PAS spectra of a protonated coal
(#4, subbit.C).

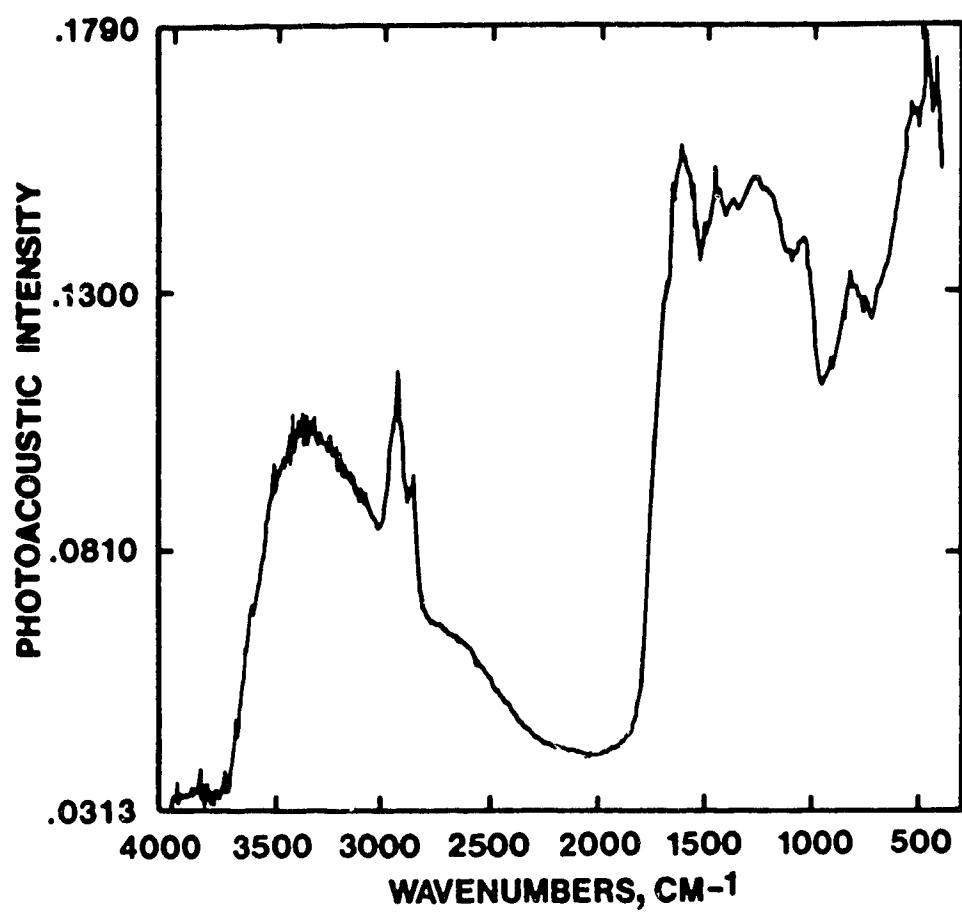


Fig.14b Typical FTIR-PAS spectra of a Ba-exchanged coal
(#4, subbit.C).

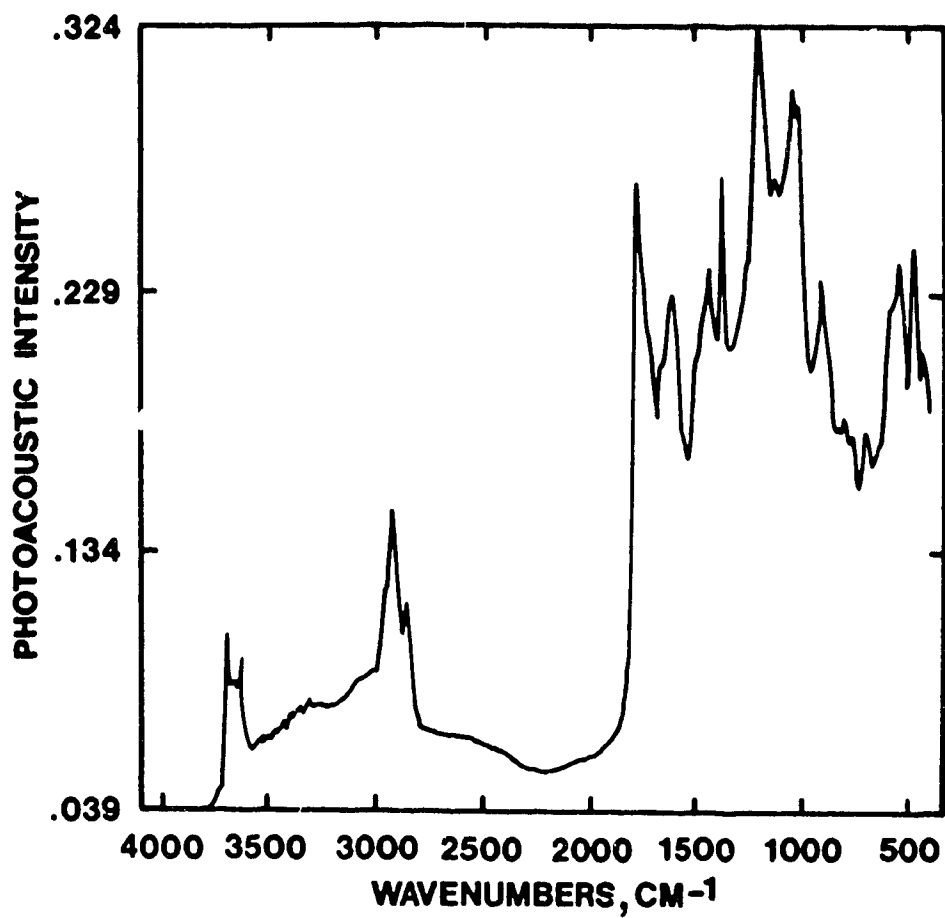


Fig.14c Typical FTIR-PAS spectra of an acetylated coal (#4, subbit.C).

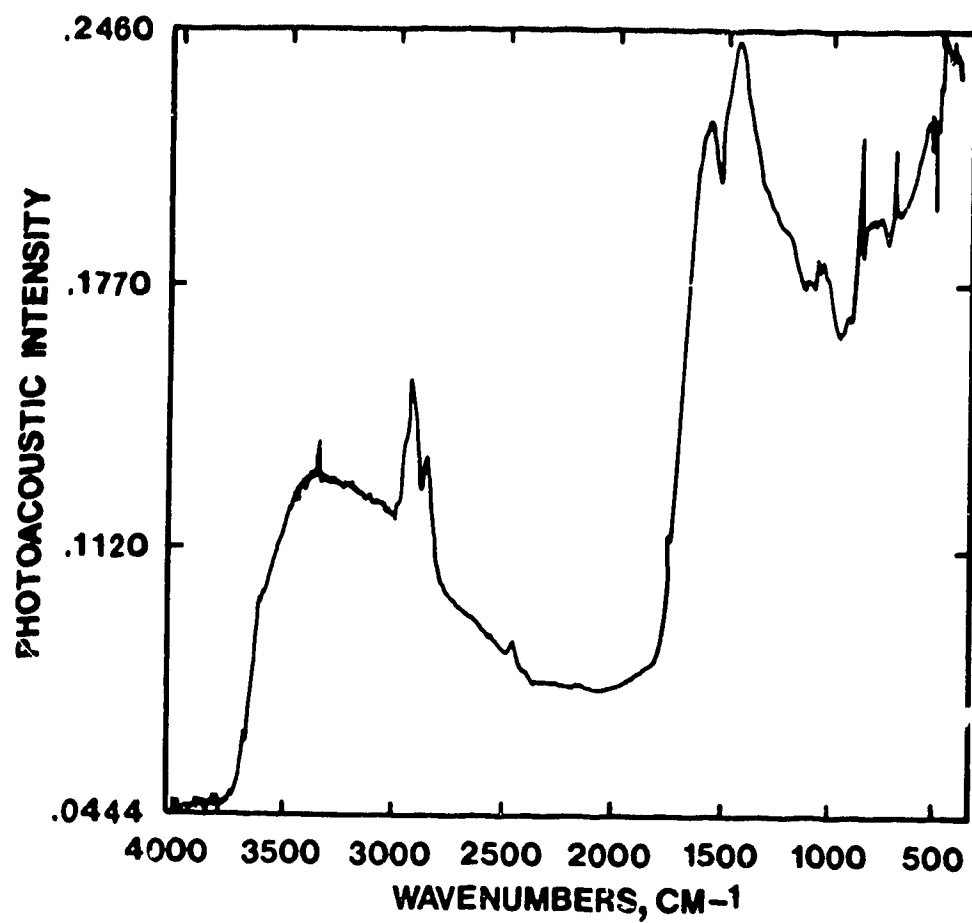


Fig.14d Typical FTIR-PAS spectra of a coal (#4, subbit.C.)
hydrolysed after acetylation.

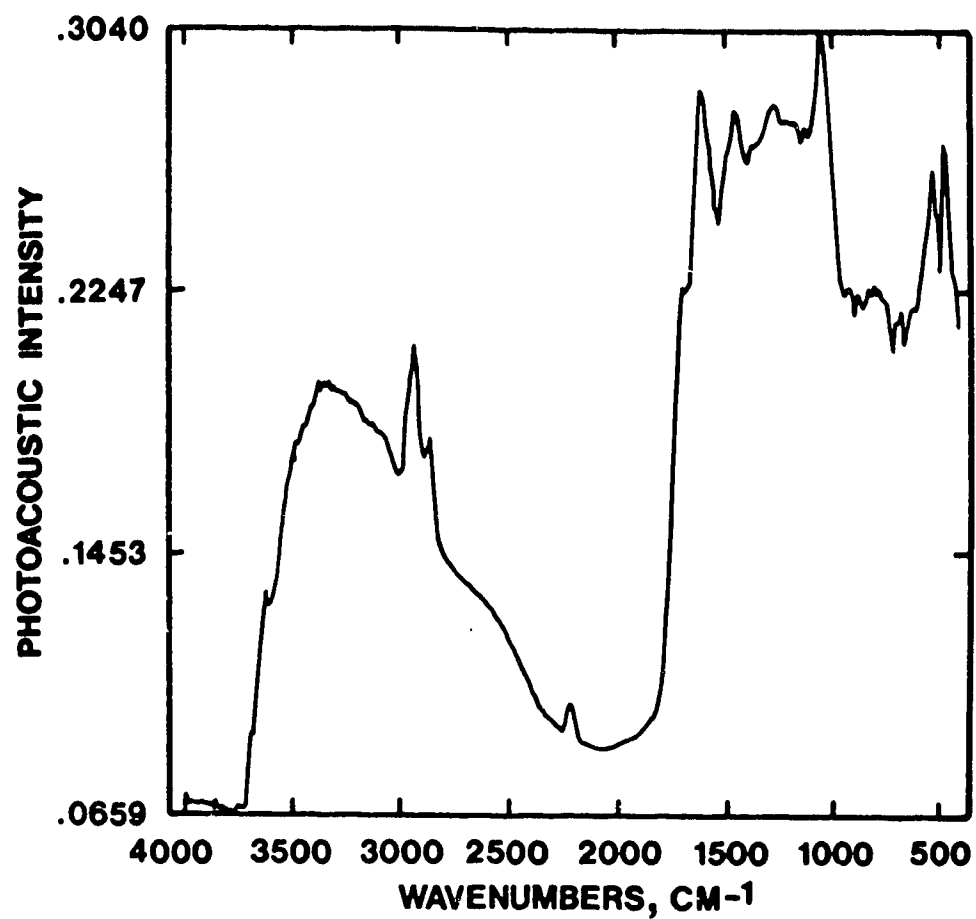


Fig.14e Typical FTIR-PAS spectra of an oxidized coal (#11 subbit.C)

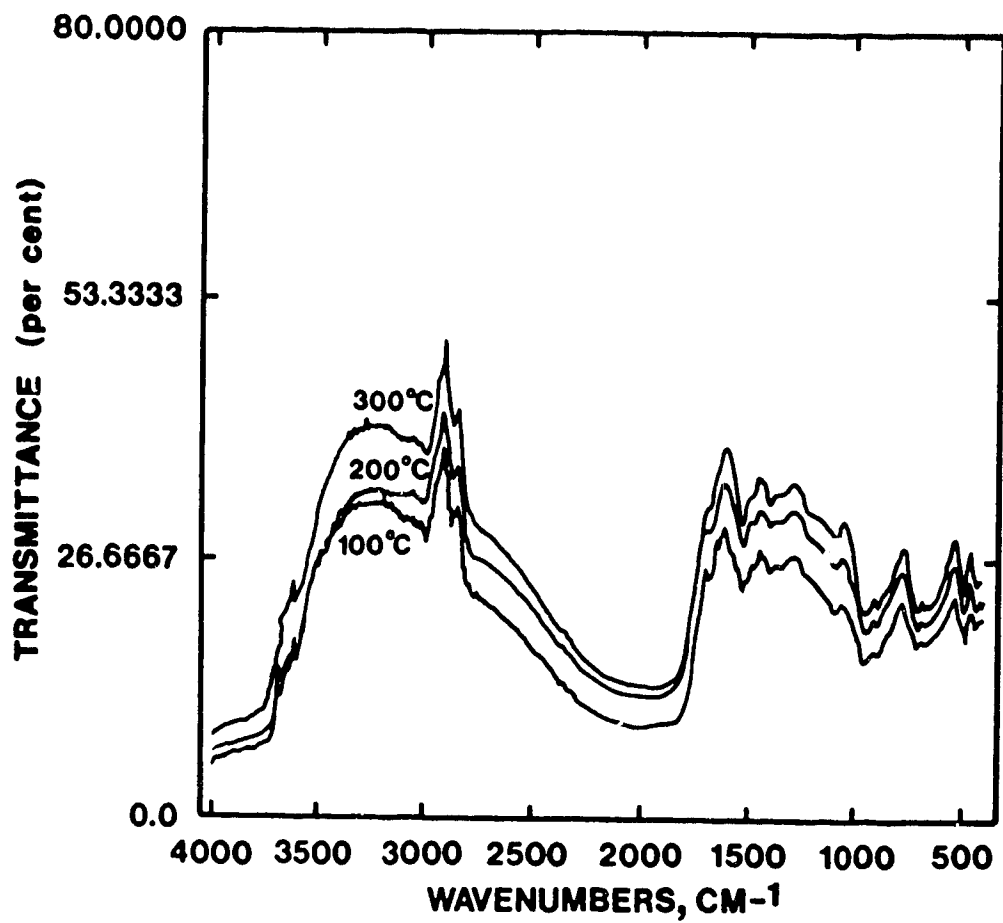


Fig. 5.5 FTIR-PAS spectra of coal #11 (subbit.C) after
slow heating at 200°C (20h) and 300°C (0.5h) in N₂
(8cc/min)

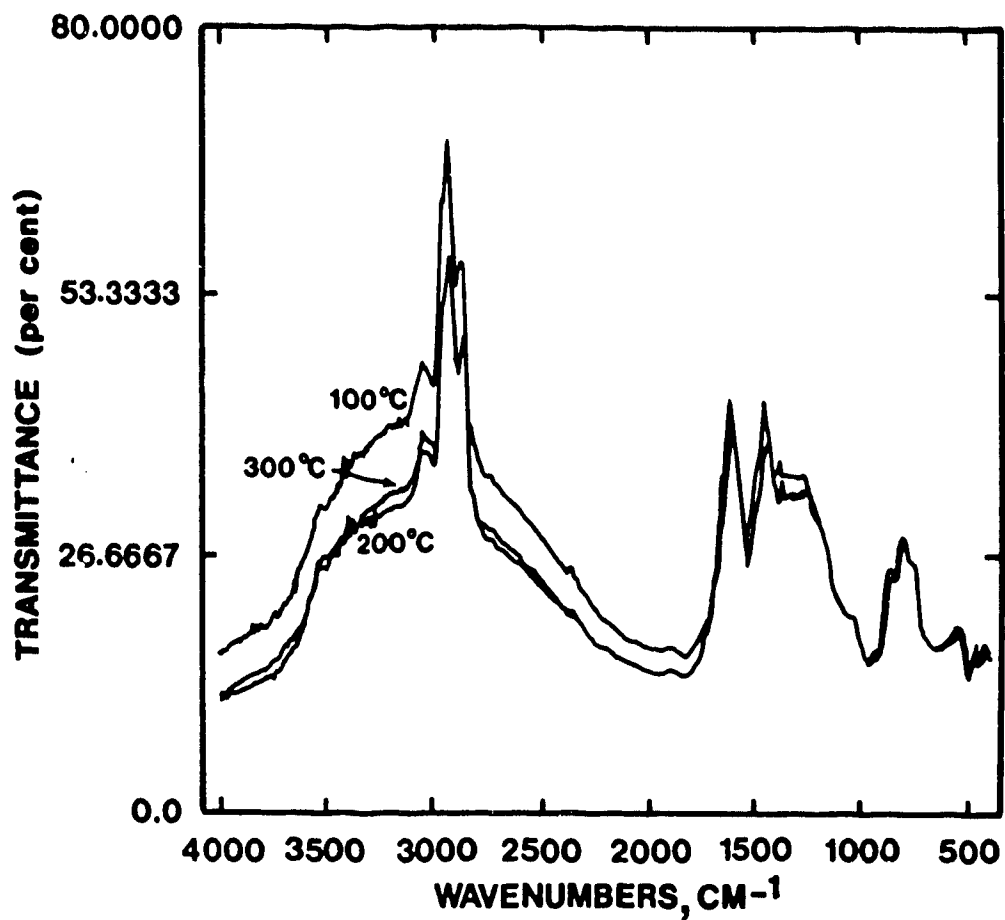


Fig. 5.6 FTIR-PAS spectra of coal #14 after slow heating at 200°C (20h) and 300°C (0.5h) in N₂ (8cc/min), compared with coal dried at 100°C in vacuo (20h).

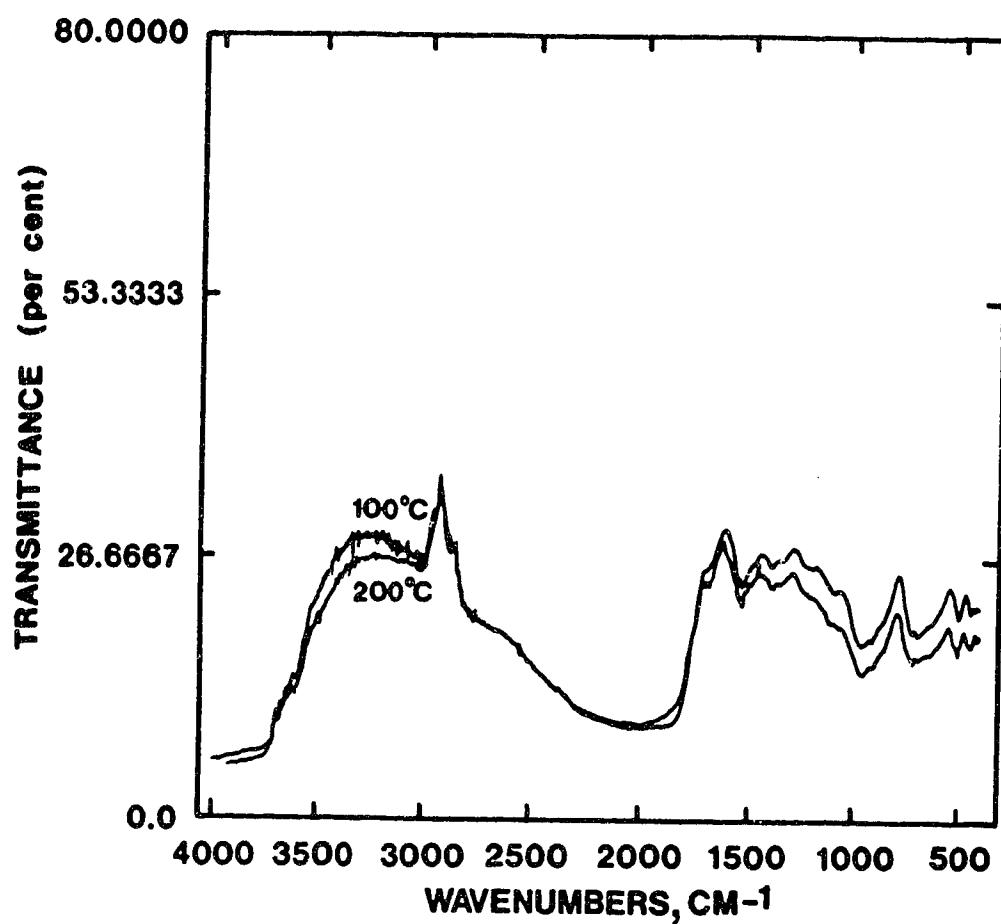


Fig. 5.7 FTIR-PAS spectra of coal #9 (subbit. C) after slow heating at 200°C (20h) in N₂ (8cc/min) compared with the original coal dried in vacuo at 100°C (20h).

Appendix 5

List of Chemicals and Time Table of Experimental Plan

CHEMICALS AND SUPPLIES

All chemicals were ACS grade and were obtained from Fisher Scientific unless otherwise indicated.

Barium acetate crystals

Barium Hydroxide Crystals

Phosphate Buffer Solutions pH 4.0, 8.0. 7.0

Potassium Hydrogen Phthalate crystals

Hydroxylamine Hydrochloride

Silver nitrate crystals

Concentrated HCl

Spectrograde Pyridine

Acetic Anhydride

Sodium Hydroxide Pellets

Amberlite Rexyn-H ion exchange resin (Aldrich Chemicals)

Whatman Filter paper - ashless #50 7cm,5cm

Glass vials for sample storage

Kapak heat seal pouches and Heat sealer

UHP nitrogen

Vacuum flasks

250 ml Heating mantles

Condensers

Plastic Erlenmeyer flasks 125ml, 250ml, 500ml

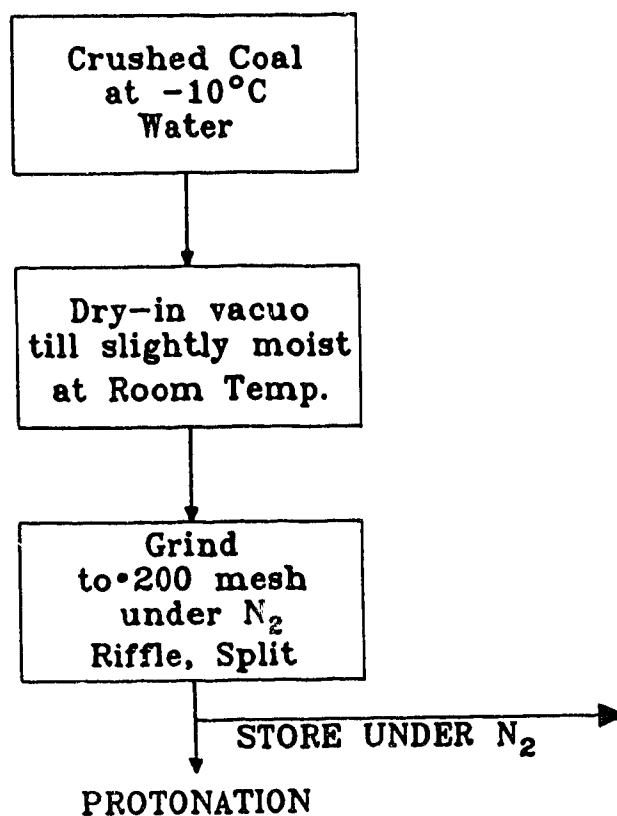
Plastic Buchner Funnels 5cm,7cm

Magnetic Stirrers

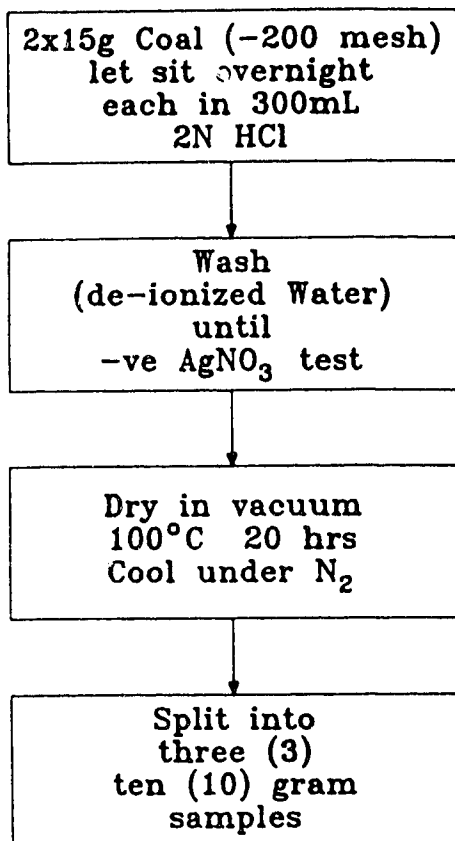
Vacuum pumps

Desiccators

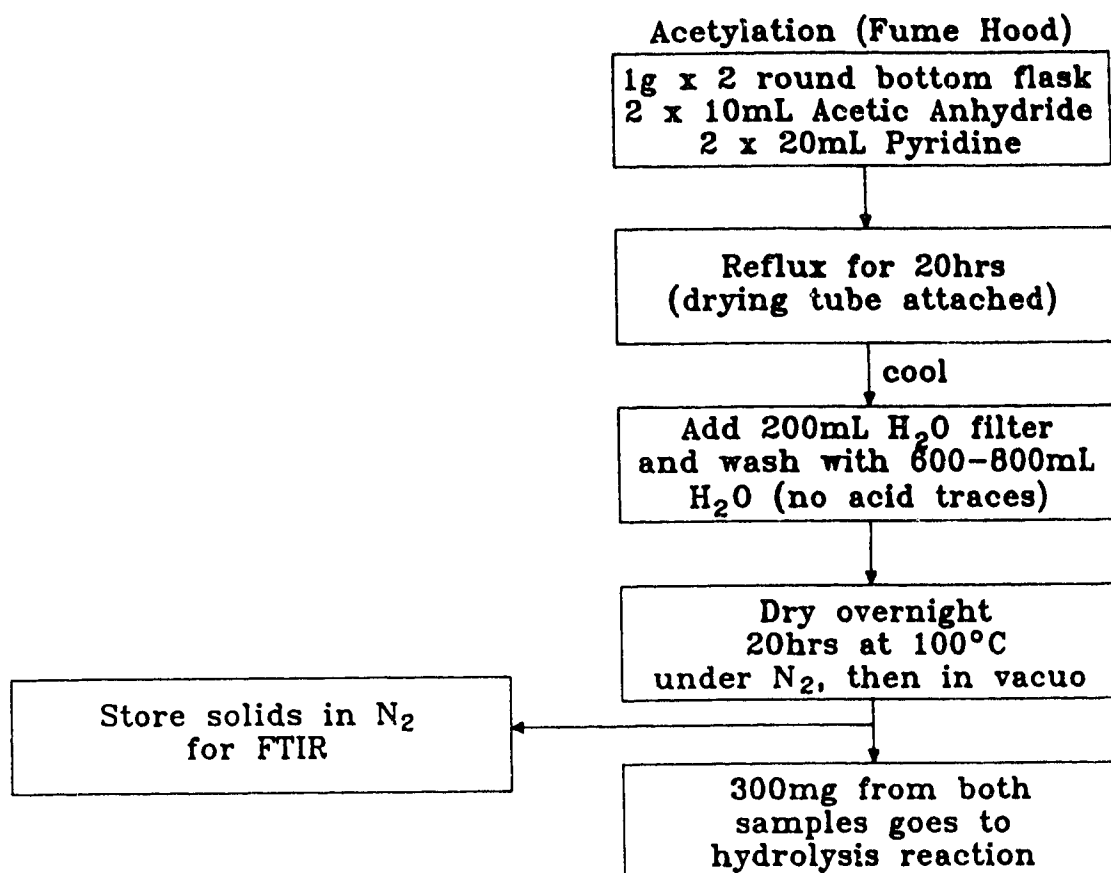
SAMPLE PREPARATION (1-2 WEEKS)



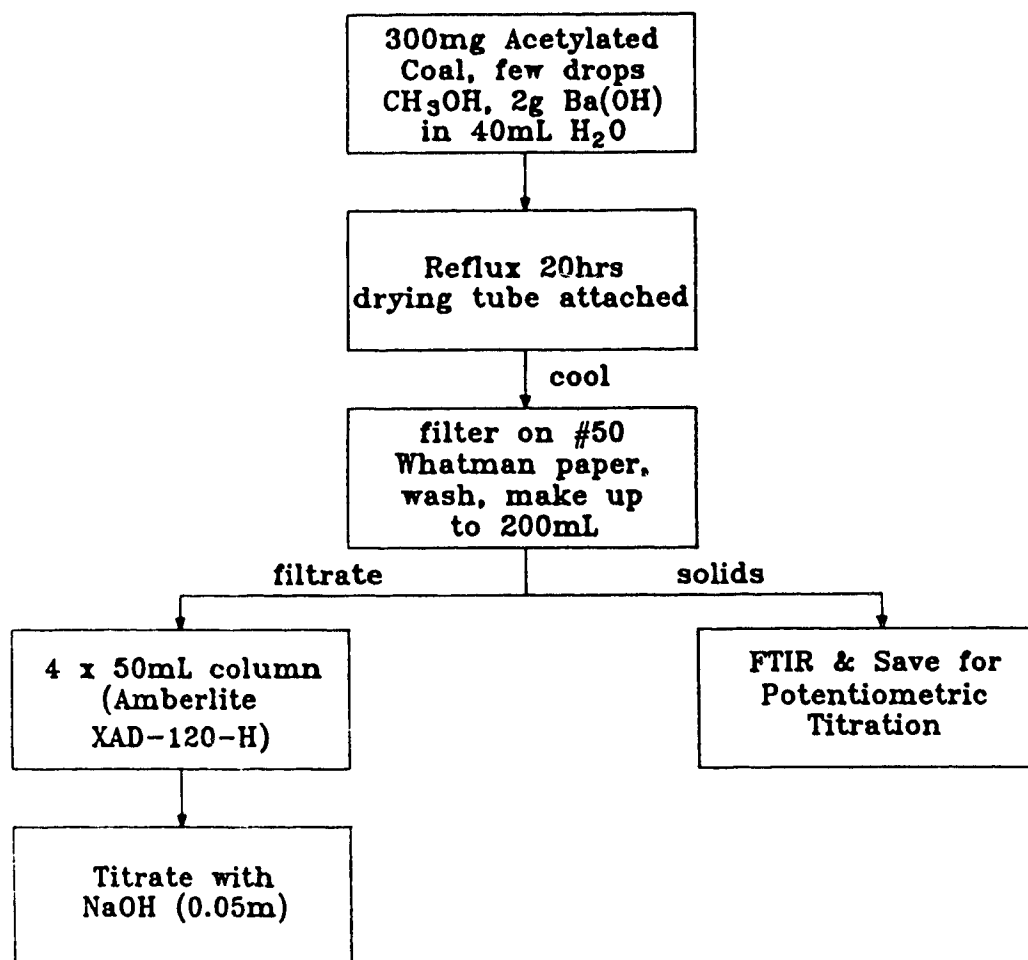
PROTONATION



HYDROXYL DETERMINATION (2 WEEKS)

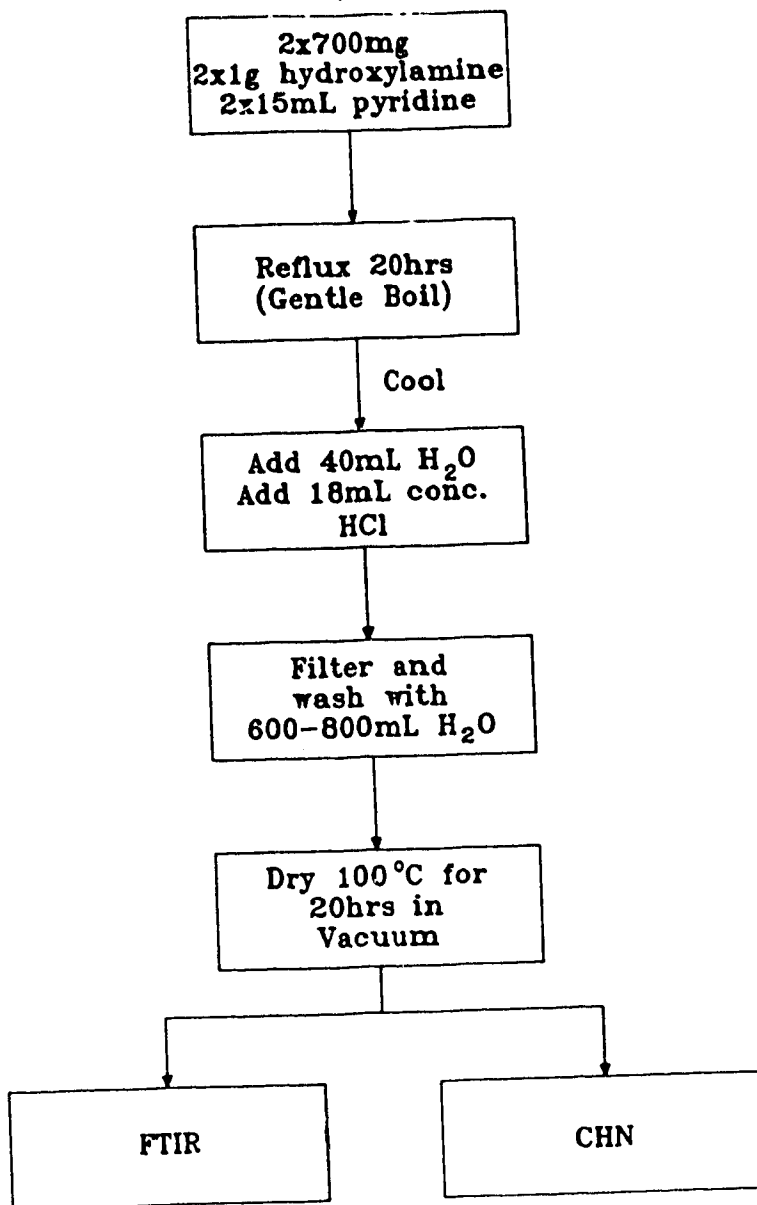


HYDROLYSIS



CARBONYL OXYGEN (2 WEEKS)

Oximation (Fume Hood)



CARBOXYLIC ACID (1 WEEK)

